Optimizing the Culture Medium for Little-leaf Mockorange (*Philadelphus microphyllus*) by Using Statistical Modeling and Spectral Imaging

A Dissertation

Presented in Partial Fulfillment of the Requirements for the

Degree of Doctor of Philosophy

with a

Major in Plant Sciences

in the

College of Graduate Studies

University of Idaho

by

Razieh Khajehyar

Approved by:
Major Professor: Robert Tripepi, Ph.D.
Committee Members: Stephen Love, Ph.D.; William Price, PhD.; Timothy Prather, PhD.
Department Administrator: Juliet Marshall, Ph.D.

May 2022

Abstract

Native plants are very important in urban landscape systems, as they have been adopted to the environment and are resistant to different biotic or abiotic stresses in the area. Little-leaf mockorange is a native plant in the western United States, and is a good choice for urban landscape use, while difficulties in its propagation through regular methods is a concern. In a series of studies, the potential of tissue culture to propagate this plant species was evaluated. During the completion of these studies, adjustment of tissue culture medium by changing different cytokinins and minerals was completed either as individual experiments or in the form of one experiment to run Response Surface Methods (RSM) to develop a statistical model. At the end of experiments, the feasibility of application of ASD spectroradiometer was also checked to estimate the foliar mineral status of tissue-cultured plants for studying a non-destructive method of foliar mineral prediction. Results showed that little-leaf mockorange grew best on ½ strength MS medium containing 32.5 to 35 mM N, 1.8 mM Ca, and 0.6 mM P, supplemented with 1.1 µM Zeatin. Also, using a spectroradiometer for hyperspectral imaging showed that N and Ca could be accurately estimated by developing models based on Random Forest regression models. Hyperspectral features such as, minimum external of the wavelength and asymmetric point of the wavelengths throughout the hyperspectral bands, as well as vegetation indices such as double peak index (DPI) or cellulose absorption index (CAI) were useful to provide informative data to predict foliar content of N and Ca in tissue-cultured little-leaf mockorange. this research resulted in an optimized tissue culture medium for efficient reproduction of little-leaf mockorange, so that commercial propagators can use these results to propagate this selected plant for the landscape industry.

Acknowledgment

Before everything, I want to show my respect and sincere gratitude to my major advisor, Dr. Robert Tripepi, whose help and support throughout my PhD education will never be forgotten. I will always remember his support during my hard days, while his precise and delicate comments, suggestions and advice to complete this dissertation were like a light on my academic path. I learned a lot from him and his knowledge and will appreciate all his efforts to elevate my education.

Next, I would like to thank my committee members, Dr. Stephen Love, for his exact comments during writing this dissertation, and for his motivating comments on my preliminary exam and during the defense, Dr. William Price for all I learned from him about statistics and modeling, and for being such a nice person. I will always smile when I think about how calm and relieved I would become after talking with him about my concerns on the research and data analysis, and Dr. Timothy Prather, for accepting to serve on my committee the last moment, for his exact comments on the dissertation, and for his kind support and advice how to look for my future career, as well as his valuable comments on my teaching status.

I also want to acknowledge Dr. Jack Brown for his precious support and comments on my teaching and for the motivation he gave me toward teaching. I want to thank my friend and colleague, Jenny Knerr, for her suggestions, help and support while completing the experiments in the lab. I thank Milad Vahidi for helping me to improve my machine learning information, Kyler Beck and Mack Murdock for their help and support in Parma. I also appreciate ASHS for the opportunity they provided for me to be part of their team.

Dedication

I would never stand where I am today, if my parents and my family were not standing next to me. I need to express all my respect and love toward my Mom (Fatemeh Banoo Forsatian) and Dad (Mr. Homayoun Khajehyar) whose support, love, dedication, and life lessons were not holding me back and keeping my heart warm and feeling safe and supported all my life. I would be nothing without their love and support.

I want to thank my brother Mohamad Javad, my sister Marzieh, and my sister-in-law Sharareh, who have been always there for me, not only whenever I needed them, even whenever I wouldn't say a single word. I have always been feeling motivated, supported, and loved just because of them.

I need to thank all my family, my grandmas who I missed seeing them while I was earning my PhD and will be missed so much, my uncles and aunts, and my cousins whose love and support have always been with me and motivating me toward completing my degree.

And last but not least, I want to thank all my friends and beloved ones who have always been next to me and stood with me in my hard days. I appreciate them all and wish them all the best.

Table of Contents

Abstract …….. ii

Acknowledgment ……... iii

Dedication …….. iv

Table of Contents ……... v

List of Tables ……. ix

List of Figures …… xi

Chapter 1: Literature Review ……. 1

1.1. Hydrangeaceae Family ……. 1

1.1.1. Little-leaf Mockorange …….. 3

1.2. Tissue Culture ……... 5

1.2.1. Tissue Culture Medium Components …… 7

1.2.1.1. Inorganic Mineral Elements …… 8

1.2.1.2. Plant Growth Regulators (PGRs) …… 11

A) Auxins ……. 12

B) Cytokinins …….. 13

1.3. Hyperspectral Signatures …….. 16

1.3.1. Vegetation Indices ……. 18

1.3.2. Pathogen and disease diagnosis ……. 21

1.3.3. Plant stress detection …….. 21

1.3.4. Nutrient status and deficiency prediction …….. 22

1.3.5. Hyperspectral related terms ……... 23

1.4. Statistical Analysis and Statistical Modeling …… 26

1.5. Research objectives for my dissertation ……... 28

References …… 29

Chapter 2: Optimization of tissue culture medium for little-leaf mockorange (*Philadelphus microphyllus* A. Gray) by adjusting cytokinin and mineral components 40

Abstract …… 40

2.1. Introduction ……... 41

2.2. Objectives ……. 43

2.3. Materials and Methods ……. 43

2.3.1. Plant materials …… 43

2.3.2. Surface sterilization of stem explants …… 44

2.3.3. Micropropagation and maintenance of the shoot cultures ……. 44

2.3.4. Plant growth regulator cytokinin experiments …….. 45

2.3.4.1. Evaluation of cytokinin type and concentration ……. 45

2.3.4.2. Zeatin experiment ……... 45

2.3.5. Minerals experiments …… 46

2.3.5.1. Nitrogen (N) experiment …… 46

2.3.5.2. Iron (Fe) experiment ……... 46

2.3.5.3. Calcium (Ca) experiment …… 47

2.3.5.4. Magnesium (Mg) experiment ……. 47

2.3.5.5. Phosphorous (P) experiment …….. 47

2.3.6. Shoot harvest and data collection …….. 47

2.3.7. Statistical analysis …… 48

2.4. Results …….. 49

2.4.1. Cytokinin experiment …… 49

2.4.2. Zeatin experiment …….. 53

2.4.3. Minerals experiments …… 54

2.5. Discission …….. 58

2.6. Conclusion …… 62

References …… 63

Chapter 3: Optimization of selected minerals and a cytokinin for in vitro propagation of little-leaf mockorange (*Philadelphus microphyllus* A. Gray) using Response Surface Method (RSM) …… 69

Abstract …… 69

3.1. Introduction ……... 70

3.2. Objectives …… 73

3.3. Materials and Methods …….. 74

3.3.1. Plant materials …… 74

3.3.2. Micropropagation and maintenance of the shoot cultures ……. 74

3.3.3. Response Surface Methods experiment …… 75

3.3.3.1. Experimental design ……... 75

3.3.4. Media preparation and micropropagation …….. 77

3.3.5. Data collection ……... 78

3.3.6. Statistical analysis …….. 78

3.4. Results ……... 78

3.4.1. Number of axillary shoots …….. 79

3.4.2. Shoot length ……... 80

3.4.3. Dry weight …… 80

3.5. Discussion …… 85

3.6. Conclusion …… 86

References …… 87

Chapter 4: Using hyperspectral signatures for predicting foliar nitrogen and calcium content of tissue cultured little-leaf mockorange (*Philadelphus microphyllus* A. Gray) … 89

Abstract …… 89

4.1. Introduction …….. 89

4.1.1. Nutrient status and deficiency prediction …….. 91

4.2. Materials and Methods ……. 93

4.2.1. Plant materials and tissue culture …….. 93

4.2.2. Preparing the spectroradiometer and taking readings …… 93

4.2.3. Tissue analysis for mineral content ……... 95

4.2.4. Feature generation …….. 95

4.2.4.1. Continuum removal and feature selection……... 95

4.2.5. Correlation tests ……. 96

4.2.6. Model development ……... 96

4.2.6.1. Applied machine learning (ML) methods ……... 97

4.2.6.2. Data partitioning …… 97

4.2.7. Model evaluation criteria ……... 98

4.3. Results ……... 99

4.3.1. Vegetation indices calculation and feature generation …….. 99

4.3.2. Foliar nitrogen content ……... 100

4.3.2.1. Extraction of spectral bands with higher correlation with N content ……. 100

4.3.2.2. Model development …… 100

4.3.3. Foliar calcium content ……... 104

4.3.3.1. Extraction of spectral bands with higher correlation with Ca content …… 104

4.3.3.2. Model development …… 104

4.4. Discussion ……. 108

4.5. Conclusion …… 112

References …… 114

Conclusion to the Dissertation ……... 118

List of Tables

Table 1.1. Function and mobility within plant tissue of the 14 soil-derived essential nutrients for plant growth ……. 9

Table 1.2. The most well-known vegetation indices determined by using hyperspectral imaging in agricultural research (Data obtained and calculated from Anonymous, Index Data Base, 2021) .. 20

Table 2.1. Main effects and the interactions between cytokinins and their concentrations on the number of axillary shoots, shoot length, and dry weight of little-leaf mockorange shoot cultures. *P*-values indicate statistical significance …….. 49

Table 2.2. The effects of cytokinins type (benzyl aminopurine (BA), kinetin (Kin), zeatin (Zea), meta-topolin (MT), dimethylamino purine (2iP), and thidiazuron (TDZ)) on the number of axillary shoots, shoot length, and dry weight of little-leaf mockorange shoot cultures. *P*-values with an asterisk indicate statistical significance ……...…….. 51

Table 2.3. The effects of cytokinins (benzyl aminopurine (BA), kinetin (Kin), zeatin (Zea), meta-topolin (MT), dimethylamino purine (2iP), and thidiazuron (TDZ)) and their concentrations on mean shoots dry weights of little-leaf mockorange cultures. Six different cytokinins were tested at five concentrations on shoot explants. Data are means ± 95% confidence limits (n = 4). An interaction was observed that indicated the pattern of change over concentration differed by cytokinin type ..…….. 52

Table 3.1. The design created by SAS software to complete RSM for optimizing *in vitro* growth of little-leaf mockorange shoots ……...…….. 75

Table 3.2. The high, low, and average concentrations of selected minerals N, Ca, and P, as well as zeatin, used in different treatments combinations of culture media for *in vitro* propagation of little-leaf mockorange shoots ……..…… 77

Table 3.3. The optimum concentrations of zeatin, N, Ca, or P resulting in the optimal axillary shoot number, shoot length, and dry weight of little-leaf mockorange produced in tissue culture as determined by RSM models ...…… 86

Table 4.1. The highest correlated vegetation indices determined by using hyperspectral imaging in this study (Data obtained and calculated from Anonymous, Index Data Base, 2021) ...…… 99

Table 4.2. Fifteen wavelength ranges taken from spectra extracted from little-leaf mockorange shoot cultures by using a ASD spectroradiometer …… 100

Table 4.3. Various models developed for %N estimation in little-leaf mockorange shoots with different feature combinations and different number of trees via Random Forest algorithm …….. 103

Table 4.4. Various models developed for %N estimation of little-leaf mockorange shoots with different feature combinations and different penalty terms via SVM algorithm …….. 103

Table 4.5. Various models developed for %Ca estimation in little-leaf mockorange shoots with different features combinations and different number of trees via Random Forest algorithm …….. 107

Table 4.6. Various models developed for %Ca estimation of little-leaf mockorange shoots with different feature combinations and different penalty terms via SVM algorithm …….. 108

List of Figures

Figure 1.1. Figure 1. Flowers (left) and branches covered with tiny leaves (right) of little-leaf Mockorange (Wilson, 2012) …….. 4

Figure 1.2. Molecular structure of the natural auxin IAA molecule (left) (Anonymous, Auxin, Wikipedia, 2021) and the cytokinin Zeatin (right) (Anonymous, Zeatin, Wikipedia, 2013) ……. 13

Figure 1.3. From top, left to right: Molecular structure of the cytokinins zeatin (Zea) (Anonymous, Zeatin, Wikipedia, 2021), kinetin (Kin) (Anonymous, Kinetin, Wikipedia, 2021), benzyladenine (BA) (Anonymous, 6- Benzylamino purine, Wikipedia, 2021); Bottom: meta-topolin (MT) (Anonymous, Phytotech Lab, 2013), dimethylallylamino purine (2iP) (Anonymous, Sigma Aldrich, 2021), thidiazuron (TDZ) (Anonymous, Wikipedia, 2020) ……... 16

Figure 1.4. Spectra represent a) multispectral waves with 5 wide bands, and b) hyperspectral waves consisted of several narrow bands, sometimes even extended to hundreds and thousands of the narrow bands (Adão et al., 2017) …… 18

Figure 1.5. Assessment of Nutrient Status. (A) Reflectance pattern of a typical crop as a function of the chlorophyll AB content; (B) plotting different vegetation indices as a function of chlorophyll AB (Cab) content illustrates that some classical vegetation indices [normalized difference vegetation index (NDVI) and enhanced vegetation index (EVI)] saturate and are less sensitive to subtle differences in chlorophyll AB (Cab) levels when Cab is relatively high, in contrast to green NDVI (GNDVI) and normalized difference red edge (NDRE) index. Created from simulations using Fluspect-B model in SCOPE v1.70. Constant parameters were as follows: canopy height = 0.7 m, leaf area index (LAI) of 2.5 m2 m_2, N = 2.5; Cdm = 0.01; Cw = 0.05; Cs = 0; spherical leaf distribution assumed. EVI = 2.5 (NIR _ R)/(NIR + 6R _ 7.5B + 1); GNDVI = (NIR _ G)/(NIR + G); GRVI = (G _ R)/(G + R); NDRE = (NIR _ RE)/(NIR + RE). NIR, near-infrared spectrum; RE, red edge reflectance (Maes and Steppe, 2019) ……... 22

Figure 1.6. Correlation coefficients (r) between the spectral bands and the measured leaf nitrogen content (Liu et al., 2016) …….. 23

Figure 1.7. Features taken from continuum removal (right: absorption area left and right, left: absorption depth) …… 25

Figure 2.1. Effects of different cytokinins (benzyl aminopurine (BA), kinetin (Kin), zeatin (Zea), meta-topolin (MT), dimethylamino purine (2iP), and thidiazuron (TDZ)) *in vitro* growth of little-

leaf mockorange shoots averaged over their concentrations. Number of axillary shoots (top) and shoot length (bottom). Data are means (n = 4) and bars indicate ± 95% confidence limits …..…. 50

Figure 2.2. The interaction between cytokinins (benzyl aminopurine (BA), zeatin (Zea), and thidiazuron (TDZ)) selected for their strong, positive, and negative effects and their concentrations on dry weight of little-leaf mockorange shoot cultures. Bars indicate ± 95% confidence limits (n = 4) ……..….. 50

Figure 2.3. The effects of different concentrations of MT on the number of axillary shoots formed by little-leaf mockorange shoot cultures. Data are means (n = 4) and bars indicate ± 95% confidence limits …… 52

Figure 2.4. Comparison between different concentrations of MT (left) and BA (right) on shoot length of little-leaf mockorange cultures. Data are means (n = 4) and bars indicate ± 95% confidence limits ……..…….. 52

Figure 2.5. The effects of different concentrations of TDZ on shoot length of little-leaf mockorange shoot cultures. Data are means (n = 4) and bars indicate ± 95% confidence limits …… 53

Figure 2.6. The effect of 0, 0.55, 1.1, 1.65, or 2.2 µM zeatin on shoot length (left) and dry weight (right) of little-leaf mockorange. Data are means (n = 4) and bars indicate ± 95% confidence limits ……... 54

Figure 2.7. Effects of different N concentrations on number of axillary shoots (A), shoot length (B), and dry weight (C) of little-leaf mockorange shoots in tissue culture. Data are means (n = 4) and bars indicate ± 95% confidence limits ……..…… 56

Figure 2.8. Effects of different N concentrations on dry weight of little-leaf mockorange shoots in tissue culture. Data are means (n = 4) and bars indicate ± 95% confidence limits …… 56

Figure 2.9. Effects of different Fe concentrations on shoot length (left), and dry weight (right) of little-leaf mockorange shoots in tissue culture. Data are means (n = 4) and bars indicate ± 95% confidence limits ……..…. 57

Figure 2.10. Effects of 0, 25, 50, 75, or 100 µM Fe on shoot length (left) and dry weight (right) of little-leaf mockorange shoots in tissue culture. Data are means (n = 4) and error bars indicate ± 95% confidence limits ……... 57

Figure 2.11. Effects of different Ca concentrations on shoot length (left) and dry weight (right) of little-leaf mockorange shoots in tissue culture. Data are means (n = 4) and error bars indicate ± 95% confidence limits ……..... 57

Figure 2.12. Effects of different Mg concentrations on shoot length of little-leaf mockorange shoots in tissue culture. Data are means (n = 4) and error bars indicate ± 95% confidence limits …….. 58

Figure 2.13. Effects of different P concentrations on shoot length (left) and dry weight (right) of little-leaf mockorange shoots in tissue culture. Data are means (n = 4) and error bars indicate ± 95% confidence limits ……58

Figure 3.1. Response surface of N versus Ca (top) or N versus zeatin (bottom) on the number of axillary shoots (left) or shoot length (right) for little-leaf mockorange shoots produced in vitro. Blue color indicated poor growth and red demonstrated the optimum growth. Values on contour lines indicate the level of response (shoot number or length (cm)). Values of other tested components when fixed, were zeatin 1.095 µM, P 0.625 mM, K 10 mM, and Ca 1.5 mM ……...……. 81

Figure 3.2. Response surface of N versus P (top) or zeatin versus Ca (bottom) on shoot number (left) and shoot length (right) for little-leaf mockorange shoots produced in vitro. Blue color indicated poor growth and red demonstrated the optimum growth. Values on contour lines indicate the level of response (shoot number or length (cm)). Values of other tested components when fixed, were zeatin 1.095 µM, Ca 1.5 mM, P 0.625 mM, K 10 mM, and N 29.95 mM ……..…….. 82

Figure 3.3. Response surface of P versus Ca effects (top) or P versus Zea effects (bottom) on shoot number (left) and shoot length (right) for little-leaf mockorange shoots produced in vitro. Blue color indicated poor growth and red demonstrated the optimum growth. Values on contour lines indicate the level of response (shoot number or length (cm)). Values of other tested components when fixed, were zeatin 1.095 µM, Ca 1.5 mM, K 10 mM, and N 29.95 mM …….. 83

Figure 3.4. Response surface of N versus Ca effects (top, left), zeatin (top, right), or P (bottom, left), and zeatin versus Ca effects (bottom, right) on dry weight for little-leaf mockorange shoots produced in vitro. Blue color indicated poor growth and red demonstrated the optimum growth. Values on contour lines indicate the level of response (shoot dry weight (g)). Values of other tested components when fixed, were zeatin 1.095 µM, Ca 1.5 mM, P 0.625 mM, K 10 mM, and N 30 mM …… 84

Figure 3.5. Response surface of P versus Ca effects (left) or zeatin effects (right) on dry weight for little-leaf mockorange shoots produced in vitro. Blue color indicated poor growth and red demonstrated the optimum growth. Values on contour lines indicate the level of response (shoot dry weight (g)). Values of other tested components when fixed, were zeatin 1.095 µM, Ca 1.5 mM, K 10 mM, and N 30 mM …….. 84

Figure 4.1. Schematic diagram of model development from hyperspectral bands and foliar mineral analysis for little-leaf mockorange shoots grown in tissue culture …… 98

Figure 4.2. Correlation between leaf N% and the hyperspectral signatures acquired by ASD spectroradiometer from tissue cultured little-leaf mockorange shoots. The boxes show the correlation value and the wavelength of the peak in the spectrum …….. 101

Figure 4.3. Error bar plot and scatter plot of the correlation between observed and estimated %N of little-leaf mockorange shoots by a linear regression model …….. 101

Figure 4.4. Correlation value between features or vegetation indices (VIs) and leaf nitrogen content of tissue cultured little-leaf mockorange ……. 102

Figure 4.5. Error bar plot and scatter plot of leaf %N estimated and measured test samples for little-leaf mockorange shoots via Random Forest regression …….……. 103

Figure 4.6. Error bar plot and scatter plot of leaf %N estimated and measured test samples for little-leaf mockorange shoots via Support Vector Machines regression ……..…… 104

Figure 4.7. Correlation between leaf %Ca and the hyperspectral signatures acquired by the ASD spectroradiometer from tissue cultured little-leaf mockorange shoots …… 105

Figure 4.8. Correlation value between features and VIs with leaf calcium content of little-leaf mockorange shoots ……..…… 105

Figure 4.9. Error bar plot and scatter plot of the correlation between observed and estimated %Ca of little-leaf mockorange shoots by linear regression model ……...……. 106

Figure 4.10. The importance value of generated features and selected VIs regarding leaf %Ca in little-leaf mockorange shoots via Random Forest algorithm ……..…..…… 107

Figure 4.11. Error bar plot (left) and scatter plot (right) of leaf %Ca estimated and measured test samples in little-leaf mockorange shoots via Random Forest algorithm ……..……..….. 108

Figure 4.12. Error bar plot and scatter plot of leaf %Ca estimated and measured test samples for little-leaf mockorange shoots via Support Vector Machines regression ……..…… 108

Chapter 1: Literature Review

1.1. Hydrangeaceae Family

Mockorange (*Philadelphus spp.*) from the Hydrangeaceae family is widely distributed in Asia, North America, and southeastern Europe (Anonymous, Wikipedia, 2019). Plants in the Hydrangeaceae family are dicots (Anonymous, SFGate, 2019). The name of this plant family is derived from the Latin, hydro, meaning water, and aggeion, meaning vessel or cup. The name refers to the shape of the fruit. While individual species in the Hydrangeaceae family have some distinct characteristics, these plants share many characteristics that set them apart as a group from other plant families (Anonymous, SFGate, 2019). The Hydrangeaceae (hydrangea) is a family of flowering plants, in the Cornales order and is comprised of several genera (Anonymous, The Plant List, 2013, Anonymous, Britannica, 2017) and about 250 to 260 species (Anonymous, Britannica, 2017, Anonymous, SFGate, 2019) of mostly herbaceous or woody ornamental trees, shrubs, vines, and herbs, which all are primarily native to tropical, subtropical, and north temperate regions (Anonymous, Britannica, 2017, Anonymous, SFGate, 2019).

Hydrangea shrubs are low-growing, densely branched plants that typically reach no more than 3 to 4.5 m tall. Vining hydrangeas climb or trail with the help of their tendrils to clasp onto nearby structures or objects (Anonymous, SFGate, 2019). Most plants are deciduous having large, simple, green leaves with toothed margins, which grow in an opposite arrangement along the stem (Anonymous, Britannica, 2017, Anonymous, SFGate, 2019). Some Mediterranean species are evergreen, and the typically serrated-edged leaves with net-like veins keep their color year-round and are retained in winter. However, in cooler

climates some Hydrangeaceae plants are deciduous and drop their leaves every fall (Anonymous, SFGate, 2019).

Flowers may grow as a single flower or as large clusters of branching inflorescences of star-shaped blooms (Anonymous, SFGate, 2019, Anonymous, Go Botany, 2021). The flowers are actinomorphic (radially symmetrical). Flowers have four or five sepals, fused at the base, and four or five individual petals. Some flowers are sterile, whereas fertile ones contain both pollen-bearing (antheridia, male reproductive organ) and ovule-bearing (ovary and pistils, female reproductive organ) parts. They have eight or more stamens and two to five styles (Anonymous, Britannica, 2017, Anonymous, SFGate, 2019). Colorful flowers with shades of blue, purple, pink, white or red can be seen among the Hydrangeaceae plants. Some bigleaf hydrangea species (*Hydrangea macrophylla*) change color depending on soil pH. Plants on soils with a pH higher than 5.5 typically produce pink flowers, whereas plants growing on acidic soils with a pH less than 5.5 produce blue flowers.

Hydrangeaceae flowers may be clustered in three general shapes: mopheads, lacecaps or panicles. Mophead hydrangea flowers are rounded and resemble pom-poms. Each cluster contains mainly infertile flowers that are unable to produce seeds and have large, showy sepals. Lacecap clusters are only slightly rounded and flat. These flower clusters contain several small, fertile flowers. Infertile flowers with large, showy sepals are typically found around the cluster's perimeter. Panicle hydrangea clusters are large conical or pyramidal shaped, with showy infertile blooms mixed with small fertile flowers (Anonymous, SFGate, 2019).

The fruit of hydrangea plants is typically shaped like a dry cup or capsule, but it may sometimes be berry-like, which when ripe, dehisces to release its many seeds. Seeds may be winged (Anonymous, Go Botany, 2021).

In the landscape, Hydrangeaceae plants may be grown as individual plants or be grouped together forming hedges. They grow best in a nutrient-rich, moist but well-drained soil. Plant hardiness varies depending on the species, but many of them can grow in U.S. Department of Agriculture plant hardiness zones 3 through 9. They prefer sun in the morning, but partial sun to full shade during the hot afternoon hours (Anonymous, SFGate, 2019).

The hydrangea family includes the well-known garden ornamentals that are shrubs in the genera *Deutzia*, *Hydrangea* (hydrangea), and *Philadelphus* (mockorange or sweet syringa). Other ornamental genera include *Cardiandra*, *Carpenteria*, *Decumaria, Dichroa*, *Jamesia, Kirengeshoma, Pileostegia*, *Platycrater*, *Schizophragma*, and *Whipplea* (Anonymous, The Plant List, 2013, Anonymous, Britannica, 2017).

1.1.1. Little-leaf Mockorange

Mockorange are woody shrubs (Anonymous, USDA, 2015) in the genus *Philadelphus*, includes about 65 species and cultivars, and all are flowering deciduous shrubs (Dirr and Heuser, 2006). Some of the more popular species are *P. argenteus* (Silver mockorange), *P. argyrocalyx* (Silver-cup mockorange), *P. coronarius* (sweet mockorange), *P. californicus* (California mockorange), *P. microphyllus* (little-leaf mockorange), *P. occidentalis* (Western mockorange) and *P. oreganus* (Oregon mockorange) (Anonymous, USDA, 2015).

Philadelphus microphyllus A. Gray (little-leaf mockorange) is a small to medium sized multi-stemmed, deciduous shrub with long arching stems covered with tiny, medium-green leaves with silvered aspect similar to boxwood leaves (Figure 1). Little-leaf mockorange produces flowers on previous year's wood for several weeks starting in late spring, so the plant needs to be pruned immediately after flowering (Anonymous, Gardenia, 2021). The shrub blooms with plenty of very fragrant flowers, which fill the air with their vanilla or orange-blossom like scent. Flowers, which are little-leaf mockorange most outstanding characteristic, have four white or yellowish petals and are almost 2.5 cm in diameter. Flowers may be born as single blooms or as pairs (Dirr and Heuser, 2006, Anonymous, Gardenia, 2021). The fruit is a four-valved dehiscent capsule full of seeds (Dirr and Heuser, 2006). Its height can reach to 1.5 to 2 m, while the width can be around 1 to 1.2 m. The bark appears tan to reddish-gray and peeling.

Figure 1. Flowers (left) and branches covered with tiny leaves (right) of little-leaf Mockorange (Wilson, 2012).

An important characteristic of this species is its excellent tolerance to drought, easy to grow and low maintenance requirements. It can also grow in a wide range of light conditions from light shade to full sun. The shrub usually grows in different chalk, sand, or loamy soils with a pH of 7 to 7.80, and in average, dry to medium, well-drained soils. In spring and winter, plants grow best in dryer soil around the crown rather than wet soil. (Anonymous, Missouri Botanical Garden, 2008, Anonymous, Gardenia, 2021). After

planting, it needs watering once a week for the first growing season, and then in subsequent years it should be watered every two weeks during the hottest summer weather (Wilson, 2012).

Generally, this species is insect and disease free, but it may need to be observed for leaf-spot, canker, powdery mildew and/or rust. Little-leaf mockorange is a great plant used for cut flowers, shrub beds and borders, foundation plantings, or informal flowering hedges as a screen. This species is a shrub native to United States found in California, Colorado, Utah, Nevada, Wyoming, Arizona, Texas, and New Mexico in areas, such as arid rocky slopes, cliffs, or pinyon-juniper to coniferous woods (Anonymous, Johnson Center, 2015, Anonymous, Gardenia, 2021). In general, mockorange species can be propagated by seed, summer soft-wood cuttings, hardwood cuttings and layering (Dirr and Heuser, 2006), but little-leaf mockorange is difficult to propagate through seeds or cuttings (Steve Love, University of Idaho, personal communication).

1.2. Tissue Culture

Plant tissue culture, also known as *in vitro* culture or micropropagation, is the science of growing isolated plant cells, organs, or tissues separated from a parent plant and placed on a culture medium. Tissue culture requires specific tools, a set of techniques, and sterile conditions as well as specific temperature and light conditions to be successful in the propagating plants. Plants are propagated and grown on a mineral medium in the presence of other substances, such as plant growth regulators, vitamins, and carbohydrates (Loyola-Vargas and Vázquez-Flota, 2006, George et al., 2007). Tissue culture is a fast and highly reliable asexual plant propagation method for research and is commercially applied in the greenhouse and nursery industries. Tissue culture can help researchers and growers

increase the number of selected plants in a short period of time. On the other hand, some other scientists (Street as cited by Smith, 2012) would prefer to use a broader term for plant tissue. Street mentioned as aseptic culture of any cell, tissue or organ and their components under specific physical and chemical conditions *in vitro* are considered as micropropagation techniques (cited by Smith, 2012).

The earliest steps toward plant tissue culture were first observed and introduced by Henri-Louis Duhumel du Monceau in 1756, when he was doing research on the wound-healing process in plants and after watching plants produce callus after wounding (Gautheret, 1985, Smith, 2012). Smith (2012) later mentioned that microscopic studies by other scientists (Schleiden, 1838; Schwann, 1839) led to the understanding of the cell, which stated that cell is the functional and structural unit of an organism that has potential autonomy. Studies of callus formation on the plant segments by Vöchting (1878) proved the theory (cited by Smith, 2012). Vöchting reported that the upper zones of stem segments can produce buds and lower parts produce either callus or roots regardless of stem size as long as they contain enough buds or leaf primordia to produce new parts. (Vöchting 1878 as cited by Smith, 2012). Many studies have been conducted by Skoog and his colleagues (Skoog and Tsui, 1948, Miller et al., 1955, Skoog and Miller, 1957), improved understanding tissue culture and its different aspects, such as the effects of adenine and phosphate on the production of shoots and roots by non-meristematic pith tissues in the presence of vascular tissue (Skoog and Tsui, 1948). Skoog and his colleagues also discovered the first cytokinin, (kinetin: Miller et al., 1955) and then learned the effects of kinetin strongly increasing cell division of tobacco callus tissue. Skoog and co-workers also recognized the importance of balancing the ratio between exogenous auxin and kinetin in the medium as these hormones

affected the morphogenesis of tobacco callus (Skoog and Miller, 1957, Trigiano and Gray, 2010, Smith, 2012). These studies and others led to the discovery that higher concentrations of auxin than kinetin leads to root formation, whereas the contrariwise ratio induces shoot formation, and the moderate levels of each in the medium produce callus (Smith, 2012).

One tissue culture technique, often referred to as micropropagation, involves inducing axillary shoot proliferation and growth under aseptic conditions on a culture medium in small jars or containers. The plant selected for micropropagation needs to undergo different stages during the tissue culture process beginning with surface sterilization of the stem, shoot establishment followed by shoot multiplication, and then rooting. Finally, rooted shoots must adapt to the natural environment. These steps are listed (Trigiano and Gray, 2010) as Stage 0: Stock plants care, Stage I: Establishment & stabilization, Stage II: Shoot multiplication/proliferation, Stage III: Rooting & transplant preparation, and Stage IV: Transplanting & acclimatization.

1.2.1. Tissue Culture Medium Components

Growth and development of an explant - the plant part put into culture- on a culture medium depends on its genetics, growth environment, and the components in the culture medium. The first two factors may be less easy than the third factor to manipulate to obtain optimum growth. The tissue culture medium is a combination of 95% water, macro- and micro-nutrients, plant growth regulators (PGRs), vitamins, sugar (to substitute for photosynthetic products), and other simple to complex organic materials. All together about 20 different components interacting together create the optimum growth medium for explants.

The main components in this research that I specifically have focused on are selected inorganic minerals and cytokinins, a type of plant growth regulator (Trigiano and Gray, 2010).

1.2.1.1. Inorganic Mineral Elements

Plants need 17 essential elements for optimum growth. Three of these elements can be obtained from air, water, and culture media, including oxygen (O_2), hydrogen (H_2), and carbon (C). Fourteen other essential elements (also called minerals or nutrients), that plants need to acquire to grow properly include nitrogen (N), phosphorous (P), potassium (K), calcium (Ca), magnesium (Mg), sulfur (S), as well as iron (Fe), manganese (Mn), boron (B), chlorine (Cl), copper (Cu), zinc (Zn), molybdenum (Mo), and nickel (Ni) (Mahler, 2004). Macronutrients are those elements required in millimolar (mM) quantities (the first six minerals after C, H, and O) (Trigiano and Gray, 2010). They play important roles as part of the plant structures or organelles. In contrast, micronutrients are required in lower quantities than macronutrients, and plants need these elements in micromolar (µM) amounts (the second eight minerals). Their roles are as catalysts of biochemical interactions and physiological systems (Table 1: Trigiano and Gray, 2010).

Among all these elements, I will review the importance and the role of the selected elements, used in my experiments.

a) Nitrogen (N): plants need a large amount of nitrogen to obtain optimum growth. Nitrogen is taken up in the form of nitrate (NO_3^-) or ammonium (NH_4^+) and is an important component of amino acids, amides, nucleic acids, proteins, enzymes, vitamins, coenzymes, and plant hormones. Nitrogen is also a component of the protoplast and gives vigor and dark green color to the plant foliage. Nitrogen is a mobile element, so if deficient in a plant,

it moves from the older leaves and tissues and is transported to younger leaves, causing yellowish green to yellow old leaves. If nitrogen deficiency continues, the whole plant can turn yellow.

Table 1. Function and mobility within plant tissue of the 14 soil-derived essential nutrients for plant growth.

Essential nutrient	Mobility in plant	Function of plant
Nitrogen	good	proteins, protoplasts, enzymes
Phosphorus	good	ATP, ADP, basal metabolism
Potassium	good	water relations, energy relations, cold hardiness
Sulfur	fair/good	proteins, protoplasts, enzymes
Calcium	very poor	cell structure, cell division, cell elongation
Magnesium	good	chlorophyll, enzymes
Boron	very poor	sugar translocation, cell development, growth regulators
Chlorine	good	photosynthesis
Copper	poor	enzyme activation
Iron	poor	chlorophyll synthesis, metabolism, enzyme activation
Manganese	poor	Hill reaction-photosystem II, enzyme activation
Molybdenum	poor	nitrogen fixation, nitrogen use
Nickel	unknown	iron metabolism
Zinc	poor	protein breakdown, enzyme activation

b) Phosphorus (P): this element is absorbed in the form of $H_2PO_4^-$, HPO_4^{2-}, or PO_4^{3-}, depending on soil pH. Phosphorus is necessary for producing ATP, ADP, and AMP and is necessary for basic metabolic processes, such as photosynthesis, carbohydrate catabolism, and transferring energy within the plants. Phosphorus is a mobile element, but its deficiency is difficult to diagnose visually. Its deficiency may result in stunted plants or sometimes purple-green older leaves.

c) Potassium (K): potassium can be taken up by plants in the form of K^+. It is a mobile mineral within a plant, and its deficiency is seen in older leaves' margins first. It has important roles in water and energy relationships. Potassium is also linked with plant cold hardiness and increases frost tolerance through decreasing cell sap osmosis. Potassium regulates the supply of CO_2 by controlling the stomata openings. Potassium is involved in cell division. Potassium concentration can be highest in young tissues. Also, K improves fruit color, growth, and flavor.

d) Calcium (Ca): calcium is another macronutrient, taken up as Ca^{2+} by plants roots, and is necessary for structural phenomena, such as cell division, cell elongation, and cell structure. Calcium also acts as a cofactor with some enzymes participating in ATP and phospholipids hydrolysis. It is also important for chromosome flexibility and helps cell division. Calcium concentration affects uptake of N, Fe, Zn, B, and Mn. Calcium is immobile, so its deficiency shows up in the younger growing leaves and tissues. Shoot tips may also dieback under severe Ca^{2+} deficiency.

e) Magnesium (Mg): another mobile macronutrient taken up in the form of Mg^{2+} by plants. When deficient, older plant leaves have interveinal chlorosis, which is seen as the dark green veins, and light green to yellowish green interveinal areas. Magnesium has important roles as the main component of the chlorophyll molecule and is required by some enzymes involved in P transfer. Magnesium is also necessary for formation of carbohydrates, fats, and vitamins, while enhancing P uptake and transport within plants.

f) Iron (Fe): one of the main micronutrients and an immobile element that can be taken up by plants roots in the form of Fe^{2+}. The need for Fe depends on the plant species. Iron is necessary for photosynthesis, metabolic process, as well as enzyme activation. Iron is a

very important component of cytochrome and non-heme iron proteins. Iron has a catalyst role in the formation of chlorophyll. Iron helps with various reactions, such as respiration, photosynthesis and reduction of nitrates and sulfates. Iron deficiency is seen as the interveinal chlorosis in younger leaves (Mahler, 2004, Anonymous, NCDACS, 2019).

Like any plants growing in soil in the natural environment, explants growing *in vitro*, need different minerals obtained from salts in the culture medium to grow well. The need for different minerals and their concentrations depends on the plant species, the plant organ or tissue explant used for the tissue culture, and the age of the explant.

Different basal salts are available in the market, among which the Murashige and Skoog (MS) medium is one commonly used for many plant species or for different *in vitro* goals (Murashige and Skoog, 1962). Commercial MS medium has different essential minerals at specific concentrations usually beneficial for most plant species. Among them are N at 60 mM, K at 30 mM, Ca at 3 mM, Mg at 1.5 mM, P at 1.25 mM, and Fe at 100 µM.

1.2.1.2. Plant Growth Regulators (PGRs)

Plant growth regulators, also known as phytohormones, play important roles in plant growth and development. As with *in vivo* plants, tissue cultures (*in vitro* cultures) are dependent on phytohormones for growth and development. The success of a tissue cultured explant and its growth can be highly dependent on the concentration of specific phytohormones as well as their ratio and combinations with the other phytohormones. Two main categories of phytohormones have been found in plants and are very important for tissue culture, including i) classical plant hormones (auxins, cytokinins, gibberellins, abscisic acid, and ethylene), and ii) more recently discovered natural growth substances (polyamines, oligosaccharins, salicylates, jasmonates, sterols, brassinosteroids, and

strigolactones) that have hormonal and regulatory roles in the plants (Trigiano and Gray, 2010).

Two types of PGRs among the classical group are very important and regularly used in plant tissue culture. These two types are auxins and cytokinins, each having specific roles to help explants grow better and more efficiently.

A) Auxins

This group of plant growth regulators is responsible for many actions within plants, among them are cell division, cell elongation, cell wall acidification, somatic embryogenesis, organizing meristematic tissues to form in unorganized tissues (callus) or organized tissues and defined organs (mostly roots), as well as promoting vascular differentiation and patterning. Auxins also play key roles in apical dominance in stems and buds, delay abscission, promote root formation and branching, mediate tropic (phototropic and gravitropic) responses, delay leaf senescence, and enhance fruit ripening (George et al., 2007, Trigiano and Gray, 2010, Anonymous, The Plant Cell, 2013b). Auxins are naturally occurring hormones in the plants, but auxins can also be produced synthetically. Well-known natural auxins are indole-3-acetic acid (IAA) (Figure 2) and indole-3-butyric acid (IBA). Common synthetic auxins include 1-naphetaleneacetic acid (NAA) and 2,4-dichlorophenoxyacetic acid (2,4-D). Auxins are found in high concentrations in young leaves, floral organs, developing fruits and seeds, and generally in fast-growing organs (George et al., 2007). Indole-3-acetic acid is the weakest auxin, so it is mostly used in concentrations of 0.01 to 10 µM in the tissue culture medium, whereas the more stable auxins such as IBA or NAA can be used in concentrations of 0.001 to 10 µM. In tissue culture, auxins promote initiation and enhancement of root formation by the explant or

callus. Auxin is transported basipetally in the plants, from the leaves and foliage where it is produced through stems to where it affects specific cells and enacts key physiological roles. Intensity of auxins' effects in culture depends on concentration as well as explant type, plant species, and plant growth stage.

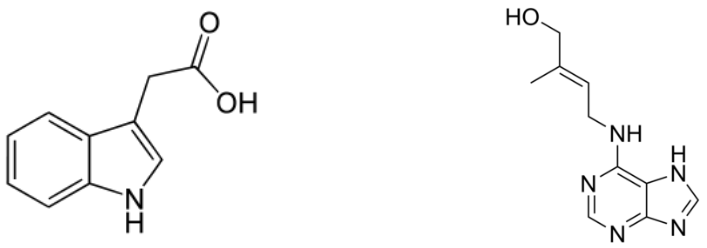

Figure 2. Molecular structure of the natural auxin IAA molecule (left) (Anonymous, Auxin, Wikipedia, 2021) and the cytokinin Zeatin (right) (Anonymous, Zeatin, Wikipedia, 2013).

B) Cytokinins

Cytokinins are included in another important group of phytohormones for managing plants in tissue culture. Cytokinins have many physiological roles including promoting cell division, shoot initiation, and shoot growth, (inducing axillary bud break), inducing adventitious shoot formation, delaying leaf senescence, regulating nutrient allocation, antagonizing auxin responses in plants, and helping induce environmental and pathogenic responses by plants. Cytokinins also inhibit root formation. Cytokinin action is light dependent. (George et al., 2007, Trigiano and Gray, 2010, Anonymous, The Plant Cell, 2013a,). Natural forms of cytokinins used in research laboratories are *trans*-zeatin (Zea) (Figure 2), and 6-(γ.γ-Dimethylallylamino) purine also named N^6-(2-Isopentenyl)adenine (2iP). Zeatin use in commercial labs is often limited due to its high cost. In contrast, synthetic forms of cytokinins are mass produced in larger amounts resulting in lower cost, including 6-benzylaminopurine (BA), kinetin (Kin), thidiazuron (TDZ), and *meta*-topolin

(MT). Effective concentrations of cytokinins in culture are different depending on the explant type, plant species, and growth stage, but are usually between 0.1 µM to 10 µM.

a) Zeatin (Zea): is a phytohormone and an adenine-derived cytokinin, which has adenine-purine bound into its molecular structure (Anonymous, Zeatin, Wikipedia, 2021). Zeatin exists in the form of a *cis*- and a *trans*-isomer and conjugates (Figure 2: right, Figure 3: top, left). Zeatin is the main natural form of cytokinin and was first discovered in immature seed kernels from the genus *Zea* (corn). Zeatin promotes the growth of lateral buds and if sprayed on meristems, can stimulate cell division, increase axillary bud breaks, and produce denser (more branched) plants (Mok and Mok, 1994). Zeatin and its derivative compounds are found in extracts from many different plant species (Anonymous, Zeatin, Wikipedia, 2021). These compounds are thought to be the active ingredient of coconut milk, which can enhance the cell growth, and is sometimes used in tissue culture medium as a complex natural ingredient (Robert Tripepi, University of Idaho, personal communication). Zeatin has important roles in plant culture protocols, such as inducing cell growth and promoting callus formation when combined with auxin.

b) Kinetin (Kin): (Figure 3: top, middle) promotes cell division. Kin was first extracted and discovered by Miller et al. (1955) from autoclaved herring sperm and detected as a result of cell-division enhancement. Kinetin is used in tissue culture medium to help induce callus-formation and to promote shoot regeneration (Anonymous, Kinetin, Wikipedia, 2021).

c) Benzyladenine (BA): 6-Benzylaminopurine (Figure 3: top, right), also known as benzyladenine (BAP or BA) and the first lab generated synthetic cytokinin, developed and evaluated by Skoog et al. (Skoog and Tsui, 1948, Anonymous, 6- Benzylamino purine,

Wikipedia, 2021). Benzyladenine stimulates cell division and influences plant growth and development, including blossom set and fruit development. Benzyladenine also inhibits respiratory kinase in plants, thus increasing postharvest life of green vegetables.

d) *Meta*-topolin (MT): *meta*-topolin [6-(3-hydroxybenzylamino)purine] is a newer class of cytokinin (Figure 3: bottom, left), first extracted from popular leaves (Werbrouck et al., 1996). In early experiments, poplar seedlings transplanted into soil, showed enhanced shoot growth after treatment with MT, as opposed to treatment with BA (Werbrouck et al., 1996). Application of MT to the culture medium, can reduce hyperhydricity in tissue cultured explants (Bairu et al., 2007).

e) Dimethylallylamino purine (2iP): 6-(γ.γ-Dimethylallylamino) purine also known as N6-(2-Isopentenyl) adenine (2iP) is a bacteria-derived riboside cytokinin (Figure 3: bottom, middle), which is used to grow plant tissues derived from callus. 2iP has been used in Schenk and Hildebrandt medium to support *in vitro* propagation of microshoot cultures from shoot tips of *Genista* plants (Anonymous, Sigma Aldrich, 2021).

f) Thidiazuron (TDZ): 1-phenyl-3- (1,2,3-thiadiazol-5-yl) urea, also known as TDZ (Figure 3: bottom, right) is a cytokinin-like PGR, which in crop production is mostly applied to and taken up by leaves. Thidiazuron was reported by Arndt et al. (1976) to be an effective cotton (*Gossypium hirsutum*) defoliant. Later TDZ became widely applied and was shown to have both auxin- and cytokinin-like effects (Guo et al., 2011, Chung and Ouyang, 2021). Thidiazuron uptake caused leaves to drop under controlled conditions prior to fruit harvest. This characteristic makes this cytokinin useful in mechanical harvest of processed fruits. A reduced tree canopy can also accelerate fruit maturation, with fewer leaves to block the sunlight. Under conditions of correct timing and dose, TDZ completely stops plant growth,

giving it herbicidal action. Thidiazuron was also reported to enhance shelf life of cut flowers when added to water (Anonymous, Wikipedia, 2020). Thidiazuron is often used as cytokinin-like hormone in tissue culture or defoliant in some countries, such as United States of America, Australia, and Mexico although agricultural use has been banned within the European Union (Anonymous, Wikipedia, 2020).

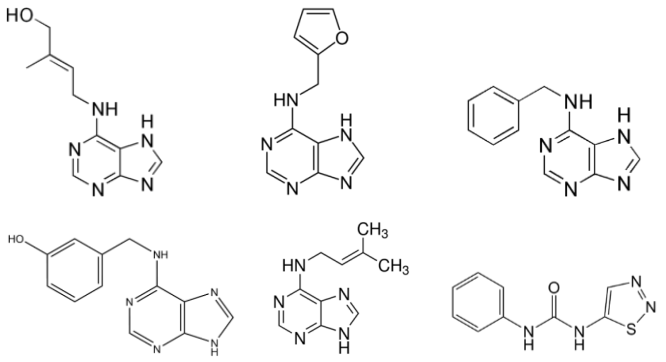

Figure 3. From top, left to right: Molecular structure of the cytokinins zeatin (Zea) (Anonymous, Zeatin, Wikipedia, 2021), kinetin (Kin) (Anonymous, Kinetin, Wikipedia, 2021), benzyladenine (BA) (Anonymous, 6-Benzylamino purine, Wikipedia, 2021); Bottom: meta-topolin (MT) (Anonymous, Phytotech Lab, 2013), dimethylallylamino purine (2iP) (Anonymous, Sigma Aldrich, 2021), thidiazuron (TDZ) (Anonymous, Wikipedia, 2020).

1.3. Hyperspectral Signatures

When light strikes a leaf, a portion of the light reflects towards the observer, and this amount of energy reflected at each wavelength is called reflectance spectrum, abbreviated as spectrum or reflectance. Many factors affect the spectrum reflectance, including the leaf surface, the internal surfaces, such as chloroplast surface and other organelles, leaf color or discoloration, physiological disorders, and water content. The chemical content, such as mineral components and their concentrations, biochemical components and their distribution inside the foliage, and other parameters also affect reflectance from the leaf and plant canopy, and their effects on reflectance can be useful to diagnose a plant's status (Martinez-Martinez et al., 2018).

Hyperspectral imaging involves capturing a large number of continuous spectral bands to determine specific reflectance characteristics of an object. Therefore, hyperspectral sensing provides a continuous and complete record of the spectral responses of a material over specific wavelengths (Robila, 2004). Hyperspectral sensing is the measurement of the spectral characteristics of materials by using remote sensing systems having more than 60 spectral bands with spectral resolutions of less than 10 nm. These bands produce a continual portion of the light spectrum defining the chemical composition of an object through its spectral signatures (Gomez, 2020). Remote sensing and hyperspectral imaging can analyze the characteristics that multispectral sensing cannot. Hyperspectral imaging can capture reflectance or fluorescence spectroscopy on every single spatial pixel of the spectral image through which the specific characteristics (e.g., plant water content) unable to be seen by human eyes can be recognized (Robila, 2004, Gomez, 2020).

The basic shape of the spectral curve is a characteristic of the parent material of the object examined by spectroscopy (Liang, 2004). In the visible (Vis) to near infrared (NIR) spectrum, water, soil, or plant canopy display characteristics that cause specific curvatures and peaks in the reflectance spectra and makes the material recognizable (Liang, 2004, Robila, 2004). The advantages of hyperspectral data compared to red-green-blue (RGB) imagery and multispectral data are that hyperspectral data can detect more accurate information of the object via more spectral bands (Figure 4). Hyperspectral acquisition devices provide information that is needed or used both for research and commercial purposes, including sensor types, acquisition modes and unmanned aerial vehicle (UAV)-compatible sensors (Adão et al., 2017). Hyperspectral sensing and unmanned aircraft systems (UAS) have been applied in many fields including material identification,

homeland security, precision agriculture (vegetative coverage, nutrition deficiencies, foliar water content, physiological disorders, etc.), environmental aspects (wetlands, hydrology, etc.), medical and health care (medical diagnoses, food safety, etc.), landmine detection, and many more applied fields (Gomez, 2020).

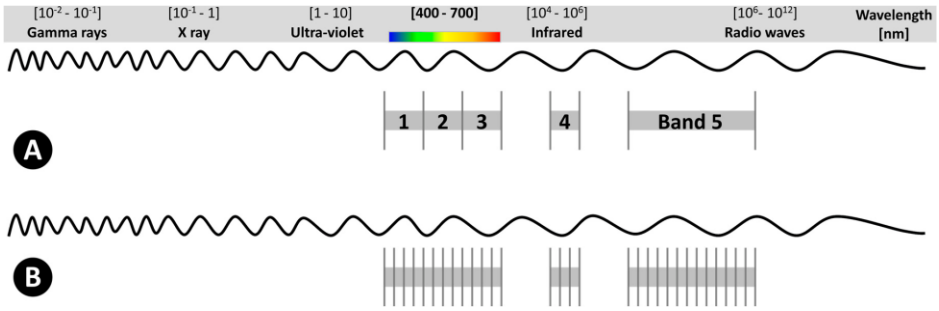

Figure 4. Spectra represent a) multispectral waves with 5 wide bands, and b) hyperspectral waves consisted of several narrow bands, sometimes even extended to hundreds and thousands of the narrow bands (Adão et al., 2017).

1.3.1. Vegetation Indices

Vegetative index (VI) describes an algorithm that processes spectral data for the purpose of determining information about plant health. Several VIs have been introduced and are used in remote sensing in agricultural fields. Some of these indices are defined in Table 2. Vegetation indices (VIs) can provide an estimation of biophysical, physiological, or even biochemical parameters in crops (Adão et al., 2017). Vegetation indices are classified into two groups of broader and narrower bands. Narrow bands are more applicable for hyperspectral data and processes (Adão et al., 2017). Some examples of the narrow-band indices are chlorophyll absorption ratio index (CARI), greenness index (GI), greenness vegetation index (GVI), modified chlorophyll absorption ratio index (MCARI), modified normalized difference vegetation index (MNDVI), simple ratio (SR) including narrowband variants 1–4, transformed chlorophyll absorption ratio index (TCARI), triangular

vegetation index (TVI), modified vegetation stress ratio (MVSR), modified soil-adjusted vegetation index (MSAVI) and Photochemical Reflectance Index (PRI).

Detectable indices and vegetation properties from remote sensing can be either a leaf biochemical or a canopy structural variable, including leaf chlorophyll content (LCC), leaf water content (LWC), leaf area index (LAI), fractional photosynthetically active radiation (FPAR) absorbed by canopy, surface roughness, and phenology, which are some of the most critical inputs to land surface process models (Liang, 2004, Morcillo-Pallarés et al., 2019).

The goal of improving these plant phenotyping technologies is to increase the ability to collect plant morphological and physiological traits in large scales, such as extensive fields or large forests, rapidly and non-destructively (Pandey et al., 2017). Accurate, objective, reliable, and timely crop yield predictions and estimations are necessary for farmers owning large areas of lands to make planning decisions for fertilization, irrigation, and chemical application. Yield predictions are very important for precision agriculture management to help farmers save time and obtain financial benefits (Liang, 2004).

Reflectance of the visible wavelengths (VIS, between 400 and 700 nm) is dependent on the photosynthetic pigments, such as chlorophyll. In contrast, reflectance from the near infrared wavelengths (NIR, between 700 and 1300 nm), lacks strong absorption features caused by twisted or contorted surface of the leaf. The shortwave infrared region (SWIR, between 1300 nm and 3000 nm) presents variable reflectance values mainly linked to the absorption characteristics of water and other compounds (Martinez-Martinez et al., 2018).

Hyperspectral data evaluation and management involves several steps including calibration of the hyperspectral device, taking spectral images or hyperspectral signatures (reflectance, spectrum), spectral/spatial processing, dimensionality reduction, and computation related operations, such as feature detection, selection, analysis, etc. (Adão et al., 2017).

Table 2. The most well-known vegetation indices determined by using hyperspectral imaging in agricultural research (Data obtained and calculated from Anonymous, Index Data Base, 2021).

Index Name	**Abbreviation**	**Formula**
Cellulose Absorption Index	CAI	$CAI= 0.5\ (\rho_{2000} + \rho_{2200}) - \rho_{2100}$
Chlorophyll Absorption Ratio Index	CARI	$CARI= (700nm/670nm)\ \sqrt{(a\cdot 670+670nm+b)^2}\ /(a2+1)^{0.5}$
Disease water stress index	DWSI	$DWSI= 802nm + 547nm/1657nm + 682nm$
Anthocyanin Reflectance Index	ARI	$ARI2= \rho_{800}\ [\frac{1}{\rho 550} - \frac{1}{\rho 700}]$
Normalized difference vegetation index	NDVI	NDVI = (Bnear_IR - Bred) / (Bnear_IR + Bred)
Leaf Area Index	LAI	LAI = leaf area / ground area
Double Peak Index	DPI	$DPI= 688nm+710nm / 697nm^2$
Normalized Difference Water Index	NDWI	NDWI = (Bnear_IR - Bmiddle_IR) / (Bnear_IR + Bmiddle_IR)
Normalized Difference Nitrogen Index	NDNI	$NDNI= \frac{\log(\frac{1}{\rho 1510}) - \log(\frac{1}{\rho 1680})}{\log(\frac{1}{\rho 1510}) + \log(\frac{1}{\rho 1680})}$
Normalized Difference Lignin Index	NDLI	$NDLI= \frac{\log(\frac{1}{\rho 1754}) - \log(\frac{1}{\rho 1600})}{\log(\frac{1}{\rho 1754}) + \log(\frac{1}{\rho 1600})}$
Red-Edge Stress Vegetation Index	RVSI	$RVSI= (718nm+748nm/2) - 733nm$

Agriculture has been using hyperspectral technology to address the needs for improved crop production. Hyperspectral images have been applied to diagnose pathogens and disease problems, physiological disorders caused by biotic or abiotic stresses, and last but not least to detect nutrient deficiencies or toxicities in plants tissues.

1.3.2. Pathogen and insect diagnosis

Hyperspectral signatures can be highly effective in detecting pathogen infections during very early stages (Maes and Steppe, 2019). Sadeghi et al. (2021) applied hyperspectral signatures to determine if leaf reflectance from different host plant species affected the preference level of the Hessian fly to choose its host. Beck (2019) applied the hyperspectral remote sensing and narrowband spectral vegetation indices to diagnose the pink root disease at the leaf and canopy level of onions in Parma, ID, USA. Hruška et al. (2018) applied the narrow bands spectral indices to detect anomalies in grape leaves as a method to take appropriate preventative action to stop the infection and guarantee crops yield and health. Martinez-Martinez et al. (2018) applied leaf canopy spectroscopy to estimate and detect the severity of angular leaf spot in beans. Tian et al. (2021) applied hyperspectral remote sensing to detect leaf blast infection of rice from asymptomatic stages through the mild stage.

1.3.3. Plant stress detection

Hyperspectral techniques have been used to detect the effects of environmental stresses, such as drought. Many studies have applied hyperspectral indices to study the effects of field water status and water blockage due to *Verticillium* affecting stomatal conductance of olive trees (Calderón et al., 2013), water stress effects on water content of citrus trees (Delaliuex et al., 2014), water stress effects on the stomatal conductance and leaf water potential of citrus trees (Zarco-Tejada et al., 2012), and plant status and biomass of wheat (Golzarian et al., 2011).

1.3.4. Nutrient status and deficiency prediction

Due to the importance of nitrogen increasing yield efficiency and crop health, modern application of remote sensing and hyperspectral signatures in preventing nitrogen deficiencies in field crops has become widespread. Hence, much research has been conducted to determine using remote sensing and applying hyperspectral signatures to define nitrogen deficiency of field crops (Liu et al., 2016, De Oliveira et al., 2017). Using hyperspectral imaging to study required rates of fertilizers to increase crop production or the amount of nitrogen uptake by plants can improve agricultural production and yield efficiency (Maes and Steppe, 2019) (Figure 5).

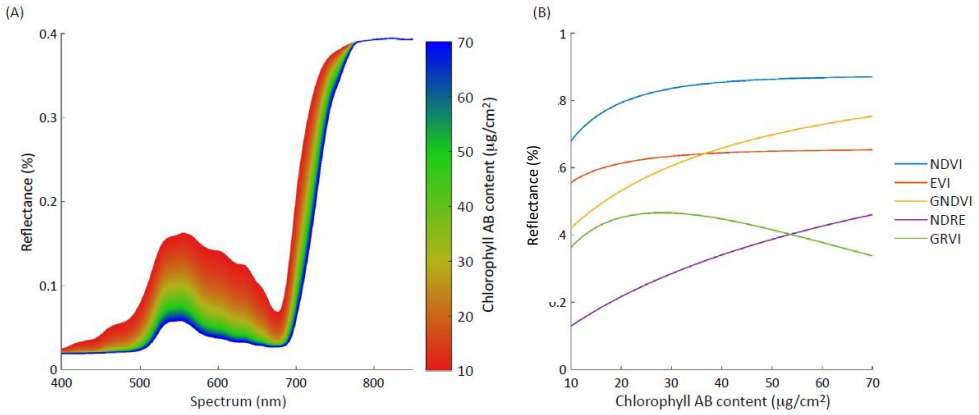

Figure 5. Assessment of Nutrient Status. (A) Reflectance pattern of a typical crop as a function of the chlorophyll AB content; (B) plotting different vegetation indices as a function of chlorophyll AB (C_{ab}) content illustrates that some classical vegetation indices [normalized difference vegetation index (NDVI) and enhanced vegetation index (EVI)] saturate and are less sensitive to subtle differences in chlorophyll AB (C_{ab}) levels when C_{ab} is relatively high, in contrast to green NDVI (GNDVI) and normalized difference red edge (NDRE) index. Created from simulations using Fluspect-B model in SCOPE v1.70. Constant parameters were as follows: canopy height = 0.7 m, leaf area index (LAI) of 2.5 m^2 m^{-2}, N = 2.5; C_{dm} = 0.01; C_w = 0.05; C_s = 0; spherical leaf distribution assumed. EVI = 2.5 (NIR _ R)/(NIR + 6R _ 7.5B + 1); GNDVI = (NIR _ G)/(NIR + G); GRVI = (G _ R)/(G + R); NDRE = (NIR _ RE)/(NIR + RE). NIR, near-infrared spectrum; RE, red edge reflectance (Maes and Steppe, 2019).

De Oliveira et al. (2017) applied vegetation indices to estimate foliar N concentration in three Eucalyptus tree clones. Liu et al. (2016) applied multiple linear regression and neural

network analysis to find a relationship between the leaf nitrogen content of winter wheat and vegetative indices in narrow bands of the spectrum (Figure 6).

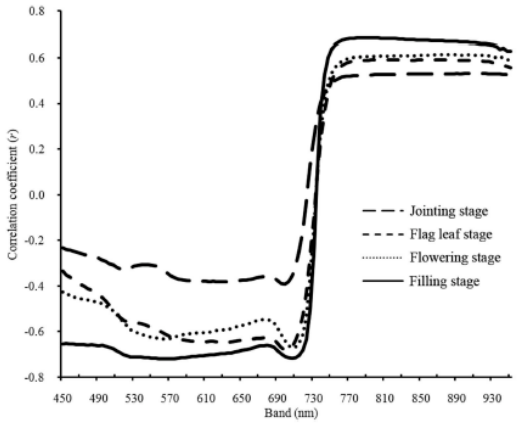

Figure 6. Correlation coefficients (r) between the spectral bands and the measured leaf nitrogen content (Liu et al., 2016).

Other studies have used hyperspectral indices to check the nutrition status in plants, including sodium and potassium content in grass (Capolupo et al., 2015), potassium deficiency level in canola (Severtson et al., 2016), nitrogen concentration in oat (Van Der Meij et al., 2017), corn (Gabriel et al., 2017), rice (Wen et al., 2018), and wheat (Zhu et al., 2018), and different macro- and micro-nutrients as well as water content in corn (Pandey et al., 2017).

1.3.5. Hyperspectral related terms

- Reflectance: is the ratio of the amount of light leaving a target to the amount of light striking the target.
- Hyperspectral Vegetation Indices: vegetative index (VI) describes an algorithm that processes spectral data for the purpose of determining information about plant health. Several VIs have been used in remote sensing in agricultural fields. Some of these indices are presented in Table 2.

- Continuum Removal: for quantification of absorption features in spectra, the overall concave shape of a spectrum should be removed. To normalize reflectance spectra and compare individual absorption features from a common baseline, one uses continuum removal (Harris Geospatial Solutions, Inc., 2021). This normalization procedure is referred to as ‘continuum removal’ or ’convex-hull’ transformation and allows comparison of spectra that are acquired by different instruments or under different light conditions. Continuum removal or convex hull fit over the top of a spectrum using straight-line segments which connect local spectra maxima. The first and last bands in the output continuum-removed spectrum file are equal to 1.0.

Continuum Removal is completed by dividing it into the actual spectrum for each pixel in the image:

$S_{cr} = (S / C)$, Where:

S_{cr} = Continuum-removed spectra

S = Original spectrum

C = Continuum curve

Continuum removal provides features that can help obtaining information necessary to detect plant status from the hyperspectral images. These features are shown in Figure 7.

D= The absorption depth (the lowest point in the continuum region)

$$\text{Area} = \text{Area}_{\text{left}} + \text{Area}_{\text{right}}$$

$$\text{Asymmetry} = \frac{\text{Area left}}{\text{Area right}}$$

- Feature generation: In regression problems, obtaining successful regressions is dependent on the number of features (such as absorption depth, area of absorption curvature, etc.) assigned within the feature space, which becomes even more critical when

hyperspectral data sets are used. As a result of the large number of spectral bands in hyperspectral datasets, researchers try to determine which features, either spectral bands or spectral vegetation indices generated from spectral bands, are more associated with foliar mineral or physiological status. To answer this question and define plant status, the use of feature selection approaches has been suggested to develop the regression model with less but the most informative features.

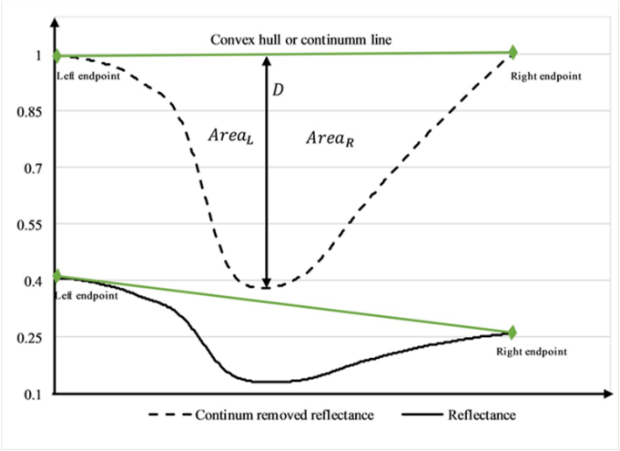

Figure 7. Features taken from continuum removal (right: absorption area left and right, left: absorption depth).

- Feature selection method: the main goal of applying feature selection is to ignore features with negative or low impacts on model development and to select those informative features with positive effects on model development. Effective and informative variables must be included in the model being developed. Importing many features may increase complexity in developing the model, and in some cases, cause unacceptable results in the developed regression model. Hence, the potential of the model to predict the plant status may become lost due to too many low impact features included in the model. In the feature selection process, in addition to removing features, we can also apply statistical criteria to identify informative features for the model. The lower the

number of the features, the more acceptable the model can be considered for computation and development. Therefore, using dimension reduction has the advantages of removing extra features, identifying informative features, and reducing computational complexity.

- Model training (development): to train (in machine learning model development is called model training) a model, different regression methods can be tested. Some of these methods includes:

- Linear Regression: is a linear model, that assumes a linear relationship between the input variables (x) and the single output variable (y).
- Random Forest Regression: RFR is a learning algorithm that uses ensemble learning method for regression.
- Support-Vector Machines: SVM are learning models with associated learning algorithms that analyze data for classification and regression analysis.

1.4. Statistical Analysis and Statistical Modeling

For a plant scientist, the goal of any scientific experiment is to introduce a better or the best method or treatment to improve some aspect of plant growth. To choose among the experimental treatments, one needs to conduct an experiment, collect data from the trials, and analyze the data collected via statistics (Aydar, 2018). Depending on the experiment, number of the treatments and their combinations, the goal of the experiment, and other desired factors, different experimental designs and methods of data analysis can be used. One statistical analysis method used to reduce the number of treatments in a large factorial experiment is the response surface method. Response surface methodology (RSM) is a set of tools or statistical procedures that first was mentioned in the journal of “the Royal Statistical Society, series B” from a work done by Box and Wilson (1951). They started to

develop a statistical model to determine efficient and optimum treatments or application conditions on a set of controllable variables that provides the optimum response in chemical and/or biological experiments (Khuri, 2006). This methodology is an approach that combines both mathematical and statistical tools and techniques and helps developing, improving, and optimizing the experiment procedures. Response surface methodology helps to evaluate the relative significance of the variables and helps to reduce the number of less influential variables (Naghipour et al., 2016). Response surface methodology in statistics examines the relationship between different explanatory variables and those response variables of interest to researchers (Anonymous, Wikipedia, 2020).

The experimental design to fit and develop a response surface model includes choosing treatments among several selected designs. Many criteria, such as environmental or nutritional conditions for plants must be considered to select the suitable design to accomplish the goal of an experiment and obtain the most favorable results. Some of these special designs are known as robust parameter designs, split-plot designs, mixture experiment designs, and designs for generalized linear models (Anderson-Cook et al., 2009). The final goal of RSM is to use a sequence of designed experiments to get an optimal response from one experiment (Anonymous, Wikipedia, 2020).

The best way to obtain an appropriate estimation of a first-degree polynomial model is using either a factorial design experiment or a fractional factorial design experiment. Using either of these designs helps to determine which of the explanatory variables affect the response variable(s) of interest. Later more complicated designs like central composite design can be used to estimate the second-degree polynomial model to optimize (maximize, minimize) the target response variable(s) (Anonymous, Wikipedia, 2020). For

RSM, experiments need to focus on statistical designs suitable for fitting quadratic models. These designs can provide the lack of fit detection to help determine if a higher-order model is needed (NIST, 2012).

1.5. Research objectives for my dissertation:

Experimentation reported in my dissertation research was directed by two major objectives.

1. Optimize concentrations and ratios of selected minerals and plant growth regulators as components within a specific culture medium to produce optimal growth of little-leaf mockorange shoot cultures.

2. Determine the feasibility of using of hyperspectral signatures to measure the nutrient status of plants in tissue culture and to model the spectrum to allow prediction of optimal foliar mineral contents of shoot explants.

References

Adão, T., Hruška, J., Pádua, L., Bessa, J., Peres, E., Morais, R., Sousa, J. J., 2017. Hyperspectral imaging: A review on UAV-based sensors, data processing and applications for agriculture and forestry. *Remote Sensing*, 9, 1110; doi:10.3390/rs9111110.

Anderson-Cook, C.M., Borror, C.M., Montgomery, D.C., 2009. Response surface design evaluation and comparison. *Journal of Statistical Planning and Inference*, Vol. 139, 629-641, ISSN 0378-3758, Available on: https://doi.org/10.1016/j.jspi.2008.04.004.

Anonymous, 2008. *Philadelphus microphyllus* 'June Bride' - Plant Finder. Missouri Botanical Garden. Accessed in October 2019. Available on: www.missouribotanicalgarden.org/PlantFinder/PlantFinderDetails.aspx?taxonid=268016&isprofile=1&gen=Philadelphus.

Anonymous, 2013. Cytokinins. The Plant Cell a, Vol 22, June 2010, tpc.110.tt0610, https://doi.org/10.1105/tpc.110.tt0610. *Amer. Soc. Plant Biol.*, Available on: www.plantcell.org/cgi/doi/10.1105/tpc.110.tt0610.

Anonymous, 2013. Meta-topolin. PhytoTech Labs. Accessed in March 2019. Available on: https://phytotechlab.com/meta-topolin.html.

Anonymous, 2013. The plant list. Version 1.1. Accessed in January 2019. Available on: www.theplantlist.org/.

Anonymous, 2013. The story of auxin. The Plant Cell b, Vol. 22, April 2010, tpc.110.tt0410, https://doi.org/10.1105/tpc.110.tt0410. *Amer. Soc. Plant Biol.*, Available on: www.plantcell.org/cgi/doi/10.1105/tpc.110.tt0410.

Anonymous, 2013. Zeatin. Wikipedia. Accessed in March 2020. Available on: https://en.wikipedia.org/wiki/Zeatin.

Anonymous, 2015, Plant Database: *Philadelphus microphyllus*. Lady Bird Wildflower Johnson Center, The University of Texas at Austin. Accessed in October 2019. Available on: www.wildflower.org/plants/result.php?id_plant=phmi4.

Anonymous, 2015. Plants profile for *Philadelphus microphyllus* (little-leaf mockorange). USDA. Accessed in January 2019. Available on: www.plants.usda.gov/core/profile?symbol=phmi4.

Anonymous, 2017. The Editors of Encyclopaedia. "Hydrangeaceae". Encyclopedia Britannica, Accessed in August 2021. Available on: www.britannica.com/plant/Hydrangeaceae.

Anonymous, 2019. Home guides: Characteristics of the Hydrangeaceae Plant Family. SFGate. Accessed in October 2019. Available on: www. homeguides.sfgate.com/characteristics-hydrangeaceae-plant-family-68624.html.

Anonymous, 2019. Hydrangeaceae. Wikipedia. Accessed in October 2019. Available on: https://en.wikipedia.org/wiki/Hydrangeaceae.

Anonymous, 2019. Plant nutrients. North Carolina Department of Agriculture & Consumer Services (NCDACS). Accessed in October 2019. Available on: www.ncagr.gov/CYBER/kidswrld/plant/nutrient.htm.

Anonymous, 2020. Thidiazuron. Wikipedia. Accessed in October 2021. Available on: https://en.wikipedia.org/wiki/Thidiazuron.

Anonymous, 2020. Response surface methodology. Wikipedia. Available on: https://en.wikipedia.org/w/index.php?title=Response_surface_methodology&oldid=934975962.

Anonymous, 2021. 6-(γ.γ-Dimethylallylamino)purine. D7660, Sigma-Aldrich. Accessed in October 2021. Available on: https://www.sigmaaldrich.com/US/en/product/SIGMA/D7660.

Anonymous, 2021. 6-Benzylaminopurine. Wikipedia. Accessed in October 2021. Available on: https://en.wikipedia.org/wiki/6-Benzylaminopurine.

Anonymous, 2021. Auxin. Wikipedia. Accessed in March 2020. Available on: https://en.wikipedia.org/wiki/Auxin.

Anonymous, 2021. Family: Hydrangeaceae, Native Plant Trust: *Go Botany* (3.6). Accessed in October 2019. Available on: www. gobotany.nativeplanttrust.org/family/hydrangeaceae/.

Anonymous, 2021. Index Data Base. Accessed in October 2021. Available on: https://www.indexdatabase.de/.

Anonymous, 2021. Kinetin. Wikipedia. Accessed in: October 2021. Available on: https://en.wikipedia.org/wiki/Kinetin.

Anonymous, 2021. Meta-Topolin. Phytotech Lab. Accessed in October 2021. Available on: https://phytotechlab.com/meta-topolin.html.

Anonymous, 2021. *Philadelphus microphyllus* (little-leaf mockorange). *Gardenia: Create Gardens*. Accessed in October 2021. Available on: www.gardenia.net/plant/philadelphus-microphyllus.

Anonymous, 2021. Zeatin. Wikipedia. Accessed in: October 2021. Available on: https://en.wikipedia.org/wiki/Zeatin.

Arndt, F.R., Rusch, R., Stillfried, H.V., Hanisch, B., Martin, W.C., 1976. A new cotton defoliant. *Plant Physiol.*, 57, S99.

Aydar, A.Y., 2018. Utilization of response surface methodology in optimization of extraction of plant materials, statistical approaches with emphasis on design of experiments applied to chemical processes, *Valter Silva, IntechOpen*, 157-169. InTechOpenScience. DOI: 10.5772/intechopen.73690. Available on: www.intechopen.com/books/statistical-approaches-with-emphasis-on-design-of-experiments-applied-to-chemical-processes/utilization-of-response-surface-methodology-in-optimization-of-extraction-of-plant-materials.

Bairu, M.W., Stirk, W.A., Dolezal, K., Van Staden, J., 2007. Optimizing the micropropagation protocol for the endangered *Aloe polyphylla*: can *meta*-topolin

and its derivatives serve as replacement for benzyladenine and zeatin? *Plant, Cell, Tissue, Org. Cult. (PCTOC)*. 90, 15–23. DOI 10.1007/s11240-007-9233-4.

Beck K. D., 2019. Evaluating the use of hyperspectral remote sensing and narrowband spectral vegetation indices to diagnose onion pink root at the leaf and canopy level. M.Sc. Thesis. *University of Idaho*.

Box, G.E.P., Wilson, K.B., 1951. On the experimental attainment of optimum conditions (with discussion). *J. Royal Stat. Soc. Series*. B13. 1–45.

Calderón, R., Navas-Cortés, J., Lucena, C., Zarco-Tejada, P. 2013. High-resolution airborne hyperspectral and thermal imagery for early detection of *Verticillium* wilt of olive using fluorescence, temperature, and narrow-band spectral indices. *Remote Sensing Environment*, 139, 231–245.

Capolupo, A., Kooistra, L., Berendonk, C., Boccia, L., Suomalainen, J. 2015, Estimating plant traits of grasslands from UAV-acquired hyperspectral images: A comparison of statistical approaches. *ISPRS Int. J. Geo-Inf.* Vol. 4, 2792–2820.

Chung, H. H., Ouyang, H.-Y, 2021. Use of thidiazuron for high-frequency callus induction and organogenesis of wild strawberry (*Fragaria vesca*). *Plants*, 10, 67. https://doi.org/10.3390/plants10010067.

Delalieux, S., Zarco-Tejada, P.J., Tits, L., Bello, M.Á.J., Intrigliolo, D.S., Somers, B., 2014. Unmixing-based fusion of hyperspatial and hyperspectral airborne imagery for early detection of vegetation stress. *IEEE J. Sel. Top. Appl. Earth Obs. Remote Sens.*, Vol. 7, 2571- 2582.

De Oliveira, L.F.R., De Oliveira, M.L.R., Gomes, F.S., Santana, R.C., 2017. Estimating foliar nitrogen in *Eucalyptus* using vegetation indexes. *Scientia Agricola*, Vol. 74, 142-147. http://dx.doi.org/10.1590/1678-992X-2015-0477.

Dirr, M.A., Heuser, C.W., 2006. The reference manual of woody plant propagation, from seed to tissue culture, 2nd Ed., 410 pp, *Varsity Press, Inc*.

Gabriel, J.L., Zarco-Tejada, P.J., López-Herrera, P.J., Pérez-Martín, E., Alonso-Ayuso, M., Quemada, M., 2017. Airborne and ground level sensors for monitoring nitrogen status in a maize crop. *Biosyst. Eng.*, Vol. 160, 124–133.

Gautheret, R.J., 1985. History of plant tissue and cell culture: A personal account, in cell culture and somatic cell genetics of plants (Vasil, I. K., ed.), Vol. 2, *Academic Press*, New York, pp. 1–59.

George, E.F., Hall. M.A., De Klerk, G., 2007. Plant Propagation by tissue culture: Volume 1. The Background, *Springer*, ISBN 978-1-4020-5005-3 (e-book).

Golzarian M.R., Frick, R.A., Rajendran, K., Berger, B., Roy, S., Tester, M., 2011. Accurate inference of shoot biomass from high-throughput images of cereal plants. *Plant Methods*, 2011 7:2. DOI:10.1186/1746-4811-7-2.

Gomez R., 2020. Professional short course on: Hyperspectral and multispectral imaging. *Applied Technology Institute*. Available on: https://aticourses.com/.

Guo, B., Abbasi, B.H., Zeb, A., Xu, L.L., Wei, Y.H., 2011. Thidiazuron: A multi-dimensional plant growth regulator. *Afr. J. Biotech*. 10, 8984–9000.

Harris Geospatial Solutions, Inc., 2021. Accessed in October 2021. Available on: https://www.l3harrisgeospatial.com/.

Hruška, J., Adão, T., Padua, L., Peres, E., Sousa, J. J., 2018. Evaluation of narrow-band vegetation indices for anomaly detection in grapevine leaves. IX National conference on cartography and geodesy. *Portugal Publication Identifiers*. 1-7.

Khuri, A.I., 2006. Response surface methodology and related topics, *World Scientific Publishing Co*. 472 pp. Available on: https://doi.org/10.1142/5915.

Liang, S., 2004. Quantitative remote sensing of land surfaces, *Wiley*, New York. Print ISBN: 9780471281665. DOI: 10.1002/047172372X.

Liu, H., Zhu, H., Wang, P., 2016. Quantitative modelling for leaf nitrogen content of winter wheat using UAV-based hyperspectral data, *Intl. J. Remote Sens.*, Vol. 38, 2117–2134. DOI: 10.1080/01431161.2016.1253899.

Loyola-Vargas V.M., Vázquez-Flota F., 2006. An introduction to plant cell culture. In: Loyola-Vargas V.M., Vázquez-Flota F. (eds) Plant cell culture protocols. *Methods in Molecular Biology*™, Vol. 318. Humana Press. https://doi.org/10.1385/1-59259-959-1:003.

Maes, W.H., Steppe, K., 2019. Perspectives for remote sensing with unmanned aerial vehicles in precision agriculture. *Trends in Plant Science*, Vol. 24. https://doi.org/10.1016/j.tplants.2018.11.007.

Mahler, R. L., 2004. Nutrients plants require for growth. *University of Idaho*. CIS 1124.

Martinez-Martinez, J.V., Gomez-Gil1, M.L. Machado, F. Pinto, A.C., 2018. Leaf and canopy reflectance spectrometry applied to the estimation of angular leaf spot disease severity of common bean crops. *Public Library of Science (PLoS ONE)*. Vol. 13 e0196072. Available on: https://doi.org/10.1371/journal.pone.0196072.

Miller, C.O., Skoog, F., Von Saltza, M.H., Strong F.M., 1955. Kinetin, a cell division factor from deoxyribonucleic acid. *J. Amer. Chem. Soc.*, Vol. 77, 1392. DOI: 10.1021/ja01610a105.

Mok, D.W.S., Mok, M.C., 1994. Cytokinins: chemistry, activity, and function. *CRC Press*. ISBN 0-8493-6252-0.

Morcillo-Pallarés, P., Rivera-Caicedo, J. P., Belda, S., De Grave, C., Burriel, H., Moreno, J., Verrelst, J., 2019. Quantifying the robustness of vegetation indices through global sensitivity analysis of homogeneous and forest leaf-canopy radiative transfer models. *Remote Sens*., 11, 2418. 1-23. DOI:10.3390/rs11202418.

Murashige, T., Skoog, F., 1962. A revised medium for rapid growth and bioassays with tobacco tissue cultures. *Physiol. Plant.*, Vol. 15, 473-497. Available on: https://doi.org/10.1111/j.1399-3054.1962.tb08052.x.

Naghipour, D., Taghavi, K., Jaafari, J., Mahdavi, Y., Ghanbari Ghozikali, M., Ameri, R., Jamshidi, A., Mahvi, A.H., 2016. Statistical modeling and optimization of the phosphorus biosorption by modified *Lemna minor* from aqueous solution using response surface methodology (RSM), *Desalination Water Treat. (DESALIN)*, 57, 19431-19442. DOI: 10.1080/19443994.2015.1100555.

NIST/SEMATECH, 2012. e-Handbook of statistical methods, http://www.itl.nist.gov/div898/handbook/, Accessed in October 2021. Available on: https://doi.org/10.18434/M32189.

Pandey, P., Ge1, Y., Stoerger, V., Schnable, J.C., 2017. High throughput *in vivo* analysis of plant leaf chemical properties using hyperspectral imaging. *Front. Plant Sci.*, 8:1348. DOI: 10.3389/fpls.2017.01348.

Robila, S. A., 2004. An analysis of spectral metrics for hyperspectral image processing, 2004 IEEE International Geoscience and Remote Sensing Symposium, Anchorage, AK, USA, 20–24 September 2004. *IEEE*, 5, 3233-3236.

Sadeghi, R., Odubiyi, S., Nikoukar, A., L. Schroeder, K., Rashed, A., 2021. *Mayetiola destructor* (Diptera: Cecidmyiidae) host preference and survival on small grains with respect to leaf reflectance and phytohormone concentrations. *Sci. Rep.*, 11:4761. https://doi.org/10.1038/s41598-021-84212-x.

Schleiden, M.J., 1838. On the development of the organization in phaenogamous plants. London: *R. & J.E. Taylor*. 42 pp.

Schwann, T., 1839, Microscopical researches into the accordance of the structure and growth of animals and plants. *Sydenham Society*. 268 pp.

Severtson, D., Callow, N., Flower, K., Neuhaus, A., Olejnik, M., Nansen, C., 2016. Unmanned aerial vehicle canopy reflectance data detects potassium deficiency and green peach aphid susceptibility in canola. *Precis. Agric.*, Vol. 17, 659–677.

Skoog, F., Miller, C.O., 1957. Chemical regulation of growth and organ formation in plant tissue cultured *in vitro*. *Sym. Soc. Exp. Biol.*, Vol. 11, 118-131.

Skoog, F.K., Tsui, C., 1948. Chemical control of growth and bud formation in tobacco stem segments and callus cultured in vitro. *Amer. J. Botany*, Vol. 35, 782-787. DOI:10.1002/J.1537-2197.1948.TB08148.X.

Smith, R. H., 2012. Plant tissue culture: techniques and experiments. Netherlands: *Elsevier sci.,* 208 pp. ISBN 9780124159853, 0124159850.

Tian, L., Xue, B., Wang, Z., Li, D., Yao, X., Cao, Q., Zhu, Y., Cao, W., Cheng, T., 2021. Spectroscopic detection of rice leaf blast infection from asymptomatic to mild stages with integrated machine learning and feature selection. *Remote Sen. Env.*, 257- 112350. https://doi.org/10.1016/j.rse.2021.112350.

Trigiano, R.N., Gray, D.J., 2010. Plant tissue culture, development, and biotechnology, 1st Ed. CRC Press: *Taylor & Francis Group*. 583 pp. ISBN 978-1-4200-8326-2.

Van Der Meij, B., Kooistra, L., Suomalainen, J., Barel, J.M., De Deyn, G.B., 2017. Remote sensing of plant trait responses to field-based plant–soil feedback using UAV-based optical sensors. *Biogeosci*., Vol. 14, 733–749.

Vöchting, H. 1878. About organ formation in the plant kingdom. Max Cohen: Bonn, Germany.

Wen, D., Tongyu, X., Fenghua, Y., Chunling, C., 2018. Measurement of nitrogen content in rice by inversion of hyperspectral reflectance data from an unmanned aerial

vehicle. *Ciência Rural*, Santa Maria, Vol. 48. Available on: https://doi.org/10.1590/0103-8478cr20180008.

Werbrouck, S.P. O., Strnad, M., Van Onckelen, H.A., Debergh, P.C., 1996. Meta-topolin, an alternative to benzyladenine in tissue culture? *Physiol. Plant*., 98, 291-297. https://doi.org/10.1034/j.1399-3054.1996.980210.x.

Wilson, B., 2012. *Philadelphus microphyllus*: Little-leaf mockorange and desert mockorange. Las Pilitas Nursery. Accessed in October 2019. Available on: www.laspilitas.com/nature-of-california/plants/3366--philadelphus-microphyllus.

Zarco-Tejada, P., Gonzalez-Dugo, V., Berni, J., 2012. Fluorescence, temperature and narrow-band indices acquired from a UAV platform for water stress detection using a micro-hyperspectral imager and a thermal camera. *Remote Sens. Env.*, 117, 322–337.

Zhu, H., Liu, H., Xu, Y., Guijun, Y., 2018. UAV-based hyperspectral analysis and spectral indices constructing for quantitatively monitoring leaf nitrogen content of winter wheat. *Appl. Opt.*, Vol. 57, 7722–7732.

Chapter 2: Optimization of tissue culture medium for little-leaf mockorange (*Philadelphus microphyllus* A. Gray) by adjusting cytokinin and selected mineral components

Abstract

Little-leaf mockorange is a native plant species with desirable characteristics for landscape use. Conservation of phenotype and recalcitrant responses to seed and ex vitro vegetative propagation techniques makes micropropagation a good option for this species. A series of experiments were completed individually with the goal to improve *in vitro* propagation protocols by evaluating different types of cytokinins (benzylaminopurine (BA), kinetin (Kin), zeatin (Zea), *meta*-topolin (MT), and thidiazuron (TDZ)) at 0, 1.1, 2.2, 4.4, or 8.8 µM and selected minerals (N, Fe, Ca, Mg, P) as supplements in tissue culture medium. The base medium was ½ strength MS. At the end of each experiment, plant growth characteristics including number of axillary shoots, shoot height, and dry weight were measured. Of the six cytokinins tested, zeatin produced the largest increase in shoot growth. Supplementation of zeatin 1.1 µM resulted in higher shoot numbers, while shoots on 1.65 µM Zeatin produced the most dry weight. Shoots grown on medium with mineral concentrations of 60 mM N, 50 to 100 µM Fe, 3 mM Ca, 1.5 mM Mg, and 0.625 to 1.875 mM (preferably 1.25 mM) P promoted *in vitro* shoot growth of little-leaf mockorange.

2.1. Introduction

Native plants have traits that improve both sustainability and adaptability of urban landscapes when produced in geographical regions representative of their natural habitat. (Khajehyar and Tripepi, 2020). Little-leaf mockorange (*Philadelphus microphyllus* A. Gray) is a species from the Hydrangeaceae family (Anonymous, Wikipedia, 2019). This species is a shrub native to the western United States and found in California, Colorado, Utah, Nevada, Wyoming, Arizona, Texas, and New Mexico and grows in arid rocky slopes, cliffs, or pinyon-juniper to coniferous woods (Anonymous, Johnson Center, 2015, Anonymous, Gardenia, 2021). Species within the mockorange genus have historically been propagated by seeds, summer soft-wood cuttings, hardwood cuttings and layering (Dirr and Heuser, 2006), but little-leaf mockorange can be difficult to propagate as *ex vitro* cuttings and fails to breed true from seed (Steve Love, University of Idaho, personal communication), meaning a more efficacious systems, such as micropropagation, would be advantageous.

Plant tissue culture, also known as *in vitro* culture or micropropagation, is the science of growing cells, organs, or tissues on a culture medium within a container after being isolated or separated from a parent plant. Plants are propagated and grown on a mineral medium in the presence of other substances, such as plant growth regulators (PGRs), vitamins, and carbohydrates (Loyola-Vargas and Vázquez-Flota, 2006, George et al., 2007). About 20 different components interacting together create the optimum growth medium for most plant tissue-derived explants (Trigiano and Gray, 2010).

Tissue culture is a fast and highly reliable method for asexual plant propagation for research and is commercially used by the greenhouse and nursery industries for routine

product development. Finding the best culture medium and effective treatments to establish shoots followed by increasing the number of axillary shoots is important if tissue culture is to be feasible. In addition, finding the best treatments to induce shoots to form roots is quite important to complete the micropropagation process (Khajehyar and Tripepi, 2020). For efficient propagation of cultured species at each propagation stage, testing different basal salt formulations, different plant growth regulators or changing mineral concentrations in the medium are often needed. The medium ingredients may differ from species to species due to their different nutritional or hormonal requirements.

Skoog and his colleagues discovered the first cytokinin (kinetin: Miller et al., 1955) and then studied the effects of kinetin on increasing the number of cell divisions of tobacco callus. Skoog and co-workers also recognized the importance of balancing the ratio between exogenous auxin and kinetin in the medium as these hormones affected the morphogenesis of callus of cultured tobacco (Skoog and Miller, 1957, Trigiano and Gray, 2010, Smith, 2012). Scientists and propagators routinely look for combination of PGRs that can enhance shoot proliferation of different plant species, as the mineral and hormonal requirements of plants can differ from each other not only family by family, but even species by species within a genus.

In this chapter I focused on adjusting concentrations of several components including inorganic minerals (such as N, P, Ca, Mg, and Fe) and cytokinins (benzylaminopurine (BA), kinetin (Kin), zeatin (Zea), *meta*-topolin (MT), thidiazuron (TDZ), and dimethylallylamino purine (2iP)).

2.2. Objectives

The objectives of this study were to, 1) determine optimal type and concentration of cytokinin , and 2) determine the optimal concentrations of selected minerals (N, Fe, Ca, Mg, or P) within a culture medium, to enhance the optimal growth of little-leaf mockorange shoot cultures.

2.3. Materials and Methods

2.3.1. Plant materials

In 2019, stems from little-leaf mockorange (*Philadelphus microphyllus*) derived from a selection held at the University of Idaho Aberdeen Research and Extension Center, Aberdeen, Idaho, USA were acquired by the Plant Tissue Culture Lab in the Plant Sciences Department at University of Idaho, Moscow, Idaho, USA. The original plant of this accession was collected from the Goshutes Mountains, south of Wendover in Elko County, Nevada in 2012 by Dr. Stephen Love. This selected little-leaf mockorange plant was chosen based on several key landscape traits. First, this plant had a very compact and dense habit, not necessarily dwarf but showing a shortened height and density in comparison with typical representatives of this species. Second, the plant had leaves that expressed an attractive silvery color. Most plants of the species have indistinct medium green leaves. Last, the plant lacked a species-common tendency to produce random, long, leggy sprouts. Taken altogether, traits expressed by this selection provided an aesthetically pleasing plant that would complement any landscape. Another important characteristic of this plant is that Dr. Love found the plant failed to produce true-to-type from seeds, meaning that to

maintain these exceptional traits, vegetative propagation was essential (Stephen Love, University of Idaho, personal communication).

2.3.2. Surface sterilization of stem explants

Leaves were removed from stems, then stems soaked in dilute soap solution (2 drops per 100 ml) for 5 minutes and washed with tap water. Stems, cut into pieces containing two to three nodes each, dipped into 70% ethanol (v/v) for 30 seconds, followed by placement into a 10% bleach solution (v/v) for 20 minutes. Finally, stem pieces were rinsed in sterile distilled water three times. Each stem piece was cut at both ends to remove damaged tissue and put into individual culture tubes (2*15 cm) containing half strength Murashige and Skoog (½ MS, 0.5 mg thiamine-HCl, 0.25 mg nicotinic acid, 0.25 mg pyridoxine-HCl, 1 mg glycine, and 0.05 g myo-inositol, pH = 5.6) medium (Murashige and Skoog, 1962) supplemented with 0.5 µM BA.

2.3.3. Micropropagation and maintenance of the shoot cultures

Shoot cultures were maintained on culture medium for at least 6 months and were subcultured monthly to stabilize the shoot cultures. Every subculture cycle was completed by cutting the stems into several pieces of about 1.5 cm and placing six stem explants into each of the baby food jars (195 ml) used for culture maintenance. Explants were incubated in a SG-30S germinator (Hoffman Manufacturing Inc., Albany, OR) at 25 ± 1°C under a 16-h photoperiod (cool-white fluorescent lamps), with 38 $\mu mol \cdot m^{-2} \cdot s^{-1}$ photosynthetic photon flux (PPF). This process was completed every month to maintain and increase the number of shoot cultures to use for producing stem explants for later experiments. Stable shoot cultures were used in all subsequent experiments.

2.3.4. Plant growth regulator cytokinin experiments

2.3.4.1. Evaluation of cytokinin type and concentration

In an experiment designed to optimize conditions for axillary shoot proliferation and growth of little-leaf mockorange shoot cultures, different concentrations of six cytokinins were tested individually. Stem explants (1.5 to 2 cm) were placed on ½ strength MS medium supplemented with different cytokinin compounds including benzyladenine (BA), kinetin (Kin), zeatin (Zea), *meta*-topolin (MT), dimethylallylamino purine (2iP), or thidiazuron (TDZ), each at concentrations of 0, 1.1, 2.2, 4.4, or 8.8 µM. Other components in the media were at their standard amounts in ½ MS medium, also 3 g sucrose, 0.05 mg thiamine-HCl, 0.025 mg nicotinic acid, 0.025 mg pyridoxine-HCl, 0.1 mg glycine, and 0.005 g myo-inositol were added into each 100 ml medium treatments. The pH of the media were 5.6. Shoot explants were transferred onto the culture medium in baby food jars, and six explants were placed in each jar.

2.3.4.2. Zeatin experiment

During cytokinin evaluation, explants grown on culture medium supplemented with zeatin at concentrations between 1.1 to 2.2 µM were visibly growing better than other shoot cultures on media supplemented with other cytokinins. Hence, another experiment with only zeatin in a narrower concentration range was completed to determine the best concentration suitable for increasing shoot proliferation of little-leaf mockorange. Explants were put onto ½ MS medium supplemented with zeatin at concentrations of 0, 0.55, 1.1, 1.65 or 2.2 µM and kept on the medium for 4 weeks, subcultured and placed on the same treatment for 4 more weeks.

2.3.5. Minerals experiments

The standard basal MS salt consisted of 60 mM N, 3 mM Ca, 1.5 mM Mg, 1.25 mM P, and 100 µM Fe. The custom medium tested in these series of experiments were all provided by BioWorld Molecular Life Sciences, Dublin, OH, USA. Each custom medium lacked one of the minerals (N, Fe, Ca, Mg, or P). A separate stock solution of each of these minerals were then made to later combine with the custom ½ strength MS to obtain the concentrations needed to test in each mineral experiment.

2.3.5.1. Nitrogen (N) experiment

As the most important inorganic element, nitrogen was the first mineral evaluated at different concentrations for its effects on shoot proliferation and explant growth. Nitrogen at concentrations of 0, 7.5, 15, 30, or 60 mM were added into a ½ MS salts that lacked N. Shoots placed on regular ½ MS basal salts, described above, were used as a positive control. By the end of this experiment, the highest N concentration, had negative effects on the shoot cultures, severely inhibiting their growth. A second experiment was completed to help refine a recommendation - with N at concentrations of 0, 22.5, 30, 37.5, or 45 mM to avoid this effect.

2.3.5.2. Iron (Fe) experiment

Iron was second mineral that was tested in the culture medium since it is an important essential micronutrient. Five concentrations of Fe (0, 0.5, 5, 50, or 500 µM) were used to find the best Fe concentration in the culture medium to increase shoot multiplication and growth of little-leaf mockorange. Half-strength MS (½ MS) custom medium lacking Fe was prepared, and the media were supplemented with the selected Fe concentrations. At

the end of the experiment, all plants on the highest concentration of Fe died. Another experiment with a reduced range of Fe concentrations was therefore completed with 0, 25, 50, 75, or 100 µM Fe in ½ MS custom medium without iron.

2.3.5.3. Calcium (Ca) experiment

Another experiment was conducted testing different concentrations of Ca at 0, 0.75, 1.5, 2.25, or 3 mM into ½ MS tissue culture medium that lacked Ca and one regular commercial ½ MS culture medium (as positive control), to determine the best concentration of Ca promoting growth of little-leaf mockorange shoot cultures.

2.3.5.4. Magnesium (Mg) experiment

The next experiment tested Mg at concentrations of 0, 0.375, 0.75, 1.125, or 1.5 mM in ½ MS tissue culture medium that lacked Mg and one commercial ½ MS culture medium (as positive control), to determine the best Mg concentration to improve shoot growth of little-leaf mockorange.

2.3.5.5. Phosphorous (P) experiment

Phosphorous at concentrations of 0, 0.312, 0.625, 0.937, or 1.25 mM into ½ MS tissue culture medium that lacked P (custom medium) and one standard ½ MS culture medium (as positive control) were tested on shoot cultures of little-leaf mockorange.

2.3.6. Shoot harvest and data collection

After three months on culture medium (2 monthly subcultures) for the cytokinins experiment or two months on the culture medium (1 subculture) for the Zeatin, N, Fe, Ca, Mg, or P experiments, shoots were harvested, and data were collected. The growth

parameters evaluated were percentage of survival based on the proportion of dead shoots, number of axillary shoots formed, length of the longest shoot on each explant, the number of roots (if any) on each explant and their length, and shoot dry weight (biomass) for each individual explant. To determine the biomass, samples were dried at 70°C for 72 hours and then weighed. After weighing shoots, samples were ground in a mortar to a fine powder and sent to a tissue analysis lab (Brookside Laboratories, Inc., New Bremen, OH) to determine tissue mineral concentrations. They applied a combustion method using a Carlo Erba 1500 C/N analyzer to estimate total N content (method B2.20, Miller et al., 2013). For the rest of the minerals, they used nitric acid and hydrogen peroxide in a closed Teflon vessel and digested in a CEM Mars Microwave and analyzed on a Thermo 6500 Duo ICP (method B4.30, Miller et al., 2013).

2.3.7. Statistical analysis

The cytokinins experiment was completed as a complete randomized block design in the form of factorial design with two factors, including the type of the cytokinin with six levels and the concentration of the cytokinin with five levels. All the data were analyzed with SAS software version 9.4 (SAS, 2016). A generalized linear mixed model (Proc GLIMMIX) was completed with cytokinin type and concentrations (in the cytokinin experiment), and zeatin or mineral concentrations (in zeatin and minerals experiments) were fixed effects and blocks were random effects. These models assumed a normal distribution for dry weight and shoot length, and a Poisson distribution for shoot number with a log link (Stroup, 2014). For significant effects, pair-wise comparisons of marginal means were used to assess treatment differences. Roots were rarely observed for any of the

treatments, consequently for these variables, treatments did not show significant results, hence, root data were excluded from statistical analysis.

2.4. Results

2.4.1. Cytokinin experiment

Different concentrations of the various cytokinins had significant effects on shoot growth, such as number of axillary shoots, shoot length (Figure 1), and dry weight (Figure 2) of little-leaf mockorange shoots in culture (Table 1). Only shoot dry weight was affected by an interaction between cytokinins and their concentrations (Table 1, Figure 2). Due to this interaction the effects of concentration on shoots dry weight were analyzed only for each separate cytokinin (Table 1).

Table 1. Main effects and the interactions between cytokinins and their concentrations on the number of axillary shoots, shoot length, and dry weight of little-leaf mockorange shoot cultures. *P*-values indicate statistical significance.

Treatment	**Shoot growth**		
	Axillary shoot number	**Shoot length**	**Dry weight**
Cytokinin	$p < 0.0001$ *	$p < 0.0001$ *	$p < 0.0001$ *
Concentrations	$p = 0.0085$ *	$p = 0.0075$ *	$p = 0.0001$ *
Cytokinin*Concentrations	$p = 0.7225$	$p = 0.0905$	$p = 0.0187$ *

Meta-topolin concentration had an increasing effect ($p = 0.02$) on the mean number of axillary shoots (Table 2). *Meta*-topolin at concentration of 8.8 µM produced the highest level of bud break (number of axillary shoots) (4.3 fold), whereas MT at 1.1, 2.2 and 4.4 µM increased shoot number less than MT 8.8 µM, but still more than the control (Figure 3).

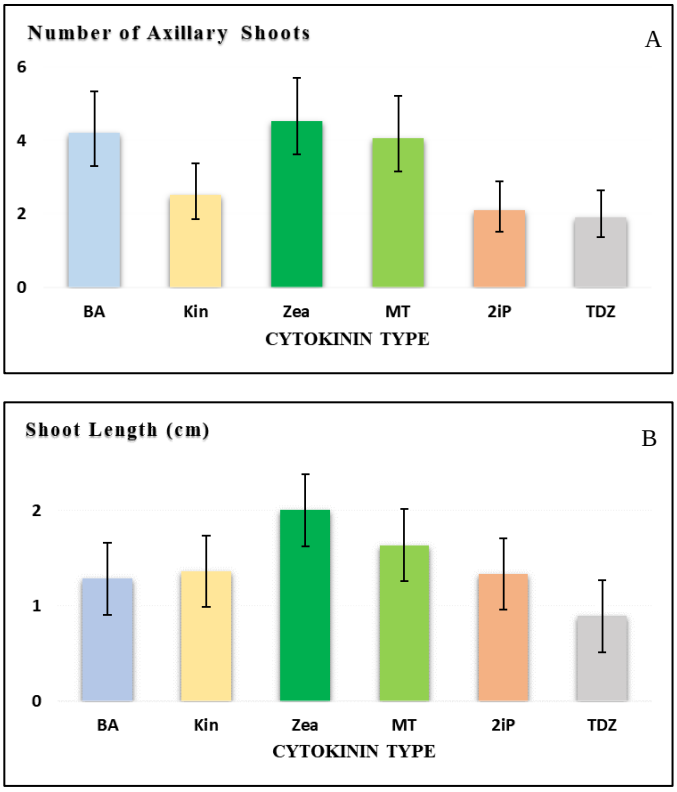

Figure 1. Effects of different cytokinins (benzyl aminopurine (BA), kinetin (Kin), zeatin (Zea), meta-topolin (MT), dimethylamino purine (2iP), and thidiazuron (TDZ)) *in vitro* growth of little-leaf mockorange shoots averaged over their concentrations. Number of axillary shoots (top) and shoot length (bottom). Data are means (n = 4) and bars indicate ± 95% confidence limits.

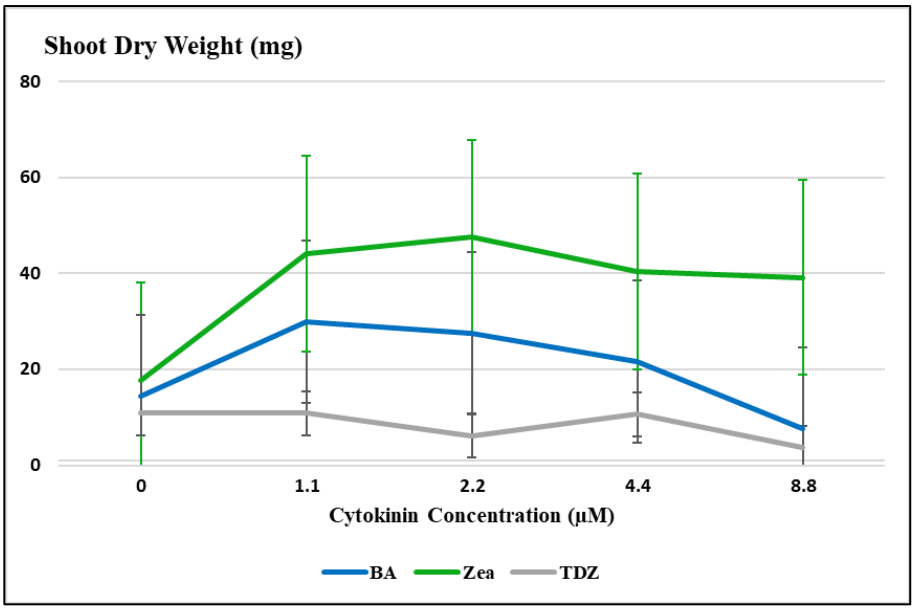

Figure 2. The interaction between cytokinins (benzyl aminopurine (BA), zeatin (Zea), and thidiazuron (TDZ)) selected for their strong, positive, and negative effects and their concentrations on dry weight of little-leaf mockorange shoot cultures. Bars indicate ± 95% confidence limits (n = 4).

Table 2. The effects of cytokinins type (benzyl aminopurine (BA), kinetin (Kin), zeatin (Zea), meta-topolin (MT), dimethylamino purine (2iP), and thidiazuron (TDZ)) on the number of axillary shoots, shoot length, and dry weight of little-leaf mockorange shoot cultures. *P*-values with an asterisk indicate statistical significance.

Treatment	Shoot growth		
	Axillary shoot number	Shoot length	Dry weight
BA	$p = 0.1407$	$p = 0.0031$*	$p = 0.0475$ *
Kin	$p = 0.5691$	$p = 0.8727$	$p = 0.0312$ *
Zea	$p = 0.3205$	$p = 0.5246$	$p = 0.0007$*
MT	$p = 0.0213$ *	$p = 0.0063$ *	$p = 0.0949$
2iP	$p = 0.7596$	$p = 0.9972$	$p = 0.0380$ *
TDZ	$p = 0.9544$	$p = 0.1003$	$p = 0.0880$

Meta-topolin also, affected shoot length, with shoots on 1.1 and 2.2 µM MT growing two times taller than control shoots (Figure 4A). Shoots grew the tallest on BA at 1.1 µM, followed by BA at 2.2 µM, but concentrations of BA at 4.4 or 8.8 µM decreased shoot length to even shorter than the control explants (Figure 4B).

Benzyladenine affected shoot length and dry weight (Table 2). Benzyladenine changed shoot dry weight, in that increasing the concentration of BA from 1.1 to 4.4 µM decreased shoot dry weight by 28% as determined by pair-wise comparisons, although this average weight was heavier than the control ($p = 0.0475$). In contrast, shoots on the medium without BA weighed 52% more than shoots on 8.8 µM BA (Table 3).

Kinetin also affected shoot dry weight (Table 2). Shoots on medium supplemented with 2.2 µM Kin or higher weighed at least 1.5-fold more than control shoots as determined by pair-wise comparisons. Shoots on 4.4 or 8.8 µM Kin also weighed at least 49% or 59% more, respectively, than shoots grown on 1.1 µM Kin.

Table 3. The effects of cytokinins (benzyl aminopurine (BA), kinetin (Kin), zeatin (Zea), meta-topolin (MT), dimethylamino purine (2iP), and thidiazuron (TDZ)) and their concentrations on mean shoots dry weights of little-leaf mockorange cultures. Six different cytokinins were tested at five concentrations on shoot explants. Data are means ± 95% confidence limits (n = 4). An interaction was observed that indicated the pattern of change over concentration differed by cytokinin type.

	Shoot dry weight (mg)				
	Cytokinin concentration (µM)				
	0	**1.1**	**2.2**	**4.4**	**8.8**
BA	14.4 ± 7.7	30.0 ± 7.7	27.5 ± 7.7	21.6 ± 7.7	7.6 ± 7.7
Kin	12.4 ± 4.2	15.5 ± 4.2	19.3 ± 4.2	23.1 ± 4.2	24.6 ± 4.2
Zea	17.8 ± 9.3	44.2 ± 9.3	47.5 ± 9.3	40.4 ± 9.3	39.2 ± 9.3
MT	12.0 ± 9.8	34.5 ± 9.8	31.7 ± 9.8	24.2 ± 9.8	38.4 ± 9.8
2iP	10.9 ± 2.7	17.0 ± 2.7	18.6 ± 2.7	17.1 ± 2.7	18.2 ± 2.7
TDZ	11.0 ± 2.1	10.8 ± 2.1	6.2 ± 2.1	10.6 ± 2.1	3.6 ± 2.1

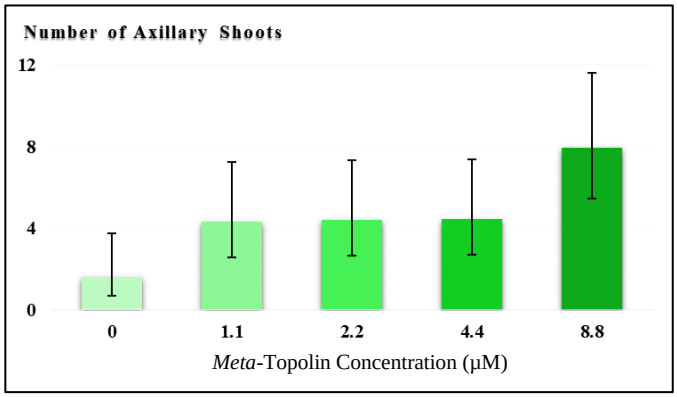

Figure 3. The effects of different concentrations of MT on the number of axillary shoots formed by little-leaf mockorange shoot cultures. Data are means (n = 4) and bars indicate ± 95% confidence limits.

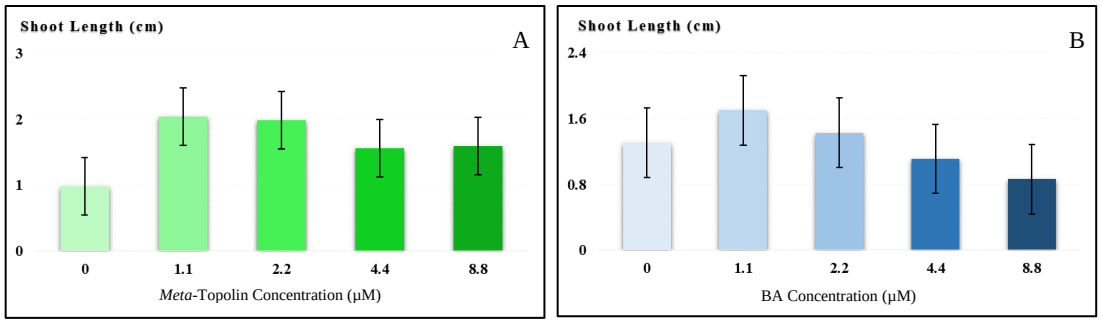

Figure 4. Comparison between different concentrations of MT (left) and BA (right) on shoot length of little-leaf mockorange cultures. Data are means (n = 4) and bars indicate ± 95% confidence limits.

2iP concentrations influenced shoot dry weight (Table 2). Mean shoot dry weights among all 2iP concentrations were similar to each other, yet they produced at least 70% more dry weight than control shoots.

zeatin significantly increased shoot dry weight of little-leaf mockorange. Similar to 2iP, any zeatin concentration resulted in shoots producing at least 2.2 fold more dry weight than control shoots. Mean shoot dry weights among the four zeatin concentrations tested were similar (Table 2). Regardless of concentration, zeatin increased shoot number and shoot height (Figure 1).

TDZ failed to affect any of the growth parameters (Table2). All explants placed on culture medium supplemented with any concentration of TDZ died. Plants growing on TDZ first showed very low growth, and eventually died, especially at high concentrations (Figure 5).

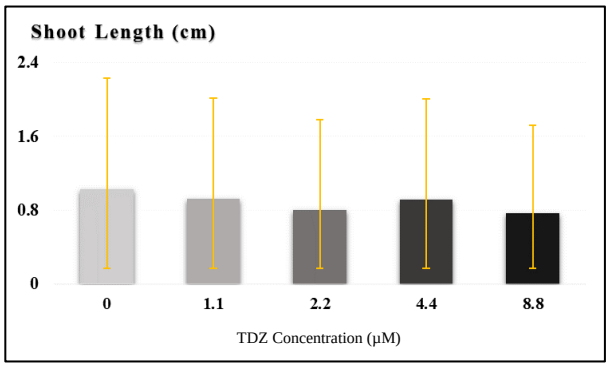

Figure 5. The effects of different concentrations of TDZ on shoot length of little-leaf mockorange shoot cultures. Data are means (n = 4) and bars indicate ± 95% confidence limits.

2.4.2. Zeatin experiment

In the zeatin experiment, shoots on medium with 1.65 µM zeatin produced the most biomass (dry weight), and those on 0.55 µM zeatin or higher concentrations grew taller than control explants (Figure 6). Shoots on 0.55, 1.1, or 2.2 µM zeatin were at least 64% taller than control shoots.

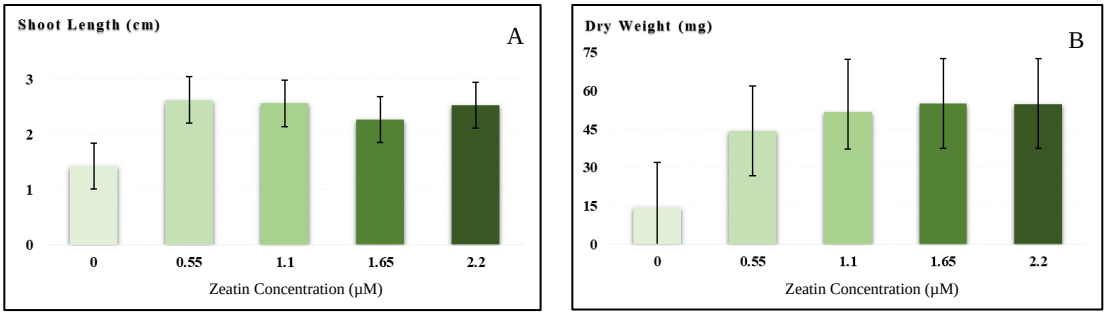

Figure 6. The effect of 0, 0.55, 1.1, 1.65, or 2.2 µM zeatin on shoot length (left) and dry weight (right) of little-leaf mockorange. Data are means (n = 4) and bars indicate ± 95% confidence limits.

2.4.3. Minerals experiments

In the first experiment testing different N concentrations in the culture medium, increasing N from 0 to 30 mM increased the number of axillary shoots by 6-fold. Increasing N from 30 (mean value 1.8) to 60 mM (1.0 mean value) caused a severe decrease in the shoot number. The number of axillary shoots formed on explants grown on 30 mM N or the positive control (½ MS medium), were similar (Figure 7A).

Regarding shoot length and dry weight, the same trend was seen if applying N from 0 to 60 mM with shoots on 30 mM N being 66% taller and producing 8 fold more dry weight than shoots on medium without N. In contrast, shoots on the positive control medium grew 38% taller and produced 84% more dry weight compared to shoots on 30 mM N (Figure 7B and 7C).

In the second N experiment, only shoot dry weight differed among the treatments. Dry weights of shoots on 22.5 or 30 mM N were almost 12 fold higher than dry weights of control shoots. Although statistically, dry weights of shoots on 37.5 or 45 mM N were lower than weights of shoots on 22.5 or 30 mM N (Figure 8).

Only shoot length and dry weight were affected by Fe concentrations. Increasing Fe from 0 to 50 µM, increased shoot length 43% and doubled the dry weight (Figure 9). The

percentage of survival on Fe 500 µM was zero, as this concentration killed all the explants. Figure 9B shows decreased dry weight on Fe 500 µM compared to the other concentrations.

In the second Fe concentration experiment, shoot length (p = 0.02) and dry weight (p = 0.005) were also significant. Shoots on 25 µM Fe or higher grew at least 75% taller and produced 70% more dry weight (Figure 10).

Shoot length and dry weight of explants grown on media with varied Ca concentrations were significantly different. Plants grown on 1.5 mM Ca were 2.5 fold taller than the shoots on control, but shoots heights between different Ca concentrations were statistically similar. Shoot length resulting from culture on ½ MS control explants were taller than shoots grown on other Ca concentrations. Shoots grown on 0.75 mM Ca or higher, as well as positive control (½ MS) explants produced the most shoot biomass compared to the zero control (Figure 11).

Only shoot length was significantly affected by changes in Mg concentration ($p < 0.0001$). Shoots grown on 0.75 mM Mg were tallest, although were shorter than shoots grown on ½ MS (Figure 12). From Mg at 0 to 0.75 mM shoot height tended to increase, whereas from 0.75 to 1.5 mM heights tended to decrease, although shoot heights of explants on medium with any level of Mg were similar.

Shoot length and dry weight were significantly affected by P concentration. Shoots on medium supplemented with 0.31 mM or higher grew at least 2.8 fold taller (Figure 13A) and produced 3.6 fold more shoot dry weight compared to shoots on the negative control medium (Figure 13B).

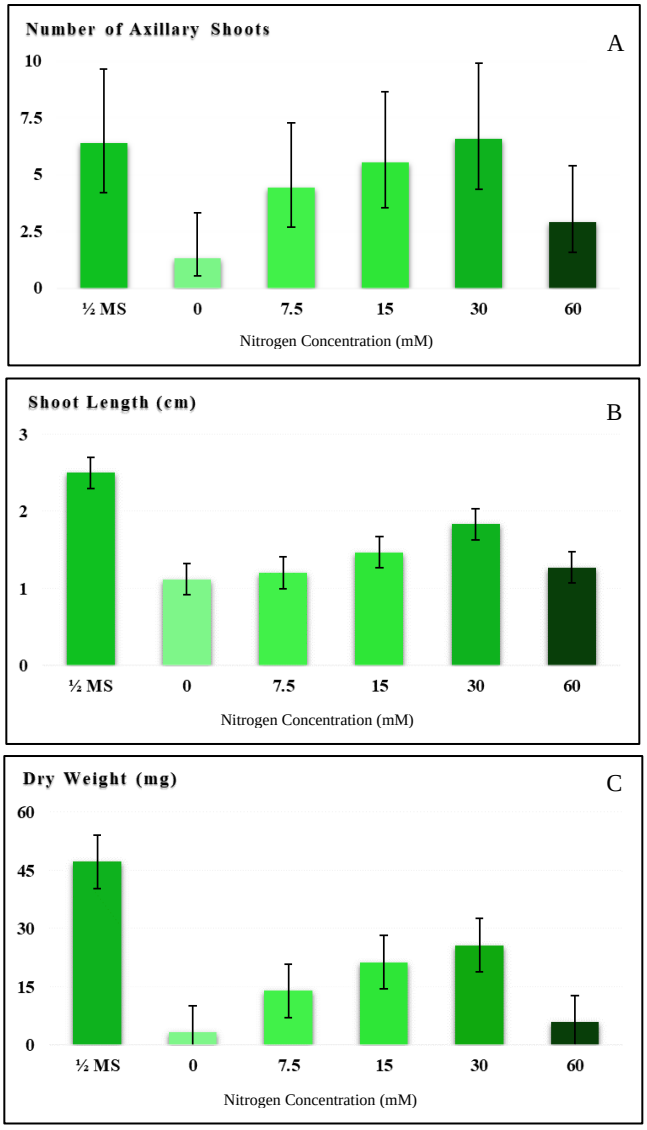

Figure 7. Effects of different N concentrations on number of axillary shoots (A), shoot length (B), and dry weight (C) of little-leaf mockorange shoots in tissue culture. Data are means (n = 4) and bars indicate ± 95% confidence limits.

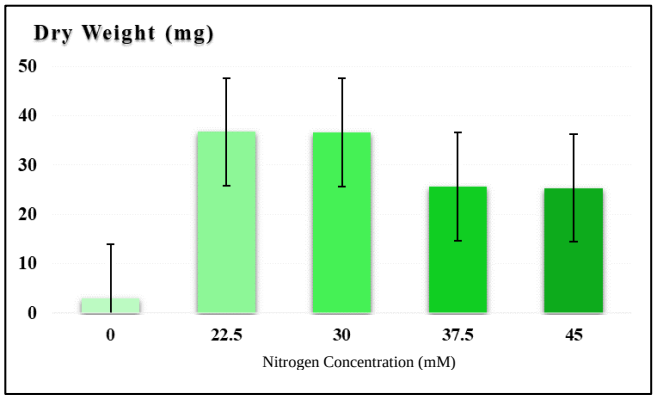

Figure 8. Effects of different N concentrations on dry weight of little-leaf mockorange shoots in tissue culture. Data are means (n = 4) and bars indicate ± 95% confidence limits.

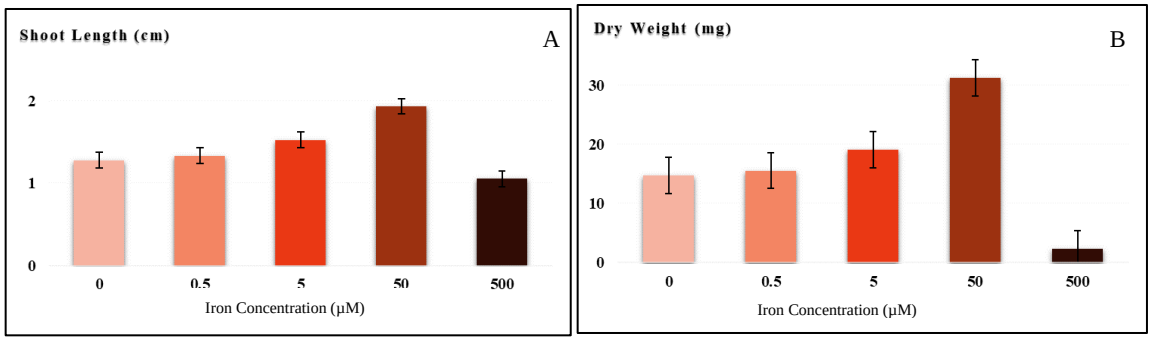

Figure 9. Effects of different Fe concentrations on shoot length (left), and dry weight (right) of little-leaf mockorange shoots in tissue culture. Data are means (n = 4) and bars indicate ± 95% confidence limits.

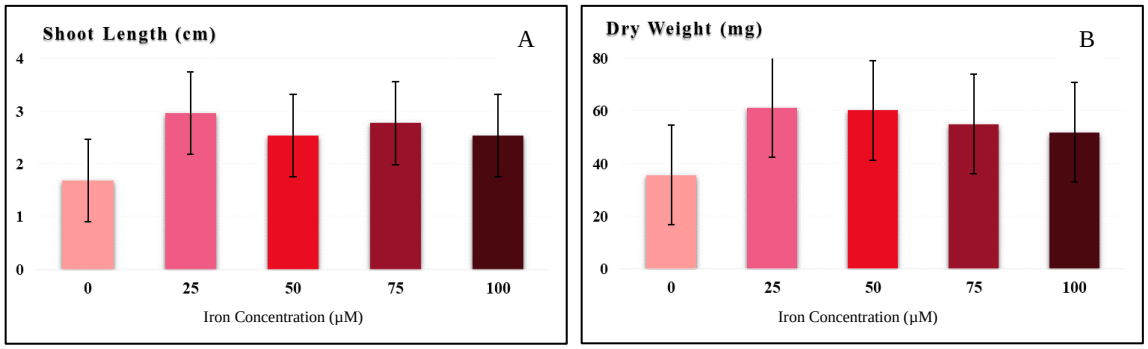

Figure 10. Effects of 0, 25, 50, 75, or 100 µM Fe on shoot length (left) and dry weight (right) of little-leaf mockorange shoots in tissue culture. Data are means (n = 4) and error bars indicate ± 95% confidence limits.

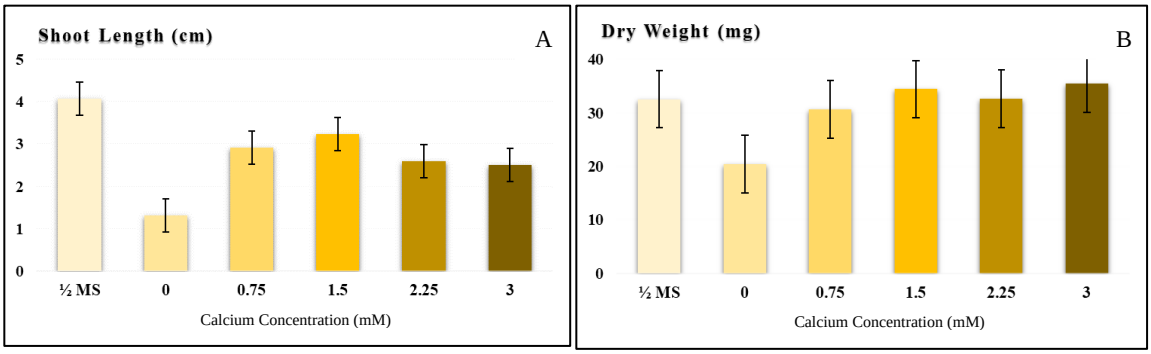

Figure 11. Effects of different Ca concentrations on shoot length (left) and dry weight (right) of little-leaf mockorange shoots in tissue culture. Data are means (n = 4) and error bars indicate ± 95% confidence limits.

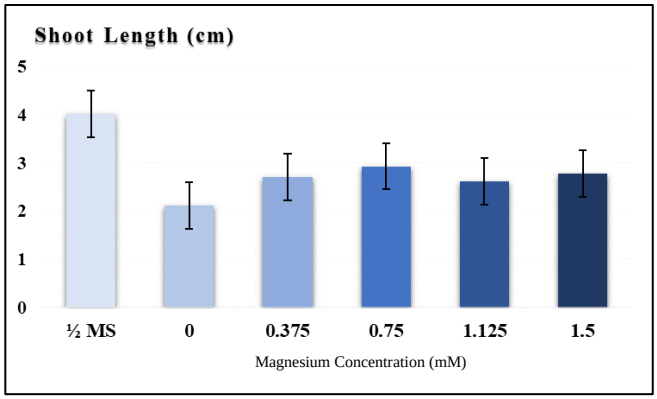

Figure 12. Effects of different Mg concentrations on shoot length of little-leaf mockorange shoots in tissue culture. Data are means (n = 4) and error bars indicate ± 95% confidence limits.

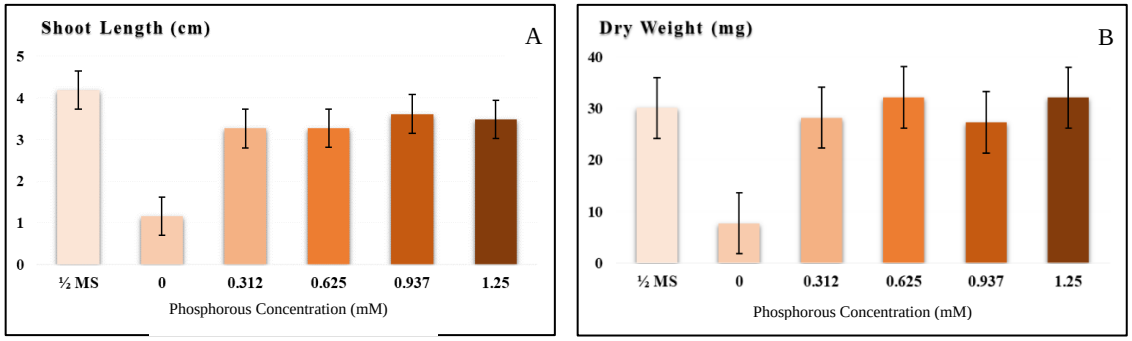

Figure 13. Effects of different P concentrations on shoot length (left) and dry weight (right) of little-leaf mockorange shoots in tissue culture. Data are means (n = 4) and error bars indicate ± 95% confidence limits.

2.5. Discussion

In this study, overall shoot growth, as indicated by increasing shoot length and dry weight of little-leaf mockorange was promoted best by a medium supplemented with zeatin, followed closely by medium supplemented with MT. Shoots treated with 1.1 µM MT produced 28% less dry weight and were 11% shorter than those on medium supplemented with 1.1 µM zeatin. Similar results were reported from other studies showing zeatin either by itself or in combination with another cytokinin promoted shoot proliferation of various plant species, such as the combination of zeatin and BA in micropropagation of olive (Ali et al., 2009). Zeatin promoted more shoot proliferation in dwarf raspberry shoot cultures as compared to BA (Debnath, 2005). Zeatin combined with TDZ increased shoot multiplication of lingonberry (Ostrolucká et al., 2004). In contrast, zeatin failed to increase

shoot growth of tissue cultured phlox shoots (Khajehyar, unpublished data). Overall, using zeatin within a range of 1.65 to 2.2 µM promoted shoot growth (more biomass production and taller shoots), which should help growers to obtain more healthy propagules within a shorter period of time.

Zeatin is the natural form of the cytokinin, and the positive responses of little-leaf mockorange to this cytokinin were probably due to this fact. Plant species and their genetics should also be considered when examining the effects of zeatin or other phytohormones on the growth of *in vitro* shoot cultures. The concentration used for each plant species at different ages can be an important factor to consider while applying any phytohormone in the culture medium. Debnath (2004) stated that increasing the concentration of zeatin enhanced shoot proliferation yet caused high mortality of explants of red raspberry. Combining zeatin with other cytokinins for each plant species may enhance the effects of zeatin on axillary shoot proliferation or shoot elongation.

The results obtained from this study were in agreement with that of other researchers studying and reporting the positive effect of MT on shoot proliferation, such as the positive effect of MT on improving axillary shoot number of firechalice (Alosaimi and Tripepi, 2018), the positive effect of 2 µM MT on shoot number, dry weight, and rooting percentage of sea oats (Valero-Aracama et al., 2010), and induction effect of MT at 5 µM on the best rate of shoot multiplication of *Aloe polyphylla* an endangered medicinal and ornamental aloe species (Bairu et al., 2007).

Thidiazuron failed to promote shoot proliferation of little-leaf mockorange grown *in vitro*. Thidiazuron in this experiment showed an inhibitory or toxic effects on explants growth. Increasing TDZ concentration, increased its negative effect on shoot length and dry weight.

Thidiazuron is a synthetic cytokinin-like PGR, first introduced in Germany as a cotton defoliant (Arndt et al., 1976, Dewir et al., 2018). This PGR is resistant to cytokinin oxidase, hence is very stable in culture medium (Mok et al., 1982, Dewir et al., 2018). Unlike zeatin, TDZ exhibits very slow metabolism within plant tissues (Mok and Mok, 1985). Thidiazuron resistance to cytokinin oxidase may cause accumulation of purine cytokinins in plant tissues (Horgan et al., 1988, Hare et al., 1994, Dewir et al., 2018). Zhang et al. (2006) stated that treatment of plants with TDZ induced accumulation of ethylene in plant tissues due to the expression of stress-related genes. Signaling of stress related genes, such as proline or abscisic acid, also resulted from treatment with TDZ (Murch et al., 1999, Jones et al., 2007, Dewir et al., 2018). The inhibitory effects of TDZ on plant tissue culture, is possibly also species dependent, and these effects may be more prominent in some plant species, such as little-leaf mockorange.

Cytokinins play key roles in long-distance signaling, a control mechanism for N assimilation in plants (Sakakibara et al. 2006, Rubio et al., 2009). These qualities may explain the promotive effects of cytokinins on shoot proliferation of explants *in vitro* as N is critical for vegetative growth. Increasing nitrate supply in the soil and through plants' roots, induces the expression of genes related to regulating nitrate and carbon metabolism in plants, which can be mimicked by applying cytokinin in the culture medium (Scheible et al., 2004, Brenner et al., 2005, Rubio et al., 2009). Applying or increasing the concentration of cytokinins can enhance N utilization, resulting in more bud breaks and shoot proliferation.

Selecting the best PGR for the micropropagation can be critical especially for growers considering the price of different PGRs and the purpose for using them. Growers need to

consider all aspects of their micropropagation goals and chose the best PGR beneficial for them economically and to meet proliferation goals. For little-leaf mockorange, the best cytokinin to use for *in vitro* growth of shoot cultures was zeatin. However, the high cost of zeatin may be prohibitive for some propagators, a situation in which a compound like MT may prove to be more efficacious.

Presence of N in tissue culture medium is very important and plays a key role in promoting growth as N will affect cytokinin signaling (induction of producing cytokinins) and enhance effects on shoot proliferation. Synergistically, applying or increasing cytokinins can accelerate signaling of genes responsible for N assimilation in plants (Sakakibara et al., 2006, Rubio et al., 2009).

Application of N in tissue culture medium improved shoot multiplication and growth of micropropagated Indian gooseberry (Sen and Batra, 2011). Sen and Batra (2011) also stated that the best responses were found on media including commercially standard concentrations of N, which my results with little-leaf mockorange confirmed.

Experiments demonstrated that Ca, Fe, Mg, or P were all essential for shoot growth of little-leaf mockorange, yet some of them had stronger effects, when applied in ½ MS medium.

Calcium supplementation at any level within my experimental parameters increased shoot dry weight clearly compared to negative control plants. Shoots on supplemented media grew at least 1.9 times taller than those on the control treatment. Also, addition of Ca resulted in at least 1.5 fold more shoot dry weight compared to the negative control. Supplementation resulted in similar results to the positive control, showing that using

regular ½ strength MS medium can be sufficient for little-leaf mockorange optimum growth.

Addition of magnesium provided significant improvements only to shoot length, resulting in plantlets at least 1.2 times taller than those grown without Mg in the medium.

Lee and Fossard (1977) and Ramage (1999) stated that phosphorus is an important mineral both for explant growth and morphogenesis (Ramage and Williams, 2002). Shoot lengths and dry weights were significantly improved by P supplementation to culture media. Shoots on medium supplemented with 0.31 to 1.25 mM P were similar in length and dry weight but at least 2.6 times taller and produced 3.6 times more dry weight than shoots on medium that lacked P.

2.6. Conclusion

In this study, little-leaf mockorange grew best on ½ MS medium supplemented with 1.65 to 2.2 µM Zeatin. If the price of the cytokinin is a key factor in choosing the cytokinin source, then MT at 2.2 µM is suggested for use instead, because of the economic issues.

Regarding the adjustment and optimization of the minerals in the tissue culture medium, I suggest that N at 22.5 to 30 mM (standard amount of N in regular ½ strength MS) be used in the culture medium. For Fe, amounts between 25 to 50 µM (regular concentration of Fe in ½ strength MS) can improve shoot growth of little-leaf mockorange. Calcium, magnesium, and phosphorous each promoted shoot growth at standard concentrations in ½ strength Murashige and Skoog medium.

Considering all these points, I suggest utilization of 1.65 to 2.2 µM Zea in the regular half-strength MS medium for efficient micropropagation of little-leaf mockorange.

References

Ali, A., Ahmad, T., Abbasi, N.A., Hafiz, I.A., 2009. Effect of different media and growth regulators on in vitro shoot proliferation of olive cultivar 'Moraiolo'. *Pak. J. Bot.*, 41, 783-795.

Alosaimi, A.A., Tripepi, R.R., 2018. Micropropagation of *Epilobium canum garretti* (firechalice) by axillary shoot culture. *HortScience*, 53, 62-66.

Anonymous, 2015, Plant Database: *Philadelphus microphylls*. Lady Bird Wildflower Johnson Center, The University of Texas at Austin. Accessed in October 2019. Available on: www.wildflower.org/plants/result.php?id_plant=phmi4.

Anonymous, 2019. Hydrangeaceae. Wikipedia. Accessed in: October 2019. Available on: https://en.wikipedia.org/wiki/Hydrangeaceae.

Anonymous, 2021. *Philadelphus microphyllus* (little-leaf mockorange). Gardenia: Create Gardens. Accessed in October 2019. Available on: www.gardenia.net/plant/philadelphus-microphyllus.

Arndt, F.R., Rusch, R., Stillfried, H.V., Hanisch, B., Martin, W.C., 1976. SN: 49537, a new defoliant (abstract). *Plant Physiol.*, 57(99).

Bairu, M.W., Stirk, W.A., Dolezal, K., Van Staden, J., 2007. Optimizing the micropropagation protocol for the endangered *Aloe polyphylla*: can *meta*-topolin and its derivatives serve as replacement for benzyladenine and zeatin? *Plant, Cell, Tissue, Organ Cult.,* 90, 15–23. DOI 10.1007/s11240-007-9233-4.

Brenner, W.G., Romanov, G.A., Köllmer, I., Bürkle, L., Schmülling, T., 2005. Immediate-early and delayed cytokinin response genes of *Arabidopsis thaliana* identified by genome-wide expression profiling reveal novel cytokinin-sensitive processes and suggest cytokinin action through transcriptional cascades. *Plant J.*, 44, 314–333. DOI:10.1111/j.1365-313X.2005.02530.x.

Debnath, S.C., 2004. Clonal propagation of dwarf raspberry (*Rubus pubescens* Raf.) through in vitro axillary shoot proliferation. *Plant Growth Regul.*, 43, 179–186.

Debnath, S.C., 2005. A two-step procedure for adventitious shoot regeneration from *in-vitro*-derived lingonberry leaves: shoot induction with TDZ and shoot elongation using Zea. *HortScience*, 40, 189-192.

Dewir, Y.H., Nurmansyah, Naidoo, Y., Teixeira da Silva, J.A., 2018. Thidiazuron-induced abnormalities in plant tissue cultures, *Plant Cell Reports*, 37, 1451–1470. Available on: https://doi.org/10.1007/s00299-018-2326-1.

Dirr, M.A., Heuser, C.W., 2006. The reference manual of woody plant propagation, from seed to tissue culture, 2nd Ed., 410 pp, *Varsity Press*, Inc.

George, E.F., Hall. M.A., De Klerk, G., 2007. Plant Propagation by Tissue Culture: Volume 1. The Background, *Springer*, ISBN 978-1-4020-5005-3 (e-book).

Hare, P.D., Staden, J., Van Staden, J., 1994. Inhibitory effect of TDZ on the activity of cytokinin oxidase isolated form soybean callus. *Plant Cell Physiol.*, 35, 11221–11125.

Horgan, R., Burch, L.R., Palni, L.M.S., 1988. Cytokinin oxidase and the degradative metabolism of cytokinins, plant growth substances. In: Pharis, R.P., Rood, S.B., (eds) Plant Growth Substances. *Springer*, pp 282–290.

Jones, M., Yi, Z., Murch, S.J., Saxena, P.K., 2007. Thidiazuron-induced regeneration of *Echinacea purpurea* L.: micropropagation in solid and liquid culture systems. *Plant Cell Rep.*, 26, 13–19.

Khajehyar, R., Tripepi, R.R., 2020. Different cytokinins and their concentrations affect shoot growth of little-leaf mockorange (*Philadelphus microphyllus* A. Gray) in tissue culture. *Supplement to HortScience, ASHS 2020 Annual Conference*. 55, 366- 367. Available on: https://doi.org/10.21273/HORTSCI.55.9S.S1.

Lee, E.C.M., Fossard, R.A., 1977. Some factors affecting multiple bud formation of strawberry (*Fragaria ananassa* Duchesne) *in vitro*. *Acta Hort*, 78, 187- 195.

Loyola-Vargas V.M., Vázquez-Flota F., 2006. An introduction to plant cell culture : Back to the future. In: Loyola-Vargas, V.M., Vázquez-Flota, F., (eds) Plant cell culture protocols. *Methods Mol. Biol.™*, 318, 3-8. Humana Press. https://doi.org/10.1385/1-59259-959-1:003.

Miller, R.O., Gavlak, R., Horneck, D., 2013. Soil, plant and water reference methods for the Western region. 4th Ed. *WREP 125*. 155 pp.

Miller, C.O., Skoog, F., Von Saltza, M.H., Strong F.M., 1955. Kinetin, a cell division factor from deoxyribonucleic acid. *J. Amer. Chem. Soc.*, Vol. 77, 1392. DOI: 10.1021/ja01610a105.

Mok, M.C., Mok, D.W.S., 1985. The metabolism of [^{14}C]-thidiazuron in callus tissues of *Phaseolus lunatus*. *Physiol. Plant*, 65, 427–432.

Mok, M.C., Mok, D.W.S., Armstrong, D.J., 1982. Cytokinin activity of N-phenyl-N-1, 2, 3-thidiiazol-5ylurea (TDZ). *Phytochemistry*, 21, 1509–1511.

Murashige, T., Skoog, F., 1962. A revised medium for rapid growth and bioassays with tobacco tissue cultures. *Physiol. Plant.*, 15, 473-497. Available on: https://doi.org/10.1111/j.1399-3054.1962.tb08052.x.

Murch, S.J., Victor, J.M.R., Krishnaraj, S., Saxena, P.K., 1999. The role of proline in thidiazuron-induced somatic embryogenesis of peanut. *In Vitro Cell Dev. Biol. Plant*, 35, 102–105.

Ostrolucká, M.G., Libiaková, G., Ondrußková, E., Gajdoßová, A., 2004. *In vitro* propagation of *Vaccinium* species. *Acta Universitatis Latviensis, Biology*, 676, 207-212.

Ramage, C.M., 1999. The role of mineral nutrients in the regulation of plant development in vitro, PhD dissertation, *The University of Queensland*.

Ramage, C.M., Williams, R.R., 2002. Mineral nutrition and plant morphogenesis. *In Vitro Cell. Dev. Biol. -Plant*, 38, 116-12.

Rubio, V., Bustos, R., Irigoyen, M.L., Cardona-Lo´pez, X., Rojas-Triana, M., Paz-Are, J., 2009. Plant hormones and nutrient signaling. *Plant Mol. Biol.*, 69: 361–373. DOI 10.1007/s11103-008-9380-y.

Sakakibara, H., Takei, K., Hirose N., 2006. Interactions between nitrogen and cytokinin in the regulation of metabolism and development. *Trends Plant Sci.*, 11: 440–448. DOI:10.1016/j.tplants.2006.07.004.

SAS Institute Inc., 2016. SAS/ACCESS® 9.4 Interface to ADABAS: Reference. Cary, NC: SAS Institute Inc.

Scheible, W.R., Morcuende, R., Czechowski, T., Fritz, C., Osuna, D., Palacios-Rojas, N., Schindelasch, D., Thimm, Ol., Udvardi, M.K., Stitt, M., 2004. Genome-wide reprogramming of primary and secondary metabolism, protein synthesis, cellular growth processes, and the regulatory infrastructure of *Arabidopsis* in response to nitrogen. *Plant Physiol.*, 136: 2483–2499. DOI: 10.1104/pp.104.047019.

Sen, A., Batra, A., 2011. Crucial role of nitrogen in in-vitro regeneration of *Phyllanthus amarus* Schum. And Thonn. *Intl. J. Pharma. Sci. Res.*, 2, 2146- 2151.

Skoog, F., Miller, C.O., 1957. Chemical regulation of growth and organ formation in plant tissue cultured *in vitro*. *Symp. Soc. Exp. Biol.*, 11, 118-131.

Smith, R. H., 2012. Plant tissue culture: techniques and experiments. *Elsevier Science*. 208 pp. ISBN 9780124159853, 0124159850.

Stroup, W.W., 2014. Rethinking the analysis of non-normal data in plant and soil science. *Agron. J*. 106, 1–17.

Trigiano, R.N., Gray, D.J., 2010. Plant tissue culture, development, and biotechnology, First Ed. CRC Press: *Taylor & Francis Group*. 583 pp. ISBN 978-1-4200-8326-2.

Valero-Aracama, C., Kane, M.E., Wilson, S.B., Philman, N.L., 2010. Substitution of benzyladenine with *meta*-topolin during shoot multiplication increases acclimatization of difficult- and easy- to- acclimatize sea oats (*Uniola paniculate* L.) genotypes. *Plant Growth Regul.*, 60, 43-49.

Zhang, C.R., Huang, X.L., Wu, J.Y., Feng, B.H., Chen, Y.F., 2006. Identification of thidiazuron-induced ESTs expressed differentially during callus differentiation of alfalfa (*Medicago sativa*). *Physiol. Plant.*, 128, 732–739.

Chapter 3: Optimization of selected minerals and a cytokinin for *in vitro* propagation of little-leaf mockorange (*Philadelphus microphyllus* A. Gray) using Response Surface Method (RSM)

Abstract

Maximizing proliferation of a new plant species upon introduction into tissue culture may require optimizing concentrations of minerals and growth regulators included in a culture medium. The objective of this study was to use Response Surface Methods to evaluate combinations of selected minerals (N, Ca, K, and P) along with zeatin to obtain optimum shoot growth of little-leaf mockorange produced in tissue culture. Forty six treatments (combinations) were designed. The concentrations of zeatin tested were 0.82, 1.095, or 1.37 µM, and the minerals were 22.5, 30, or 37.5 mM N, 1.125, 1.5, or 1.88 mM Ca, 0.31, 0.625, or 0.94 mM P, and 5, 10, or 15 mM K. Treatment concentrations were tested for their effects on the number of axillary shoots formed, shoot length, and shoot dry weight. The response surface analyses showed that the optimum concentrations of N, Ca, and P were 32.5 to 35 mM, 1.5 mM, and 0.625 mM, respectively. Potassium in the regression models resulted in nonsignificant change in responses, hence, K concentrations were limited to linear trends in the analysis. Medium supplemented with 1.1 µM zeatin affected shoot growth positively. The RSM model demonstrated that optimum concentrations of zeatin, N, Ca, and P could be determined in one experiment and could promote *in vitro* growth of little-leaf mockorange shoots.

3.1. Introduction

Plant response to propagation by tissue culture is highly dependent on the presence and amount of some minerals and nutrients supplied in the culture medium, including nitrogen (N) (Wada et al., 2015), potassium (K), calcium (Ca), phosphorous (P), magnesium (Mg), and iron (Fe). Such nutrients play key roles in plant growth and development, due to involvement in structural or metabolic actions. Hence, the mineral concentration and ratios within a culture medium impact aspects of plant morphogenesis, such as shoot multiplication and elongation, and conversely may contribute to abnormal growth, or physiological disorders (Reed et al., 2013b, Wada and Reed, 2017). Similarly, plant growth regulators (PGRs) may affect different physiological disorders (Reed et al., 2013b). Explants grown on culture media without or containing very low concentrations of auxins or cytokinins may grow poorly on and even start to die after a while. Changes in mineral concentrations in culture media are interrelated and may affect the amount of uptake of other minerals as well, thus, affecting plant growth and development (Poothong and Reed, 2014).

Although Murashige and Skoog (MS: Murashige and Skoog, 1962) salts have been used to support many kinds of plant species grown *in vitro*, this commercially available salt formulation may be suboptimal for some species causing them to grow slowly. Some plants growing on MS medium have been reported to lack vigorous growth (Poothong and Reed, 2015). Red raspberries grew poorly *in vitro* on MS medium (Poothong and Reed, 2014). Optimizing the mineral and phytohormone contents of a culture medium can enable plants to grow better if a few changes are made to the medium (Poothong and Reed, 2015). Even individual cultivars within a species may differ in their response to different mineral

combinations, meaning genotype-specific formulations of a culture medium can be highly useful for developing *in vitro* propagation procedures for many plant species (Reed et al., 2013a). Altering and developing formulations of growth media compatible for a specific cultivar can be very complicated and time consuming (Reed et al., 2013a). Developing various formulations includes changing the concentration and combination of different organic compounds or minerals, as well as different phytohormones needed by plants during each of the progressive phases of tissue culture. Completing experiments to find the best concentration of each individual mineral can take months, but combining all individual experiments into one by applying factorial combinations of nutrients and PGRs can reduce the time needed for choosing the best combination for each specific cultivar. The traditional method of optimizing the tissue culture medium was to conduct a series of trials on a single species wherein individual ingredients were tested at a range of concentrations to find the best concentration of that specific component (Poothong and Reed, 2014). Once the test ingredient was optimized, trials would begin -one at a time- on subsequent medium components. Murashige and Skoog medium was developed in this way specifically for tobacco callus cells and has been used for many plant species. Besides this systematic process being inefficient, it also fails to fully account for interactions among ingredients as concentrations of each are adjusted upward or downward.

An alternative method of designing of experiments to define optimum combinations of different treatments can be used. While consideration of all possible combinations or a large number of components can be logistically challenging or impossible, statistical methods can generate experimental designs capable of estimating optimal component settings without the need for conducting numerous serially arranged experiments on

individual minerals or PGRs (Niedz and Evens, 2007, Poothong and Reed, 2015). These experimental designs provide more flexibility and efficiency to improve tissue culture media for specific plant species (Niedz and Evens, 2007, Reed et al., 2013a). Once a design is generated, and data collected from it, optimal component levels for various responses can be estimated through response surface methodology (RSM). In RSM, linear and quadratic surface models are fit to the data. Given adequate model fit, mineral and PGR values associated with optimal conditions of the response, either minima or maxima, can then be algebraically derived from the estimated model. Wada et al. (2013, 2015) conducted a series of studies using different mineral compounds in pear tissue culture medium across five different genotypes. They reported the use of response surface methodology (RSM) (Niedz and Evens, 2007) to develop tissue culture medium for pear and found that the mesos compound ($CaCl_2$, $MgSO_4$, and KH_2PO_4) as supplements in MS medium, were important growth factors for pear. Among other things, these researchers demonstrated that varying several minerals in the culture medium at the same time is more efficient than examining only one mineral at a time (Wada et al., 2015).

Response Surface Methods (RSM) recently have also been used to model and optimize *in vitro* propagation medium by interpreting each medium component or important minerals or PGRs as a geometric dimension, which ultimately results in a geometric volume having *n* dimensions (Niedz and Evens, 2007, Reed et al., 2013a, Poothong and Reed, 2014, 2015). The geometric volume provided by the statistical analysis software is considered as the samples space for experimental design that contains the samples (treatments combinations) based on the objectives of the experiment and the results obtained from data collection of the dependent variables, such as shoot growth characteristics (Reed et al., 2013a). With the

help of the computer-aided, statistical design software, different formulations of culture media are assigned to the design. These points (treatments) are then applied and evaluated based on the plant responses of interest (dependent variables) to the treatments in order to create a multi-dimensional response surface. This information is then applied to a response surface model which is used to determine the optimal plant response and corresponding treatments (Reed et al., 2013a).

Little-leaf mockorange (*Philadelphus microphyllus* A. Gray) is native to the western US and has potential for use in managed urban landscapes. This species is very tolerant to drought, easy to grow, and has low maintenance requirements. It can also grow in a wide range of light conditions from light shade to full sun. Altogether, characteristics of this plant species makes it ideal for use in western landscapes. Although many of the worldwide mockorange species can be propagated by seed, summer soft-wood cuttings, hardwood cuttings and layering (Dirr and Heuser, 2006), little-leaf mockorange is difficult to propagate through seeds or cuttings (Steve Love, University of Idaho, personal communication).

3.2. Objectives

The objectives of this study were to optimize a tissue culture media for little-leaf mockorange shoots by using RSM on selected medium components. I proposed to evaluate important minerals, such as nitrogen (N), phosphorus (P), calcium (Ca), and potassium (K), as well as zeatin (a cytokinin growth regulator), across a range of concentrations. The responses obtained from the experiment determined best combination of the selected components to produce the optimum growth of *in vitro* shoots of little-leaf mockorange as defined by shoot number, shoot length, and dry weight.

3.3. Materials and Methods

3.3.1. Plant materials

In 2019, stems from little-leaf mockorange (*Philadelphus microphyllus*) from Aberdeen Research and Extension Center at University of Idaho, Aberdeen, Idaho, USA were collected and sent to Plant Tissue Culture Lab in the Plant Sciences Department at University of Idaho, Moscow, Idaho, USA. The original plant was collected from the Goshutes Mountains, south of Wendover in Elko County, Nevada in 2012 by Dr. Stephen Love. This specific accession was selected because of its aesthetic qualities for landscape use.

3.3.2. Micropropagation and maintenance of the shoot cultures

Shoot cultures were maintained and stabilized on culture medium for at least 26 months and were subcultured monthly. Every subculture cycle was completed by cutting the stems into several pieces of about 1.5 cm, with each explant consisting of two to three nodes. Six stem explants were placed into each baby food jar (195 ml) containing half strength Murashige and Skoog (½ MS, 0.5 mg thiamine-HCl, 0.25 mg nicotinic acid, 0.25 mg pyridoxine-HCl, 1 mg glycine, and 0.05 g myo-inositol, pH = 5.6) medium (Murashige and Skoog, 1962) supplemented with 0.5 µM BA. Explants were incubated in a SG-30S germinator (Hoffman Manufacturing Inc., Albany, OR) at 25 ± 1°C under a 16-h photoperiod (cool-white fluorescent lamps), with 38 $\mu mol \cdot m^{-2} \cdot s^{-1}$ photosynthetic photon flux (PPF). Stable shoot cultures were used in all the following experiments.

3.3.3. Response Surface Methods experiment

3.3.3.1. Experimental design

The RSM experiment was designed via the Proc Optex procedure (SAS software version 9.4, 2016). This procedure created an orthogonal balanced incomplete block design (Table 1). The algorithm used predetermined high and low values for each nutrient and then set the middle level as an average based on these values (Table 2). High and low values for each mineral were determined from previous observation and experiments.

The overall experimental design was a five-factor Response Surface design with the design points (combinations of all five factors) selected using modified D-optimal criteria suitable for fitting a quadratic polynomial equation.

Table 1. The design created by SAS software to complete RSM for optimizing *in vitro* growth of little-leaf mockorange shoots.

Treatment	**Zeatin (µM)**	**Nitrogen (mM)**	**Calcium (mM)**	**Phosphorus (mM)**	**Potassium (mM)**
1	0.82	22.5	1.5	0.625	10
2	0.82	37.5	1.5	0.625	10
3	1.37	22.5	1.5	0.625	10
4	1.37	37.5	1.5	0.625	10
5	1.095	30	1.12	0.31	10
6	1.095	30	1.12	0.937	10
7	1.095	30	1.875	0.31	10
8	1.095	30	1.875	0.937	10
9	1.095	22.5	1.5	0.625	5
10	1.095	22.5	1.5	0.625	15
11	1.095	37.5	1.5	0.625	5
12	1.095	37.5	1.5	0.625	15

13	0.82	30	1.12	0.625	10
14	0.82	30	1.875	0.625	10
15	1.37	30	1.12	0.625	10
16	1.37	30	1.875	0.625	10
17	1.095	30	1.5	0.31	5
18	1.095	30	1.5	0.31	15
19	1.095	30	1.5	0.937	5
20	1.095	30	1.5	0.937	15
21	0.82	30	1.5	0.31	10
22	0.82	30	1.5	0.937	10
23	1.37	30	1.5	0.31	10
24	1.37	30	1.5	0.937	10
25	1.095	22.5	1.12	0.625	10
26	1.095	22.5	1.875	0.625	10
27	1.095	37.5	1.12	0.625	10
28	1.095	37.5	1.875	0.625	10
29	1.095	30	1.12	0.625	5
30	1.095	30	1.12	0.625	15
31	1.095	30	1.875	0.625	5
32	1.095	30	1.875	0.625	15
33	0.82	30	1.5	0.625	5
34	0.82	30	1.5	0.625	15
35	1.37	30	1.5	0.625	5
36	1.37	30	1.5	0.625	15
37	1.095	22.5	1.5	0.31	10
38	1.095	22.5	1.5	0.937	10
39	1.095	37.5	1.5	0.31	10
40	1.095	37.5	1.5	0.937	10

41	1.095	30	1.5	0.625	10
42	1.095	30	1.5	0.625	10
43	1.095	30	1.5	0.625	10
44	1.095	30	1.5	0.625	10
45	1.095	30	1.5	0.625	10
46	1.095	30	1.5	0.625	10

3.3.4. Media preparation and micropropagation

All media contained the standard amounts of ½ MS medium including 9 mg $MgSO_4$, 1.4 mg $FeSO_4.7H_2O$, 1.86 mg $Na_2EDTA.2H_2O$, 0.85 mg $MnSO_4.H_2O$, 0.43 mg $ZnSO_4.7H_2O$, 0.31 mg H_3BO_3, 0.012 mg $Na_2MoO_4.2H_2O$, 0.001 mg $CuSO_4.5H_2O$, 0.001 mg $CoCl.6H_2O$, 3 g sucrose, 0.05 mg thiamine-HCl, 0.025 mg nicotinic acid, 0.025 mg pyridoxine-HCl, 0.1 mg glycine, and 0.005 g myo-inositol, as well as 0.7 g agar in 100 ml. Each medium pH was adjusted to 5.6 before autoclaving. Culture media were placed in baby food jars (25 ml per jar) and six shoot explants were transferred onto the culture medium in each jar. The experiment was conducted with four replications (jars) per treatment combinations. Shoot explants were maintained for 8 weeks with one subculture after 4 weeks.

Table 2. The high, low, and average concentrations of selected minerals N, Ca, and P, as well as zeatin, used in different treatments combinations of culture media for *in vitro* propagation of little-leaf mockorange shoots.

Components	Concentrations		
Zea (µM)	0.82	1.095	1.37
N (mM)	22.5	30	37.5
Ca (mM)	1.125	1.5	1.875
P (mM)	0.31	0.625	0.937
K (mM)	5	10	15

3.3.5. Data collection

Following a two month growth period, explants were harvested, and data collected. Growth parameters evaluated were number of axillary shoots formed, length of the longest shoot on each explant, and shoot dry weight (biomass) for each individual explant. To determine shoot biomass, individual shoots were dried at 70°C for 72 hours and then weighed.

3.3.6. Statistical analysis

Analysis was completed by using a Response Surface regression (SAS, 2016; Proc RSREG) with responses as a function of linear, quadratic, and two-way crossproducts of the factors N, Ca, Zeatin, and P. Due to limited response across its concentration range, K entered the model only as a linear covariate. All factor levels were standardized as (Value – mean)/(½*range) prior to estimation. Standardization, referred to as "coding" in RSM, helps alleviate differences due to changes in component units and magnitude. Separate response surface models were estimated for each response (dependent variables including number of axillary shoots, shoot length, and dry weight). Standard residual diagnostics were used on each model to assess potential outlying values and assure adequate model fit. Following model estimation and assessment, the factor values corresponding to the surface optima (in most cases maximum response) were computed as the critical values necessary to give the highest response value and optimum shoot growth.

3.4. Results

Little-leaf mockorange shoots grew well and produced the most dry weight within the range of minerals and zeatin included within the design of this experiment. Results were presented as predicted multiple design treatment points (based on the Response Surface

Method (RSM) model), hence, interpretation is often carried out through graphical representations presented as the estimated responses over the continuum of component concentrations as defined by the points tested in the design (Reed et al., 2013a). Considering components two at a time, the response surfaces can be displayed two dimensionally as a series of contour plots for each response variable. If the design points encompass an optima, the optimum value of each factor can be determined to be somewhere in the center of contour surface, represented by a circular or elliptical zone. Any value outside this zone, indicates the dependent variable, e.g., shoot growth, failed to grow well due to the imposed treatments.

Although K was tested in this study, this element in the regression models resulted in nonsignificant change in responses. Hence, K concentrations were limited to linear trends in the analyses.

3.4.1. Number of axillary shoots

The regression analysis of the Response Surface for the number of axillary shoot on little-leaf mockorange explants, showed that both linear and quadratic regressions were highly significant with *p* values of 0.0081 and 0.0005, respectively, whereas the crossproduct terms were nonsignificant. Response surfaces were created for pairs of mineral and PGR components as Ca vs. N (Figure 1, top, left), zeatin vs. N (Figure 1, bottom, left), P vs. N (Figure 2, top, left), zeatin vs. Ca (Figure 2, bottom, left), P vs. Ca (Figure 3, top, left), and P vs. zeatin (Figure 3, bottom, left). Both Ca and N show open contour lines for shoot numbers, with maximum responses occurring at the upper limits of the concentrations tested (Figure 1, top, left). This result indicated the optimal shoot growth for these minerals may be at the highest tested levels or higher. The relationship between zeatin and P,

however, was stronger and more definitive, as indicated by Figure 3, bottom, left. The complete circle surface revealed that shoot growth was optimum toward the center of the enclosed zone. Overall, the optimum number of axillary shoots were formed when shoots grew on the combination of 0.6 mM P and 1.1 µM zeatin in the culture medium.

The critical values for each medium component N, Ca, P, and zeatin were 39.28 mM, 2.95 mM, 0.25 mM, and 1.09 µM, respectively. Potassium was assumed to be constant at 10 mM. The predicted response value at this point (optimum point) was estimated as 2.2 axillary shoots.

3.4.2. Shoot length

Response surfaces were generated for Ca vs. N (Figure 1, top, right), zeatin vs. N (Figure 1, bottom, right), P vs. N (Figure 2, top, right), zeatin vs. Ca (Figure 2, bottom, right), P vs. Ca (Figure 3, top, right), and P vs. zeatin (Figure 3, bottom, right). Almost all factors exhibited a strong relationship as indicated by the enclosed contours of the figures.

Response Surface analysis showed that among the regression models only a quadratic regression was significant for shoot length of *in vitro* little-leaf mockorange, ($p < 0.0001$). The critical values for N, Ca, P, and zeatin were estimated as 36.66 mM, 1.89 mM, 0.5 mM, and 1.04 µM, respectively, and the predicted shoot length at the stationary point (optimum) of shoot length was 1.3 cm.

3.4.3. Dry weight

For explant dry weight, only the quadratic regression was significant ($p = 0.0001$). The critical values for N, Ca, P, and zeatin were calculated as 34.08 mM, 2.0 mM, 0.41 mM,

and 1.1 µM, respectively, whereas the predicted dry weight at the stationary point (optimum) was 0.021 g.

Response surfaces are given as Ca vs. N (Figure 4, top, left), zeatin vs. N (Figure 4, top, right), P vs. N (Figure 4, bottom, left), zeatin vs. Ca (Figure 4, bottom, right), P vs. Ca (Figure 5, left), and P vs. zeatin (Figure 5, right). A strong relationship was seen between almost all factors as indicated by the complete contours in the graphical representations. The center of each zone represented the optimum concentration for each selected variable (minerals or zeatin).

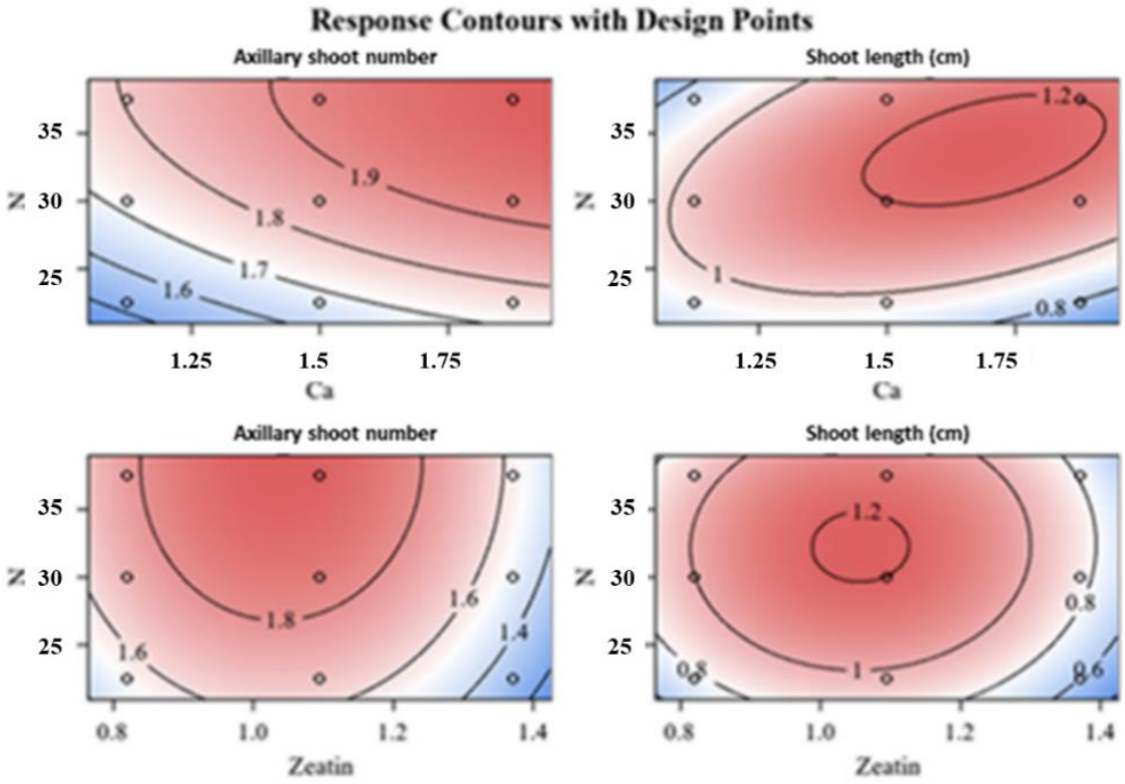

Figure 1. Response surface of N versus Ca (top) or N versus zeatin (bottom) on the number of axillary shoots (left) or shoot length (right) for little-leaf mockorange shoots produced *in vitro*. Blue color indicated poor growth and red demonstrated the optimum growth. Values on contour lines indicate the level of response (shoot number or length (cm)). Values of other tested components when fixed, were zeatin 1.095 µM, P 0.625 mM, K 10 mM, and Ca 1.5 mM.

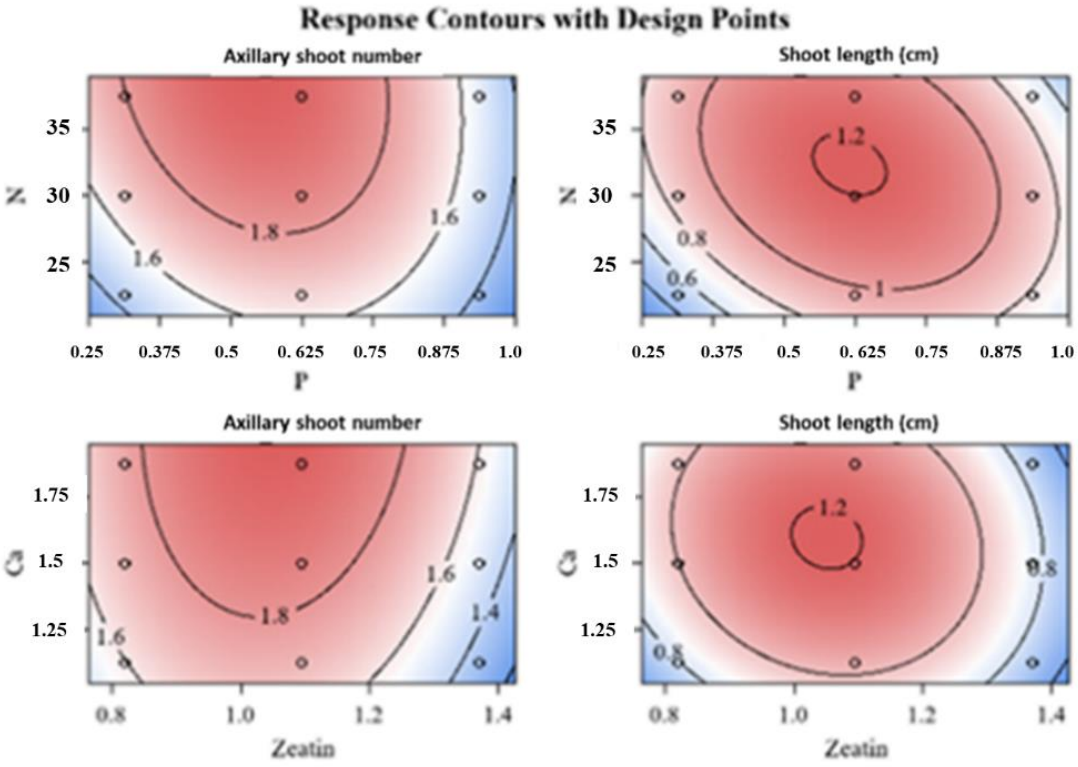

Figure 2. Response surface of N versus P (top) or zeatin versus Ca (bottom) on shoot number (left) and shoot length (right) for little-leaf mockorange shoots produced *in vitro*. Blue color indicated poor growth and red demonstrated the optimum growth. Values on contour lines indicate the level of response (shoot number or length (cm)). Values of other tested components when fixed, were zeatin 1.095 µM, Ca 1.5 mM, P 0.625 mM, K 10 mM, and N 29.95 mM.

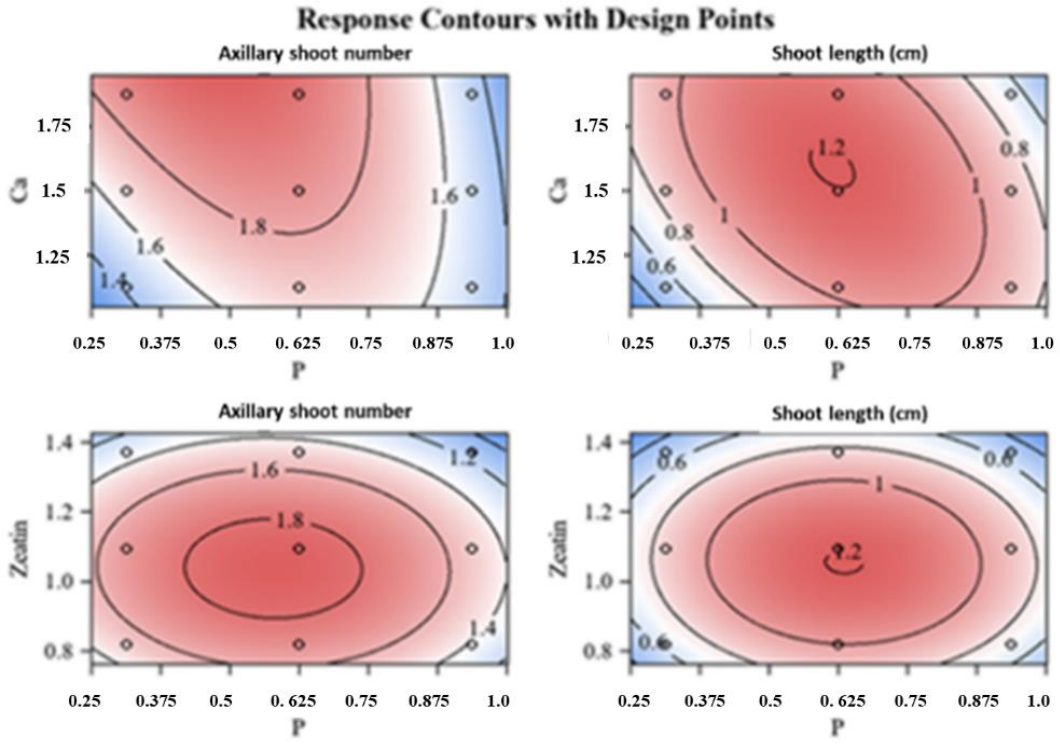

Figure 3. Response surface of P versus Ca effects (top) or P versus zeatin effects (bottom) on shoot number (left) and shoot length (right) for little-leaf mockorange shoots produced *in vitro*. Blue color indicated poor growth and red demonstrated the optimum growth. Values on contour lines indicate the level of response (shoot number or length (cm)). Values of other tested components when fixed, were zeatin 1.095 µM, Ca 1.5 mM, K 10 mM, and N 29.95 mM.

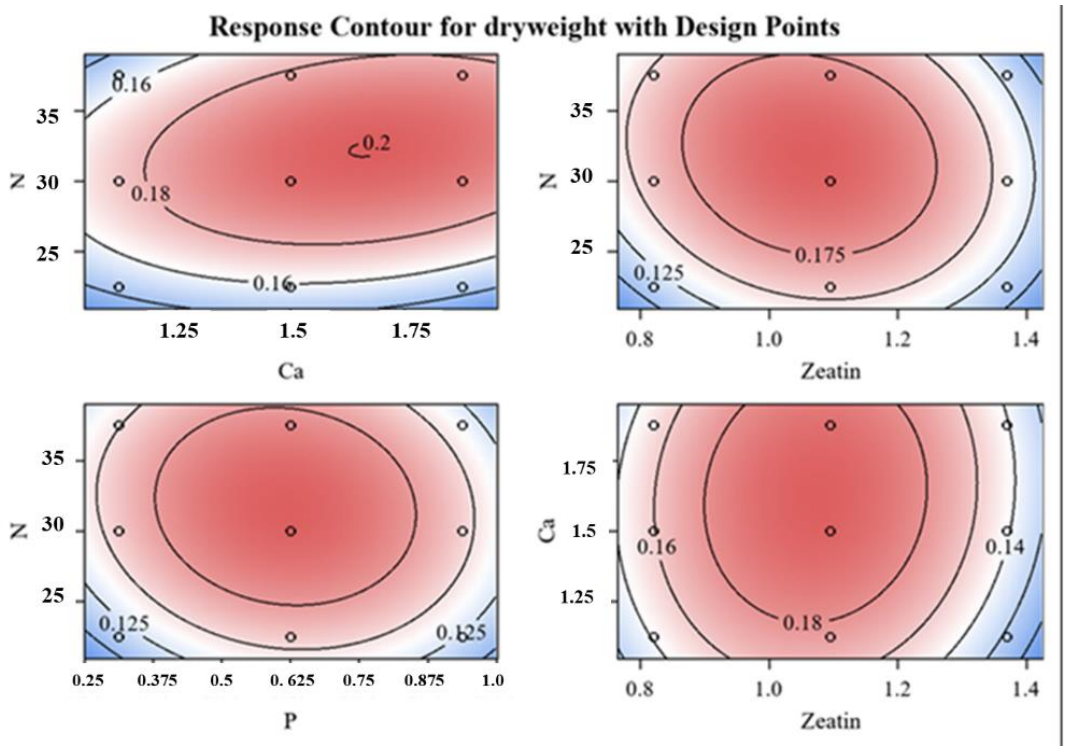

Figure 4. Response surface of N versus Ca effects (top, left), zeatin (top, right), or P (bottom, left), and Zea versus Ca effects (bottom, right) on dry weight for little-leaf mockorange shoots produced *in vitro*. Blue color indicated poor growth and red demonstrated the optimum growth. Values on contour lines indicate the level of response (shoot dry weight (g)). Values of other tested components when fixed, were zeatin 1.095 µM, Ca 1.5 mM, P 0.625 mM, K 10 mM, and N 30 mM.

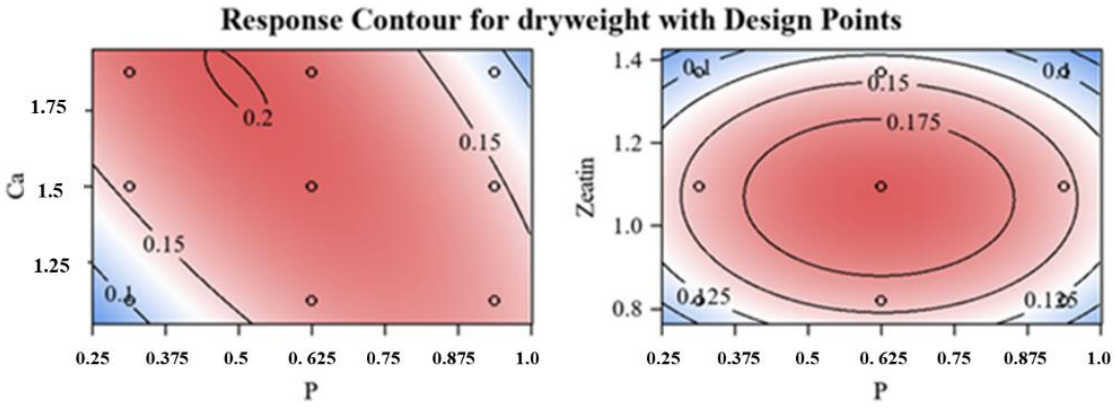

Figure 5. Response surface of P versus Ca effects (left) or zeatin effects (right) on dry weight for little-leaf mockorange shoots produced *in vitro*. Blue color indicated poor growth and red demonstrated the optimum growth. Values on contour lines indicate the level of response (shoot dry weight (g)). Values of other tested components when fixed, were zeatin 1.095 µM, Ca 1.5 mM, K 10 mM, and N 30 mM.

3.5. Discussion

Optimal concentrations of minerals and plant growth regulators in the tissue culture medium are critical for efficacious shoot multiplication. Murashige and Skoog (MS) medium contains all minerals necessary for most plant species. However, some species require modifications to MS basal salts for ideal response. Finding the optimum amount of each mineral or PGR to include in tissue culture media can be time-consuming and expensive, even without considering failed experiments. Response Surface Methods (RSM) is one of the fastest methods of coincidentally testing independent variables in biological experiments (Naghipour et al., 2016). A number of studies have been completed using RSM to modify culture media formulations for different plant species, such as determination of mineral concentrations for efficient propagation of red raspberry (Poothong and Reed, 2014, Poothong and Reed, 2015), to modify the mesos components concentrations in culture medium for pear (Wada et al., 2013), improving the culture medium for micropropagation of pear germplasm (Reed et al., 2013a), and to optimize nitrate and ammonium requirements as well as nitrogen concentrations needed in pear shoot cultures (Wada et al., 2015, Wada and Reed, 2017).

In this study unlike other studies, the response surfaces created by the RSM regression resulted in closed contours with a clear optimum point for most surfaces. This shape in the response surface allowed clear identification of optimum concentration for each component applied in the experiment. A complete circle on the surface response confirmed that the ranges of the applied components in the experiment were selected appropriately with optimum growth falling within the experimental parameters. Based on the results, optimum concentrations of zeatin, N, Ca, or P for maximizing shoot proliferation of little-

leaf mockorange were successfully identified (Table 3). Results of the axillary shoot numbers formed showed that to obtain more axillary shoots and obtaining a more complete circle on the response surface, the concentrations of N and Ca probably needed to be increased.

Results in this experiment are all from this specific little-leaf mockorange species. More experiments are needed to complete for other mockorange species to see if they will grow on the similar tissue culture medium or their requirements are different from little-leaf mockorange.

Table 3. The optimum concentrations of zeatin, N, Ca, or P resulting in the optimal axillary shoot number, shoot length, and dry weight of little-leaf mockorange shoots produced in tissue culture as determined by RSM models.

	zeatin (µM)	N (mM)	Ca (mM)	P (mM)
Axillary shoot number	1 ~ 1.1	≥ 37.5	1.75 ~ 1.875	0.56 ~ 0.625
Shoot length	1.1	32.5	1.75 ~ 1.875	0.625
Dry weight	1.1	30 ~ 32.5	1.75	0.625

3.6. Conclusion

This study determined the optimum concentration of selected minerals (N, Ca, and P) and zeatin in the culture medium used for shoot production of little-leaf mockorange. Based on response surfaces created by RSM quadratic regression models, the optimum concentrations of zeatin, N, Ca, and P were 1.1 µM, 32.5 to 35 mM, 1.875 mM, and 0.625 mM, respectively. Considering these concentrations and comparing them with standard MS medium, little-leaf mockorange shoots should grow well on ½ strength MS medium supplemented with 1.1 µM zeatin for *in vitro* propagation, saving time and money involved in creating a custom medium formulation.

References

Dirr, M.A., Heuser, C.W., 2006. The reference manual of woody plant propagation, from seed to tissue culture, 2nd Ed., 410 pp, *Varsity Press*, Inc.

Murashige, T., Skoog, F., 1962. A revised medium for rapid growth and bioassays with tobacco tissue cultures. *Physiol. Plant.*, 15, 473-497. Available on: https://doi.org/10.1111/j.1399-3054.1962.tb08052.x.

Naghipour, D., Taghavi, K., Jaafari, J., Mahdavi, Y., Ghanbari Ghozikali, M., Ameri, R., Jamshidi, A., Mahvi, A.H., 2016. Statistical modeling and optimization of the phosphorus biosorption by modified *Lemna minor* from aqueous solution using response surface methodology (RSM), *Des. Water Treat.*, 57, 19431-19442. DOI: 10.1080/19443994.2015.1100555.

Niedz, R.P., Evens, T.J., 2007. Regulating plant tissue growth by mineral nutrition. *In Vitro Cell. Dev. Biol. Plant*, 43, 370–38.

Poothong, S., Reed, B.M., 2014. Modeling the effects of mineral nutrition for improving growth and development of micropropagated red raspberries. *Scientia Horticulturae*, 165, 132-141. DOI:10.1016/j.scienta.2013.10.040.

Poothong, S., Reed, B.M., 2015. Increased $CaCl_2$, $MgSO_4$, and KH_2PO_4 improve the growth of micropropagated red raspberries. *In Vitro Cell. Dev. Biol. Plant*, 51:648–658. DOI: 10.1007/s11627-015-9720-y.

Reed, B.M., Wada, S., DeNoma, J., Niedz, R.P., 2013a. Improving in vitro mineral nutrition for diverse pear germplasm. *In Vitro Cell. Dev. Biol. Plant*, 49, 343–355. DOI: 10.1007/s11627-013-9504-1.

Reed, B.M., Wada, S., DeNoma, J., Niedz, R.P., 2013b. Mineral nutrition influences physiological responses of pear *in vitro*. *In Vitro Cell. Dev. Biol. Plant*, 49, 699-709. DOI: 10.1007/s11627-013-9556-2.

SAS Institute Inc., 2016. SAS/ACCESS® 9.4 Interface to ADABAS: Reference. Cary, NC: SAS Institute Inc.

Wada, S., Niedz, R.P., DeNoma, J., Reed, B.M., 2013. Mesos components ($CaCl_2$, $MgSO_4$, KH_2PO_4) are critical for improving pear micropropagation. *In Vitro Cell. Dev. Biol. Plant*, 49, 356–365. Available on: http://dx.doi.org/10.1007/s11627-013-9508-x.

Wada, S., Niedz, R.P., Reed, B.M., 2015. Determining nitrate and ammonium requirements for optimal *in vitro* response of diverse pear species. *In Vitro Cell. Dev. Biol. Plant*, 51, 19–27. DOI: 10.1007/s11627-015-9662-4.

Wada, S., Reed, B.M., 2017. Trends in culture medium nitrogen requirements for *in vitro* shoot growth of diverse pear germplasm. ISHS 2017. *Acta Hort*. 1155, 29-35. DOI: 10.17660/ActaHortic.2017.1155.3.

Chapter 4: Using hyperspectral signatures for predicting foliar nitrogen and calcium content of tissue cultured little-leaf mockorange (*Philadelphus microphyllus* A. Gray)

Abstract

Determining foliar mineral status of tissue cultured shoots can be costly and time consuming, yet hyperspectral signatures might be useful for determining mineral contents of these shoots. In this study, hyperspectral signatures were acquired from tissue cultured little-leaf mockorange foliage to determine the feasibility of using this technology to predict foliar nitrogen and calcium contents. After taking hyperspectral images and determining foliar N and Ca contents, the correlation between the hyperspectral bands, vegetation indices, and hyperspectral features were calculated from the spectra. Features with higher correlations were selected to develop the models via different regression methods. The results showed that non-linear regression models developed through machine learning techniques, including random forest methods and support vector machines provided satisfactory prediction models with high R^2 values (%N by RF with R^2= 0.72, and %Ca by RF with R^2= 0.99), that can estimate nitrogen and calcium content of little-leaf mockorange. Overall, Random Forest regression method provided the most accurate and satisfactory models for both foliar N and Ca estimation of little-leaf mockorange shoots grown in tissue culture.

4.1. Introduction

Hyperspectral sensing is the measurement of the spectral characteristics of materials by the using sensing systems with more than 60 spectral bands and with spectral resolutions less

than 10 nm. This resolution can produce a continuous portion of the light spectrum defining the chemical composition of an object through its spectral signatures (Gomez, 2020). With substantial developments in recording spectral bands of electromagnetic waves, hyperspectral sensors can provide data with a large number of spectral bands due to their high resolution in the range of 350 to 2500 nm, which are acquired by passive optical sensors. Spectral data are detected from any surface that can reflect, absorb, and transmit electromagnetic radiation (Hruška et al., 2018).

Hyperspectral imaging can be used to analyze characteristics that multispectral imaging cannot. Hyperspectral imaging provides the ability to complete reflectance or fluorescence spectroscopy on all single spatial pixels of a spectral image thereby discerning characteristics that cannot be seen by human eyes (Robila, 2004, Gomez, 2020). The basic shape of a curve over the spectral range is characteristic of the parent material of the object being analyzed by spectroscopy (Liang, 2004). In the visible to near infrared (NIR) spectrum (approximately between 400 and 1100 nm), characteristics of water, soil, or plant canopy give rise to specific curvatures in the reflectance spectrum, which makes them recognizable (Liang, 2004, Robila, 2004).

Perhaps the biggest advantage of hyperspectral data over simpler red-green-blue (RGB) imagery and multispectral data is that hyperspectral data can detect more accurate information of the object due to more spectral bands being recorded. Hyperspectral acquisition devices including sensor types, acquisition modes and unmanned aerial vehicle (UAV)-compatible sensors provide information that is needed or used both for research and commercial purposes, (Adão et al., 2017). Hyperspectral sensors and UAV have been useful in many areas of study including material identification, security, precision

agriculture (vegetative coverage, nutrition deficiencies, foliar water content, physiological disorders, etc.), environmental aspects (wetlands, hydrology, etc.), medical and health care (medical diagnoses, food safety, food quality assessment, etc.), landmine detection, and many more applied fields (Adão et al., 2017, Gomez, 2020).

A vegetative index (VI) describes an equation that processes spectral data for the purpose of determining information about plant health. Detectable vegetation indices (VIs) from hyperspectral signatures can provide an estimation and analysis of several plant characteristics, such as biophysical, physiological, or even biochemical parameters in crops, including leaf chlorophyll content (LCC), leaf water content (LWC), leaf area index (LAI), fractional photosynthetically active radiation (FPAR) absorbed by a canopy, surface roughness, and phenology, which are some of the most important inputs to land surface process models (Liang, 2004, Adão et al., 2017, Morcillo-Pallarés et al., 2019). These VIs can be applied in the regression models to help estimating plant status, such as foliar mineral contents.

4.1.1. Nutrient status and deficiency prediction

With the importance of nitrogen increasing yield efficiency and crop health, modern application of hyperspectral signatures in preventing nitrogen deficiencies in field have become widespread. Hence, much research has been conducted using remote sensing and applying hyperspectral signatures to determine crop nitrogen deficiency, required rates of fertilizers to increase crop production, or even the amount of nitrogen uptake by plants to improve agricultural production and yield efficacy (Maes and Steppe, 2019). De Oliveira et al. (2017) applied selected vegetation indices to estimate foliar N concentration in three Eucalyptus tree clones. Liu et al. (2016) applied multiple linear regression and neural

network analysis to find a relationship between the leaf nitrogen content of winter wheat and vegetative indices in narrow bands. Other studies have used hyperspectral indices to check the nutrition status of sodium and potassium content in grass (Capolupo et al., 2015), potassium deficiency level in canola (Severtson et al., 2016), the nitrogen concentration in oat (Van Der Meij et al., 2017), corn (Gabriel et al., 2017), rice (Wen et al., 2018), and wheat (Zhu et al., 2018), and leaf N, P, K, Ca, Mg, and few micronutrients of corn and soybean (Pandey et al., 2017).

Putting a new plant species into tissue culture medium may require adjusting the medium components to optimize desirable shoot growth from the new species. Finding the optimum concentration of each component is critical and requires time and money. Estimating an explant's foliar mineral status to check their health status is important to attain optimal *in vitro* growth. Usually, destructive methods are applied to estimate foliar mineral contents, especially for tissue cultured plants. Finding nondestructive methods, such as applying hyperspectral signatures can help growers to reduce their cost and save time.

To date, reports on using hyperspectral devices and hyperspectral vegetation indices in tissue culture environments are lacking. To check the feasibility of using of this technology to evaluate the mineral content of tissue cultured little-leaf mockorange shoots, I decided to use the ASD spectroradiometer during the shoot proliferation stage of micropropagation, to determine if this technique could help in estimating nutrition status of the explants during stage 2 of micropropagation. If hyperspectral imaging showed success, it can help tissue culture producers saving time and money by avoiding destructive methods of foliar nutrient analysis.

4.2. Materials and Methods

4.2.1. Plant materials and tissue culture

Little-leaf mockorange explants were grown on half strength Murashige and Skoog (½ MS) medium supplemented with different plant growth regulators (cytokinins such as zeatin, kinetin (Kin), benzylamino purine (BA), *meta*-Topolin (MT), thidiazuron (TDZ), or dimethylallylamino purine (2iP)) or different concentrations of minerals such as N (0, 15, 22.5, 30, 37.5, 45, or 60 mM), Fe (0, 0.5, 5, 25, 50, 75, 100, or 500 µM). Six stem explants (per jar) were placed on the culture media in baby food jars (195 ml) containing 0.5 mg thiamine-HCl, 0.25 mg nicotinic acid, 0.25 mg pyridoxine-HCl, 1 mg glycine, and 0.05 g myo-inositol, with pH = 5.6. Explants were incubated in a SG-30S germinator (Hoffman Manufacturing Inc., Albany, OR) at 25 ± 1°C under a 16-h photoperiod (cool-white fluorescent lamps), with 38 $\mu mol \cdot m^{-2} \cdot s^{-1}$ photosynthetic photon flux (PPF), for 8 weeks with one subculture onto the fresh media after the 4th week. At the end of the week eight, explants were harvested for collection of growth data and measurement of hyperspectral signatures.

4.2.2. Preparing the spectroradiometer and taking readings

For this research I used either an Analytical Spectrum Devices FieldSpec 4 High-Resolution spectroradiometer (Malvern Panalytical Ltd., Westborough, MA, USA) or an Analytical Spectrum Devices FieldSpec HandHeld-2 spectroradiometer (Analytical Spectral Devices Company, Boulder, CO, USA). After 30 minutes of spectroradiometer warm up, the device was optimized and calibrated with Spectralon white panel. During calibration, an average of 100 dark current measurements were calibrated together and an average of 50 scans of a Spectralon 99% white reference were measured every two minutes

(Labsphere Inc., North Sutton, NH, USA) (Beck, 2019). Target reference recordings displayed an average of 20 scans at an optimized integration time of approximately 1 second.

Reflectance readings of explant leaves were made immediately (within 2 minutes) after they were taken out of the jar and prior to completion of the reflectance spectra procedure. Measurements were completed in a dark-room and conducted on a black-colored bench to exclude external light and reduce outside errors. The probe was held about 5 to 10 cm over the explants to take the reflectance. Measurements were taken on all six plantlets that were grown within each culture jar. Three duplicate readings were recorded for each shoot to reduce error effects. After every 10 to 12 readings, a new calibration was completed to reduce the error from external white light. All measurements were acquired using RS3 software version 6.4 (Malvern Panalytical Ltd., Westborough, MA, USA).

Reflectance spectral data represented the full range of visible (Vis), near infrared (NIR), and short wave infrared (SWIR) light between 350 and 2500 nm, with a resolution of 1 nm. The spectral sampling interval was automatically interpolated from 1.4 nm to 1 nm at the time of each individual measurement by RS3 software, so a single value for each wavelength from 350 to 2500 nm was recorded (Beck, 2019). Data were exported by the ViewSpec Pro software version 6.2. The average of three readings of the reflectance from the group of six explants per container was used to create a single treatment reflectance spectrum.

4.2.3. Tissue analysis for mineral content

After taking the hyperspectral reflectance, the shoots were separated from the agar medium, placed in an envelope and dried in an oven at 70°C for 72 hours. Dried shoots were ground using a pestle and mortar. Dried tissues were sent to the tissue analysis lab (Brookside Laboratories, Inc., New Bremen, OH) for foliar nutrient analysis. There, tissue analysis was completed by using a combustion method employing a Carlo Erba 1500 C/N analyzer to estimate total N content (method B2.20, Miller et al., 2013). For Ca, lab procedures entailed use of nitric acid and hydrogen peroxide in a closed Teflon vessel and digested in a CEM Mars Microwave and analyzed on a Thermo 6500 Duo ICP (method B4.30, Miller et al., 2013). Results from foliar analyses were used for correlation model training with the hyperspectral signatures.

4.2.4. Feature generation

When developing regression models, the success is dependent on the number of features assigned within the feature space. The number of features used becomes more critical when hyperspectral datasets are used due to their large number of spectral bands, making it difficult to determine if spectral bands or spectral vegetation indices generated from spectral bands or both, are associated with foliar chemical or physiological status, or in this case, leaf mineral content. To answer this question, feature selection approaches have been suggested to train the model with fewer but more informative features.

4.2.4.1. Continuum removal and feature selection

To normalize reflectance spectra and compare individual absorption features from a common baseline, I used continuum removal. To use continuum removal, spectral features

were acquired and selected by using MATLAB software. Different SVIs were calculated from the spectral wavelengths and accumulated in a spread sheet. Applying RStudio version 2021.09.0. and R version 4.1.2, statistical tests were completed for correlation and *p*-values, for each hyperspectral band feature and the corresponding mineral contents received from tissue analysis.

4.2.5. Correlation tests

Pearson's correlation coefficient is the covariance of the two variables divided by the product of their standard deviations (Freedman et al., 2007). Pearson correlation coefficient was used so that features with high correlation values were first recognized and selected from the list of defined features. Numerically, Pearson correlation coefficient should be between +1 and -1. If Pearson correlation coefficient of two variables is zero or close to zero, a correlation is lacking between the two variables. If two variables have a positive coefficient close to one, the variables are directly related to each other and only one of them should be imported for regression or classifier (an algorithm that implements classification, especially in a concrete implementation). A negative coefficient close to one indicates the inverse relationship between the two variables.

4.2.6. Model development

Informative features for spectral signatures were identified for tissue cultured shoots. The next step was to 1) train the model by using machine learning methods and 2) validate their significance using test data.

4.2.6.1. Applied machine learning (ML) methods

- Linear Regression Method: is a linear model, that assumes a linear relationship between the input variable (x) and the single output variable (y).
- Random Forest Regression: RF is a supervised learning algorithm that uses ensemble learning method for regression.
- Support-Vector Machines: SVM are supervised learning models with associated learning algorithms that analyze data for classification and regression analysis.

To manage the results, the following procedures involved separately adding variables into the model and then calculating the coefficient of determination (R^2), root mean square error (RMSE) and correlation coefficient (Corr); next, a combination of variables were added to the model (multiple-inputs) and then new calculations for R^2, RMSE and Correlation were made. The best model was chosen by comparing the results and using the best R^2 and correlation values and by using error plots and scattering plots. These plots showed the error between observed and estimated values and a scatter plot of observed vs estimated values, respectively.

4.2.6.2. Data partitioning

Data sets were divided into model training and model test groups for generating the optimum regression model. Data partitioning or splitting data sets (hyperspectral recorded samples) into training and sample (test) group was one of the crucial steps in regression. To do this, the “createDataPartition” function in R software (packages “randomForest”, “neuralnet”, “rsample”, “ipred”, “readxl”, “hutils”, “xgboost”, “readr”, “stringr”, “gbm”, “class”, “FNN”, “e1071”, “caret”, and “caTools”) was used to randomly choose sample

indices based on a determined percentage. In our case 39 samples out of 56 samples (70%) were used for model training and the rest of samples were used for model testing (17 samples out of 56 samples). The training data set was then used to develop a model with wavelengths in the spectral signature and vegetation indices calculated from those spectral signatures, as well as generated features obtained from those spectral signatures correlated to the foliar nutrient content from lab analysis. The developed model was validated and evaluated by using test datasets.

4.2.7. Model evaluation criteria

To validate the performance of the model, three criteria were used; the correlation between observation values and estimated values, the RMSE (root mean square error), and correlation coefficient (R^2).

A schematic diagram of the methods used for developing a regression model from the hyperspectral bands and the mineral content in little-leaf mockorange shoots, is shown in Figure 1. All the evaluation criteria were calculated separately for foliar N or Ca contents.

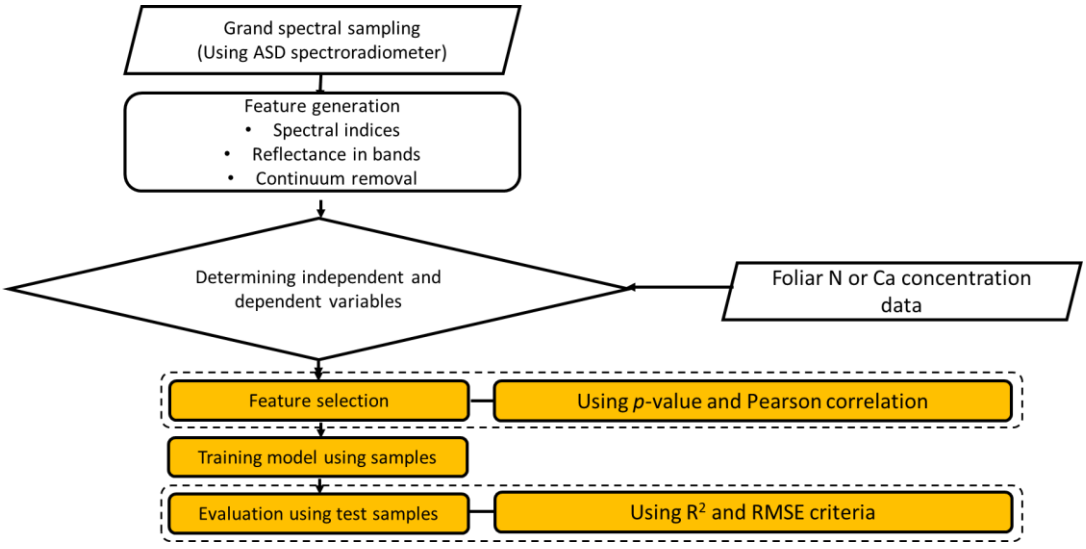

Figure 1. Schematic diagram of model development from hyperspectral bands and foliar mineral analysis for little-leaf mockorange shoots grown in tissue culture.

4.3. Results

4.3.1. Vegetation indices calculation and feature generation

Applicable vegetation indices (VI) were calculated using MATLAB (Table 1). Using MATLAB, different features were generated and calculated selecting 15 individual wavelength ranges from the hyperspectral bands. Range selection was completed based on the peaks and curvatures of the spectra. Then, dividing the spectra into 15 ranges (Table 2), specific features within these ranges, such as area under the peaks (Area), asymmetric point (asymmetry of absorption shape, a geometric feature generated from continuum removal) (Asy), minimum external peak (Min), and maximum external peak (Max) were calculated throughout the spectra.

Both VIs and features were saved in an Excel file for later mineral content predictions by the developed model.

Table 1. The highest correlated vegetation indices determined by using hyperspectral imaging in this study (Data obtained and calculated from Anonymous, Index Data Base, 2021).

Index Name	Abbreviation	Formula
Cellulose Absorption Index	CAI	$CAI = 0.5\ (\rho_{2000} + \rho_{2200}) - \rho_{2100}$
Normalized difference vegetation index	NDVI	NDVI = (Bnear_IR - Bred) / (Bnear_IR + Bred)
Leaf Area Index	LAI	LAI = leaf area / ground area
Double Peak Index	DPI	DPI= 688nm+710nm / $697nm^2$
Normalized Difference Water Index	NDWI	NDWI = (Bnear_IR - Bmiddle_IR) / (Bnear_IR + Bmiddle_IR)
Normalized Difference Lignin Index	NDLI	$NDLI = \frac{\log\left(\frac{1}{\rho 1754}\right) - \log\left(\frac{1}{\rho 1600}\right)}{\log\left(\frac{1}{\rho 1754}\right) + \log\left(\frac{1}{\rho 1600}\right)}$

Table 2. Fifteen wavelength ranges taken from spectra extracted from little-leaf mockorange shoot cultures by using a ASD spectroradiometer.

Range number	From (Lower wavelength (nm))	To (Higher wavelength (nm))
1	364	369
2	378	559
3	559	772
4	838	843
5	898	903
6	928	1057
7	1121	1258
8	1287	1670
9	1670	1714
10	1714	1819
11	1819	2150
12	2253	2332
13	2341	2389
14	2389	2419
15	2428	2490

4.3.2. Foliar nitrogen content

4.3.2.1. Extraction of spectral bands with higher correlation with N content

After calculating the correlation between the hyperspectral signatures and the %N in shoot tissues, the wavelengths at 648 to 651 nm were shown to have a moderately high correlation with %N with correlation value of 0.30 (Figure 2).

4.3.2.2. Model development

Results showed that the reflectance values at the wavelength of 648 nm, asymmetric point from 1819 to 2150 nm (Asy 11) and the area from 559 to 772 nm (Area 3) had correlation values of 0.30, 0.31 and 0.37 with %N content, and these spectral features provided information needed for predicting the %N to generate a linear model for N content measurement.

$$\%Nitrogen = 4.47*(Asy\ 11) - 3.45$$

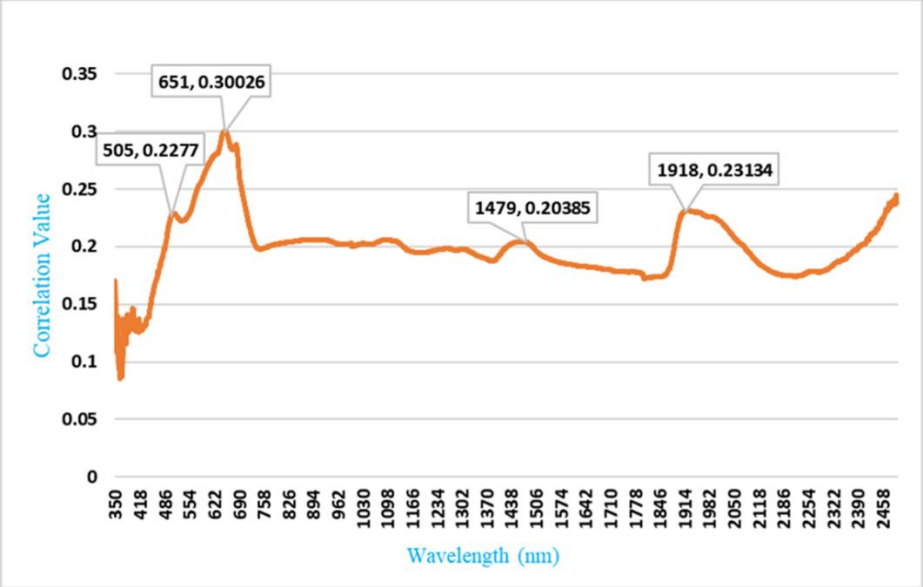

Figure 2. Correlation between leaf N% and the hyperspectral signatures acquired by ASD spectroradiometer from tissue cultured little-leaf mockorange shoots. The boxes show the correlation value and the wavelength of the peak in the spectrum.

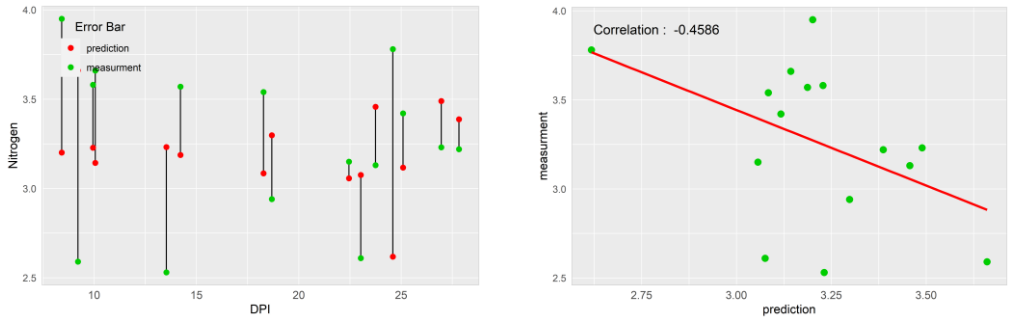

Figure 3. Error bar plot and scatter plot of the correlation between observed and estimated %N of little-leaf mockorange shoots by a linear regression model.

Based on these spectral data, N content acquired by a linear model was estimated by R^2 = 0.21, root mean square error (RMSE) = 0.54 and correlation = -0.45 (Figure 3).

Results from Random Forest (RF) algorithm model showed that the reflectance values at the wavelength of 2480 nm, asymmetric point from 1819 to 2150 nm (Asy 11) and the area from 559 to 772 nm (Area 3) had correlation values of 0.32, 0.31 and 0.37 with N% content. Based on these results, the RF regression model revealed that asymmetric point from 1819

to 2150 nm (Asy 11), asymmetric point from 559 to 772 nm (Asy 3), the reflectance values at the wavelength of 2480 nm, reflectance at wavelength of 525 nm, and Double Peak Index (DPI) were the most effective features to generate a nonparametric (non-linear) model (Figure 4).

By testing various models with different combinations of the mentioned features and/or indices, eventually the most accurate model was selected (Table 3). The fitted model with DPI index and reflectance at wavelength of 525 nm and the tree number of 5 was a more accurate model fitted by RF regression, with R^2 = 0.72 and RMSE = 0.30, and correlation = 0.84 (Figure 5).

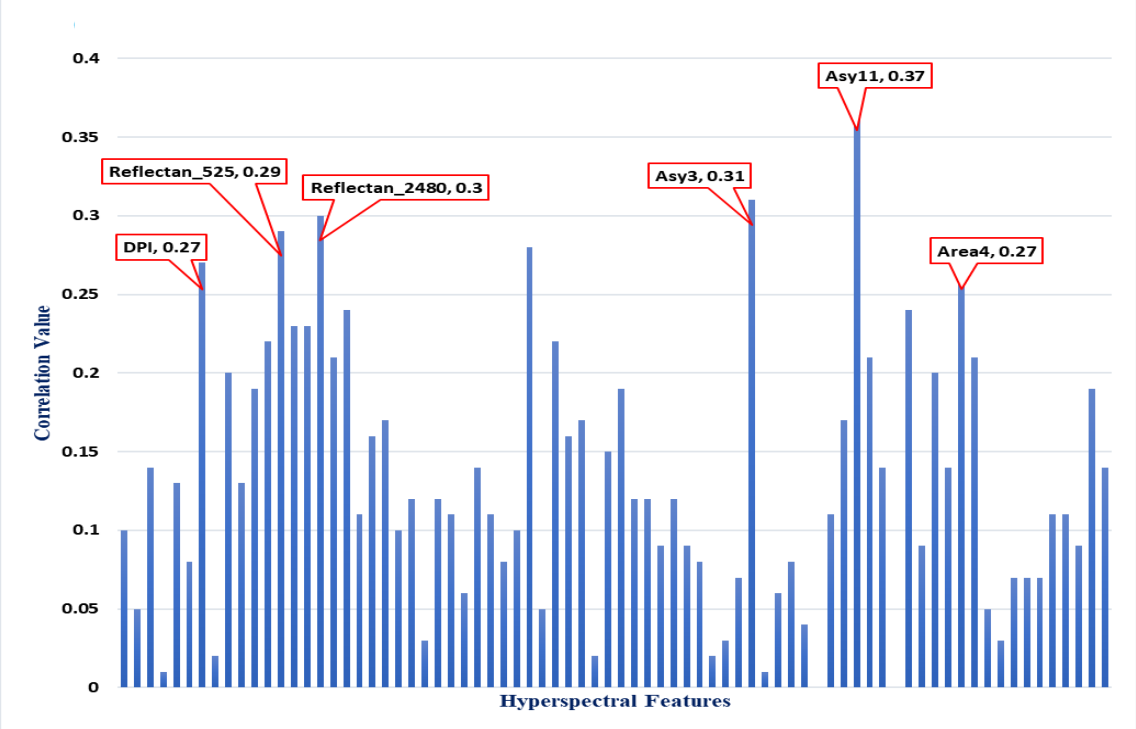

Figure 4. Correlation value between features or vegetation indices (VIs) and leaf nitrogen content of tissue cultured little-leaf mockorange.

Results also showed that the model generated by support vector machine (SVM) regression provided an acceptable estimation of foliar %N content in comparison with a linear model and the fitted SVM model including Double Peak Index (DPI) with asymmetric point from

1819 to 2150 nm (Asy 11) (Table 4), followed by a model including DPI with asymmetric point from 559 to 772 nm (Asy 3), provided an approximate accurate method to estimate foliar N content, respectively at R^2 = 0.58 and RMSE = 0.32 (Figure 6), or R^2 = 0.61 and RMSE = 0.33 for little-leaf mockorange shoots.

Table 3. Various models developed for %N estimation in little-leaf mockorange shoots with different feature combinations and different number of trees via Random Forest algorithm.

Features (N)	ntree = 5			ntree = 50			ntree = 100		
	R^2	RMSE	Correlation	R^2	RMSE	Correlation	R^2	RMSE	Correlation
2 features (DPI + Reflectance 525)	0.72	0.30	0.84	0.37	0.61	0.43	0.22	0.59	.
2 features (DPI + Asy11)	0.78	0.72	.	0.60	0.64	.	0.58	0.64	.
2 features (DPI + Asy3)	0.73	0.86	.	0.49	0.72	.	0.39	0.74	.

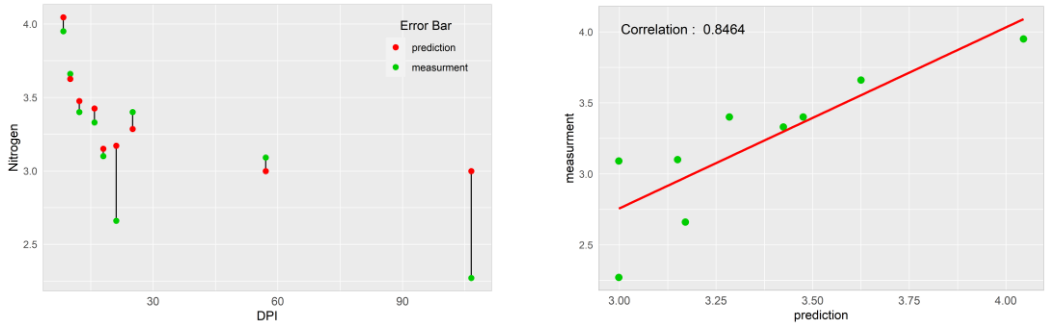

Figure 5. Error bar plot and scatter plot of leaf %N estimated and measured test samples for little-leaf mockorange shoots via Random Forest regression.

Table 4. Various models developed for %N estimation of little-leaf mockorange shoots with different feature combinations and different penalty terms via SVM algorithm.

Features (N)	cost = 10			cost = 50			cost = 100		
	R^2	RMSE	Correlation	R^2	RMSE	Correlation	R^2	RMSE	Correlation
2 features (DPI+ Asy11)	0.58	0.32	0.76	0.58	0.32	0.76	0.58	0.32	0.76
2 features (DPI+ Asy3)	0.61	0.33	0.78	0.61	0.33	0.78	0.61	0.33	0.78
2 features (DPI+ Area4)	0.56	0.34	0.75	0.56	0.34	0.75	0.56	0.34	0.75

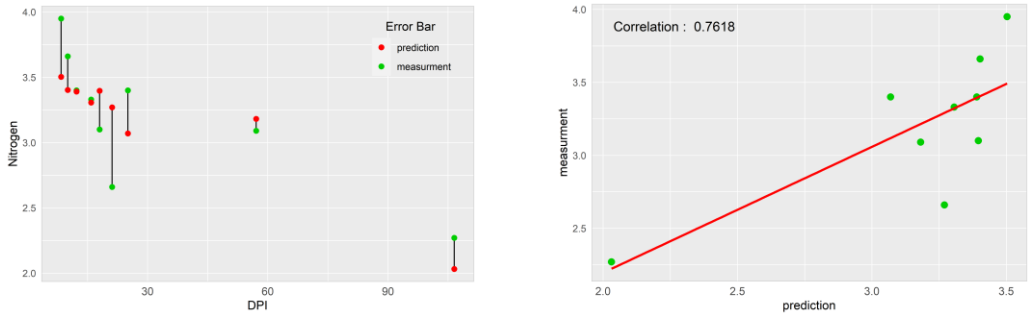

Figure 6. Error bar plot and scatter plot of leaf %N estimated and measured test samples for little-leaf mockorange shoots via Support Vector Machines regression.

4.3.3. Foliar calcium content

4.3.3.1. Extraction of spectral bands with higher correlation with Ca content

After analysis of the hyperspectral bands and checking for their correlation with the Ca content of the shoots received from the tissue analysis, I selected the bands with higher correlations, and those were 721 nm, 541 nm, 1293 nm, 1805 nm, and 2209 nm, respectively with correlation values of 0.35, 0.33, 0.30, 0.28, and 0.26 (Figure 7).

Examining the correlation values between %Ca with different features and VIs, spectra showed that the minimum external of the wavelength between 1819 to 2150 nm (Min 11), and minimum external wavelength between 1287 to 1670 nm (Min 8) had the highest correlation values with Ca, respectively 0.59 and 0.45 (Figure 8).

4.3.3.2. Model development

Results from model development showed that Ca content determined by a linear model consisted of parameters of minimum external wavelengths between 1819 to 2150 nm (Min 11) and the area from 559 to 772 nm (Area 3) could be estimated by $R^2 = 0.83$ and RMSE = 0.09. Nevertheless, the coefficient of Area 3 was low enough to ignore it to draw the error bar graph (Figure 9).

$$\%Calcium = 1.13*(Min11) + 0.08$$

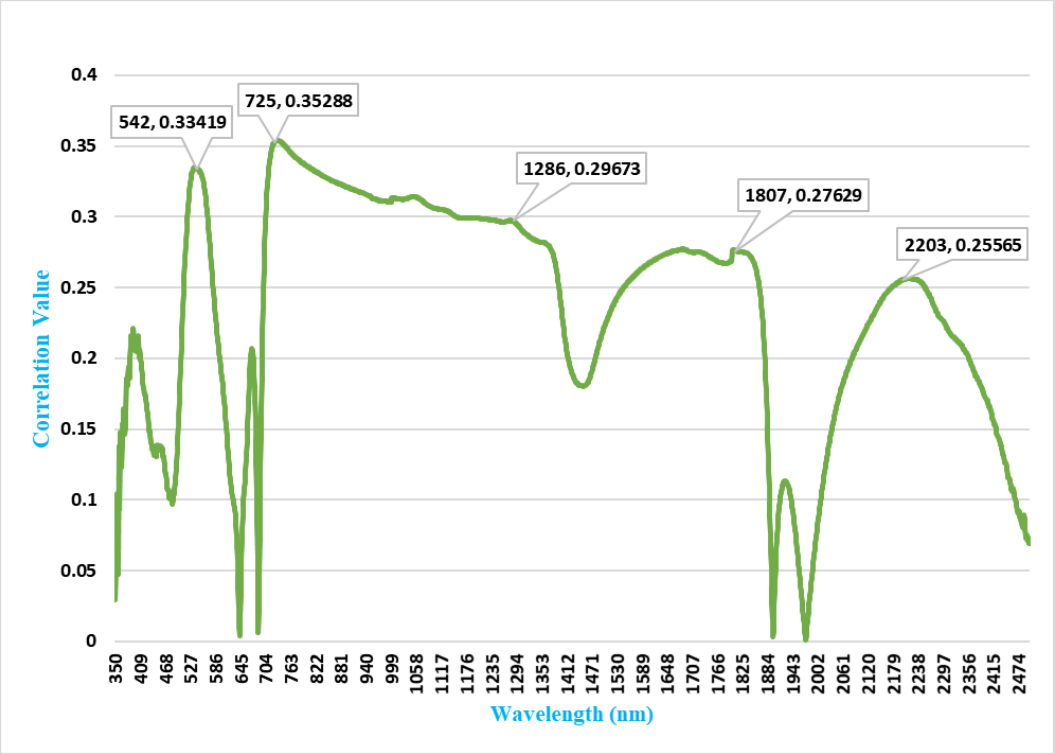

Figure 7. Correlation between leaf %Ca and the hyperspectral signatures acquired by the ASD spectroradiometer from tissue cultured little-leaf mockorange shoots.

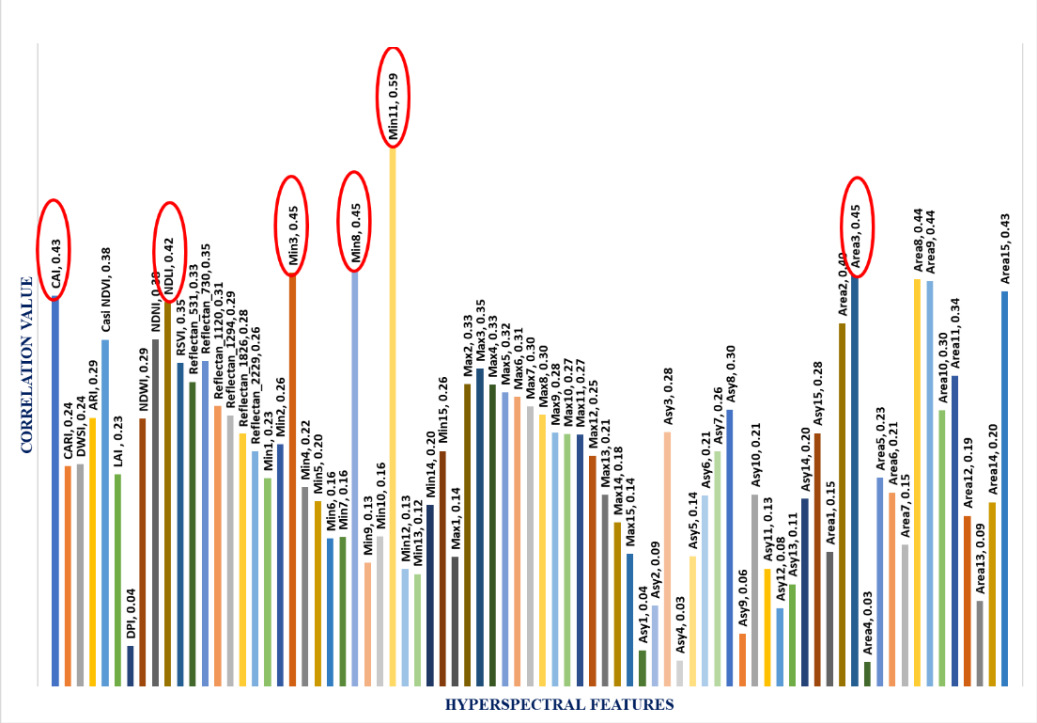

Figure 8. Correlation value between features and VIs with leaf calcium content of little-leaf mockorange shoots.

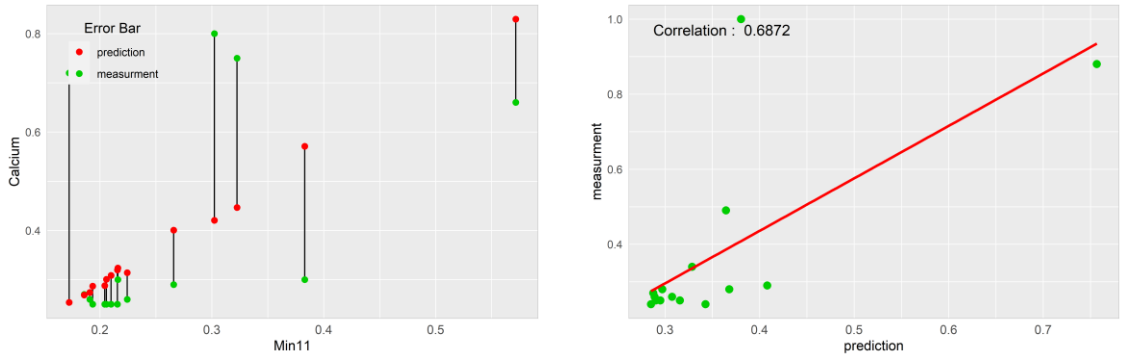

Figure 9. Error bar plot and scatter plot of the correlation between observed and estimated %Ca of little-leaf mockorange shoots by linear regression model.

The Random Forest algorithm provided a successful model to estimate the %Ca of little-leaf mockorange shoots. After examining several models with different feature combinations and tree number, results showed that the model including four features of minimum reflectance from 838 to 843 nm (Min 4), area from 2428 to 2490 nm (Area 15), asymmetric point from 1670 to 1714 nm (Asy 9), and Cellulose Absorption Index (CAI), with the tree number of 5 were the most effective features to generate a nonparametric (non-linear) model (Figure 10, Table 5), giving $R^2 = 0.99$ and RMSE = 0.03 and correlation value = 0.99 (Figure 11, right).

The results showed that using the specific spectral features and a selected index (CAI) acquired from the random forest algorithm as best to use in model development. These features were also used to develop a fitted model for SVM regression. After developing and running several models with different penalty terms (costs = 10, 50, or 100) and different kernels (linear, polynomial, or radial) (Table 6), eventually a model via linear kernel, including all four features of minimum reflectance from 838 to 843 nm (Min 4), area from 2428 to 2490 nm (Area 15), asymmetric point from 1670 to 1714 nm (Asy 9),

and Cellulose Absorption Index (CAI) with R^2 = 0.59 and RMSE = 0.16 were determined to be the better model, regardless of the penalty term (cost value) (Figure 12).

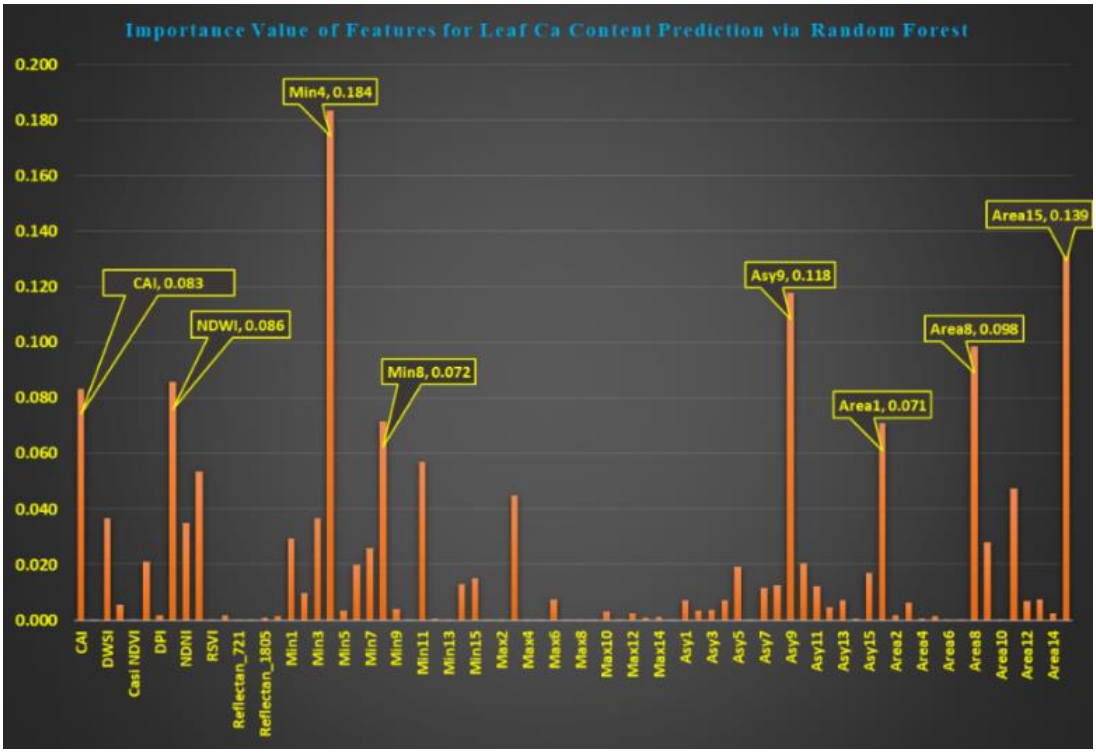

Figure 10. The importance value of generated features and selected VIs regarding leaf %Ca in little-leaf mockorange shoots via Random Forest algorithm.

Table 5. Various models developed for %Ca estimation in little-leaf mockorange shoots with different features combinations and different number of trees via Random Forest algorithm.

Features	ntree = 5			ntree = 50			ntree = 100		
	R^2	RMSE	Correlation	R^2	RMSE	Correlation	R^2	RMSE	Correlation
2 features (Min4+Area15)	0.99	0.06	0.96	0.95	0.09	0.95	0.95	0.1	0.96
3 features (Min4+Area15+CAI)	0.98	0.04	0.93	0.89	0.09	0.93	0.87	0.09	0.98
4 features (Min4+Area15+Asy9+CAI)	0.99	0.03	0.99	0.92	0.08	0.96	0.85	0.1	0.92

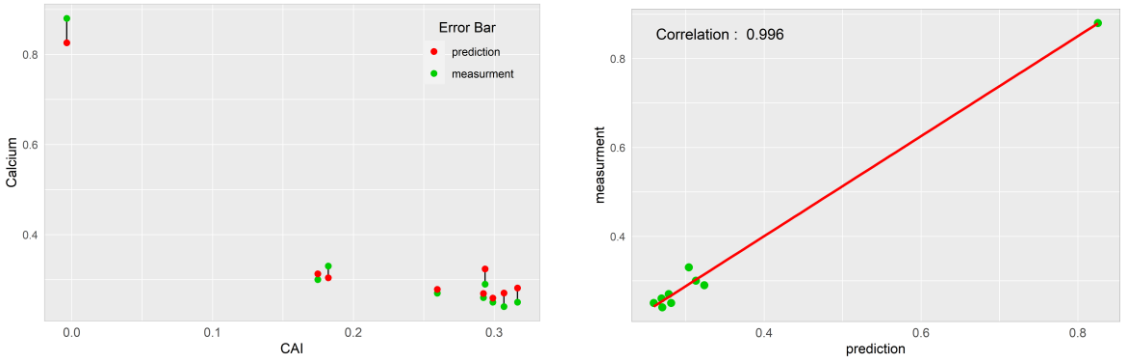

Figure 11. Error bar plot (left) and scatter plot (right) of leaf %Ca estimated and measured test samples in little-leaf mockorange shoots via Random Forest algorithm.

Table 6. Various models developed for %Ca estimation of little-leaf mockorange shoots with different feature combinations and different penalty terms via SVM algorithm.

Features	cost = 10			cost = 50			cost = 100		
	R^2	RMSE	Correlation	R^2	RMSE	Correlation	R^2	RMSE	Correlation
2 features (Min4+CAI)	0.57	0.17	0.75	0.57	0.17	0.75	0.57	0.17	0.75
3 features (Min4+Area15+Asy9)	0.18	0.22	0.42	0.18	0.22	0.42	0.18	0.22	0.42
3 features (Min4+Area15+CAI)	0.51	0.18	0.71	0.51	0.18	0.71	0.51	0.18	0.71
4 features (Min4+Area15+Asy9+CAI)	**0.59**	**0.16**	**0.76**	0.58	0.16	0.76	0.58	0.16	0.76

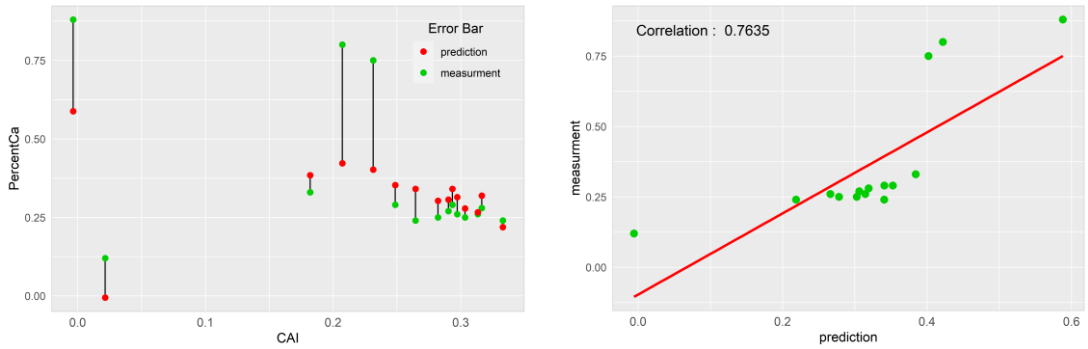

Figure 12. Error bar plot and scatter plot of leaf %Ca estimated and measured test samples for little-leaf mockorange shoots via Support Vector Machines regression.

4.4. Discussion

This research demonstrated that hyperspectral imaging can be used to predict the percentages of N and Ca in little-leaf mockorange shoots produced in tissue culture. Among the three developed regression models used to estimate and predict the foliar

nitrogen content, random forest regressions and SVM, could estimate %N more accurately than the linear regression model. Nevertheless, the models developed to predict %N were a little less accurate than those developed for predicting %Ca in the tissue cultured shoots.

In this study, the linear, Random Forest (RF) and support vector machines (SVM) regression procedures were used to obtain an accurate model to estimate the %N and %Ca in little-leaf mockorange shoots produced in tissue culture. For N, both RF and SVM gave better models than linear model, whereas RF (tree number = 5) could estimate %N better than SVM (no matter what the cost was for this regression model). For %Ca, RF model had a higher R^2 (0.99) and lower RMSE (0.03) was more successful for providing a satisfactory model than SVM with R^2 (0.59) and RMSE (0.16). Finding the best regression model and the best features or indices as well as the best wavelengths throughout the hyperspectral bands is highly important for predicting a specific mineral content or other plant characteristics, such as water content.

Although the linear regression model provided an acceptable R^2 value, the model failed to predict %Ca. Hence, random forest and SVM regression models were alternately considered. Based on the results obtained from this research, I concluded that foliar %Ca content could best be estimated using a non-linear regression model rather than a linear model. Optimal prediction features included minimum reflectance from 838 to 843 nm (Min 4), area from 2428 to 2490 nm (Area 15), asymmetric point from 1670 to 1714 nm (Asy 9), and Cellulose Absorption Index (CAI). Although these features worked for both RF regression model and SVM regression model, the RF regression had stronger R^2 and correlation, and therefore was a better model to estimate the %Ca of tissue cultured shoots of little-leaf mockorange.

Cellulose is an important component in the structure of primary cell wall of green plants (Anonymous, Wikipedia, 2021). Calcium interacts with cellulose as a cellular structural component. A high correlation between %Ca and cellulose absorbance index (CAI) is likely due to this relationship, and in the future more detailed experiments can be conducted to determine any possible relationship between %Ca and CAI index.

To date, no report has been issued using hyperspectral images to estimate shoot mineral contents of plants produced in tissue culture (*in vitro*). Some studies, however, have been conducted to estimate N content of agronomic crops in the field, such as estimating N in winter wheat at different growth stages, based on near infrared (NIR) wavelengths, via multivariate linear regression and Back Propagation (BP) neural network using vegetation indices (Liu et al., 2016); estimation of leaf N content of winter wheat via selected spectral indices and around NIR wavelengths (Zhu et al., 2018); estimating N content in field potatoes in NIR (Clevers and Kooistra, 2012); N estimation in maize via VIs such as NDVI, Renormalized difference vegetation index (RDVI) or Optimized soil-adjusted vegetation index (OSAVI) (Gabriel et al., 2017); N estimation in rice with Gaussian process regression (GPR) model (Wen et al., 2018); N estimation of eucalyptus using NDVI in red-edge and modified red-edge NDVI (De Oliveira et al., 2017); and estimation of macro- and micro nutrients such as N and Ca in soybean and maize via partial least squares regression (PLSR) models (Pandey et al., 2017).

Although some reports, describe use of NIR or lower SWIR wavelengths to provide effective estimates of N, almost all of these studies have used only vegetation indices such as NDVI or other VIs. The difference between my study and other studies was application of different geometric features, such as maximum reflectance, minimum reflectance, area

under the spectrum, and asymmetric point of the spectrum alongside the reflectance spectrum acquired from little-leaf mockorange shoots. Applying these geometric features for plants grown in an *in vitro* environment, nevertheless, resulted in satisfactory R^2 and RMSE values obtained from the regression models used to predict N and Ca contents in the shoots.

The interesting aspect of %N and %Ca estimation was that both were predictable in spectrum ranges from 1819 to 2150 nm (Range 11) and from 559 to 772 nm (Range 3). Using different features of these ranges provided information for each of these two minerals in little-leaf mockorange shoots. In addition, correlation plots of estimated and measured values for N and Ca concentrations, revealed a small gap between higher concentrations and lower concentrations of these two minerals, probably due to the limited number (less than 100) of samples used for predicting their concentrations. The other possibility for the gap was that hyperspectral images could estimate N or Ca only at higher concentrations, due to the tiny size of the leaves and stems on the shoot cultures, meaning less information was acquired from their reflectance.

A deeper look at the scatter plot of %Ca obtained from the RF algorithm (Figure 11, error bar plot), showed that samples with values higher than 0.15 of CAI features, had much lower differences between the measured and estimated values compared to the differences between measured and estimated values of CAI less than 0.15. This result indicated that for a more accurate prediction, features with higher correlation values must be selected. On the other hand, except for two samples (error bars shown in Figure 11, left), the developed model either accurately estimated or slightly over-estimated %Ca.

Most of the earlier foliar nutrient content studies have used mostly the vegetation indices to estimate canopy minerals especially N. Unfamiliarity with hyperspectral features relative to prediction of foliar mineral status may be a limitation on employment of this technique in comparison with vegetation indices. Recruitment of a team of plant scientists, plant nutritionists, and hyperspectral scientists, may provide opportunity to apply these features more effectively. This study illustrates the potential for success of such a team of a plant scientists and hyperspectral scientists.

This study showed that hyperspectral imaging could help to predict foliar nutrient contents (N and Ca particularly) of little-leaf mockorange shoots produced in tissue culture, and help to avoid destructive methods of foliar mineral analysis. This nondestructive method, can save tissue culture producers time necessary for drying, grinding, sending the samples off to a tissue analysis lab, and waiting for the analysis, and save money by avoiding to pay for shipping and foliar tissue analyses.

All these results were obtained from a specific selected mockorange plant. Application of hyperspectral imaging was successfully completed for this little-leaf mockorange grown *in vitro*, but the success of this method for other mockorange species as well as other plant species still needs to be tested.

4.5. Conclusion

This study demonstrated that strong regression models could be developed to predict N and Ca contents of tissue cultured little-leaf mockorange shoots. The best features to estimate %N were reflectance values at the wavelength of 648 nm, asymmetric point from 1819 to 2150 nm (Asy 11) and the area from 559 to 772 nm (Area 3), and reflectance at

wavelength of 1919 nm. These features were employed in a nonparametric (non-linear) model, with RF regression to provide the best model for estimation of foliar %N content. Best features to estimate %Ca in the shoots were minimum reflectance from 838 to 843 nm (Min 4), area from 2428 to 2490 nm (Area 15), asymmetric point from 1670 to 1714 nm (Asy 9), and Cellulose Absorption Index (CAI). Random forest regression provided a more accurate model to estimate %Ca than the other regression models. The best RF regression model for %N in little-leaf mockorange shoots resulted in an $R^2 = 0.72$ and correlation = 0.84. Likewise, the best RF model for %Ca estimation resulted in an $R^2 = 0.99$ and correlation = 0.99. These strong statistical values clearly demonstrated that hyperspectral imaging can be used to predict accurately %N and %Ca in tissue cultured shoots from one selected little-leaf mockorange plant. Other mockorange species as well as other plant species produced in tissue culture would need to be tested to validate using hyperspectral imaging to predict N and Ca contents of shoots produced in tissue culture.

References

Adão, T., Hruška, J., Pádua, L., Bessa, J., Peres, E., Morais, R., Sousa, J. J., 2017. Hyperspectral imaging: A review on UAV-based sensors, data processing and applications for agriculture and forestry. *Remote Sens.*, 9, 1110; doi:10.3390/rs9111110.

Anonymous, 2021. Cellulose. Accessed in December 2021. Available on: https://en.wikipedia.org/wiki/Cellulose.

Anonymous, 2021. Index Data Base. Accessed in October 2021. Available on: https://www.indexdatabase.de/.

Beck K. D., 2019. Evaluating the use of hyperspectral remote sensing and narrowband spectral vegetation indices to diagnose onion pink root at the leaf and canopy level. M.Sc. Thesis. *University of Idaho*.

Capolupo, A., Kooistra, L., Berendonk, C., Boccia, L., Suomalainen, J. 2015, Estimating plant traits of grasslands from UAV-acquired hyperspectral images: A comparison of statistical approaches. *ISPRS International Journal of Geo-Information* 4, 2792–2820.

Clevers, J.G. P.W., Kooistra, L., 2012. Using hyperspectral remote sensing data for retrieving canopy chlorophyll and nitrogen content. *IEEE Journal of Selected Topics in Applied Earth Observations and Remote Sens.*, 5 (2), 574- 583. DOI: 10.1109/JSTARS.2011.2176468.

De Oliveira, L. F. R., De Oliveira, M. L. R., Gomes, F. S., Santana, R. C., 2017. Estimating foliar nitrogen in Eucalyptus using vegetation indexes. *Scientia Agricola*. 74, 142-147. http://dx.doi.org/10.1590/1678-992X-2015-0477.

Freedman, D., Pisani, R., Purves, R., 2007. Statistics (international student edition). Pisani, R. Purves, 4th Edn. *WW Norton & amp*; Company, New York.

Gabriel, J.L., Zarco-Tejada, P.J., López-Herrera, P.J., Pérez-Martín, E., Alonso-Ayuso, M., Quemada, M., 2017. Airborne and ground level sensors for monitoring nitrogen status in a maize crop. *Biosystems Eng.*, 160, 124–133.

Gomez, R., 2020. Professional short course on hyperspectral and multispectral imaging. *Applied Technology Institute*. https://aticourses.com/.

Hruška, J., Adão, T., Pádua, L., Marques, P., Cunha, A., Peres, E., Sousa, A., Morais, R., Sousa, J. J., 2018. Machine learning classification methods in hyperspectral data processing for agricultural applications. *Association for Computing Machinery*, 137–141. DOI: https://doi.org/10.1145/3220228.3220242.

Liang, S., 2004. Quantitative remote sensing of land surfaces, *Wiley*, Print ISBN: 9780471281665. 534 p. DOI: 10.1002/047172372X.

Liu, H., Zhu, H., Wang, P., 2016. Quantitative modelling for leaf nitrogen content of winter wheat using UAV-based hyperspectral data, *Intl. J. of Remote Sen.*, 38, 2117–2134. DOI: 10.1080/01431161.2016.1253899.

Maes, W. H., Steppe, K., 2019. Perspectives for remote sensing with unmanned aerial vehicles in precision agriculture. *Trends in Plant Science,* Vol. 24, https://doi.org/10.1016/j.tplants.2018.11.007.

Morcillo-Pallarés, P., Rivera-Caicedo, J. P., Belda, S., De Grave, C., Burriel, H., Moreno, J., Verrelst, J., 2019. Quantifying the robustness of vegetation indices through global sensitivity analysis of homogeneous and forest leaf-canopy radiative transfer models. *Remote Sens*., 11, 2418. 1-23. DOI:10.3390/rs11202418.

Pandey, P., Ge1, Y., Stoerger, V., Schnable, J.C., 2017. High throughput *in vivo* analysis of plant leaf chemical properties using hyperspectral imaging. *Frontiers in Plant Science*, 8:1348. DOI: 10.3389/fpls.2017.01348.

Robila, S. A., 2004. An analysis of spectral metrics for hyperspectral image processing, 2004 IEEE International Geoscience and Remote Sensing Symposium, Anchorage, AK, USA, 20–24 September 2004. *IEEE*, 5, 3233-3236.

Severtson, D., Callow, N., Flower, K., Neuhaus, A., Olejnik, M., Nansen, C., 2016. Unmanned aerial vehicle canopy reflectance data detects potassium deficiency and green peach aphid susceptibility in canola. *Precis. Ag.*, 17: 659–677.

Van Der Meij, B., Kooistra, L., Suomalainen, J., Barel, J.M., De Deyn, G.B., 2017. Remote sensing of plant trait responses to field-based plant–soil feedback using UAV-based optical sensors. *Biogeosciences*. 14, 733–749.

Wen, D., Tongyu, X., Fenghua, Y., Chunling, C., 2018. Measurement of nitrogen content in rice by inversion of hyperspectral reflectance data from an unmanned aerial

vehicle. *Ciência Rural, Santa Maria*, 48(06) e20180008. http://dx.doi.org/10.1590/0103-8478cr20180.

Zhu, H., Liu, H., Xu, Y., Guijun, Y. 2018. UAV-based hyperspectral analysis and spectral indices constructing for quantitatively monitoring leaf nitrogen content of winter wheat. *Applied Optics*, 57: 7722–7732.

Conclusion to the Dissertation

Little-leaf mockorange (*Philadelphus microphyllus* A. Gray) was successfully propagated *in vitro* on ½ strength MS medium containing 32.5 to 35 mM N, 1.8 mM Ca, and 0.6 mM P, supplemented with 1.1 µM Zeatin. Results from testing minerals individually, as well as the experiment applying response surface methods were completely in agreement with each other and proved this statement. Stem explants growing on such medium grew more and taller axillary shoots with the most biomass. Adjustment of Zeatin concentration in the culture medium increased shoot biomass to about 100% and shoot height to about 64%. Optimizing the culture medium components including N, Ca, P, and Zeatin, using response surface methods (RSM) was successfully done, which can be help growers by saving their time and money.

Also, in this study, the feasibility of applying hyperspectral imaging to estimate tissue-cultured shoots was proved. Application of hyperspectral imaging followed by machine learning methods provided successful models to predict foliar N and Ca concentrations without the need to destructive methods, which is also another time and money saving opportunity.

Little-leaf mockorange, a plant species native to mid-west, with its beautiful flowers and adopted to the environment climate is a perfect choice for urban landscaping. Tissue culture propagation was proved to be a great method for this species. Providing nurseries and tissue culture labs growing little-leaf mockorange with the information I got in this set of experiments, can help them to improve their culture numbers.